Master in Pharmaceutical Biotechnology
School of Medicine and Surgery
University of Padova, Italy

Examining the Pathogenic Role of Molecular Layer Interneurons in Preclinical Models of Spinocerebellar ataxia type 1

Master Thesis

For the attainment of the academic degree of

Pharmaceutical Biotechnology

Supervisor: Prof Dr. Smita Saxena

Department of Neurology

Inselspital University Hospital

University of Bern

Switzerland

Submitted by

Aishwarya Thapa

Table of Contents

ABBREVIATIONS

Neurodegenerative disorders	NNDs
Central nervous system	CNS
Ataxia -telangiectasia	ATM
Peripheral nervous system	PNS
Amyotrophic Lateral Sclerosis	ALS
Parkinson's disease	PD
Huntington's disease	HD
HD gene	IT15/ HTT
Autosomal recessive cerebellar ataxias	ARCA
Autosomal dominant cerebellar ataxias	ADCA
Spinobulbar Muscular Atrophy	SBMA
Dentatorubral Pallidoluysiana Atrophy	DRPLA
Charlevoix Saguenay	ARSACS
Ataxia with oculomotor apraxia type 1	APA1
Cerebrotendinous xanthomatosis	CTX
Friedreich ataxia	FRDA
Purkinje Cells	PC
Spinocerebellar Ataxia	SCA
Spinocerebellar Ataxia type 1	SCA1
Polyglutamine	PolyQ
Polyglutamine Binding Protein 1	PQBP 1
Deep Cerebellar Nuclei	DCN
Molecular layer	ML
Granule cell Layer	GCL
Granule cell	GC
Unipolar brush cells	UBC
Climbing Fibers	CF
Parallel Fibers	PF
Inferior olive	IO
Postnatal day	P
Metabotropic glutamate receptor 1	mGluR1

Vesicular GABA transporter	VGaT
Vesicular GABA transporter 1	VGaT1
Vesicular Glutamergic Transporter 1	VGlut1
Reactive oxygen spices	ROS
Calcium binding proteins	CaBP
Endoplasmic reticulum	ER
Parvalbumin	PV
Prefrontal cortex	PFC
Induced pluripotent stem cells	iPSCs
Induced GABAergic neurons	iGNs
Long term Potentiation	LTP
Long-term Depression	LTD
Synaptotagmin 1	Synt 1

1. ABSTRACT

Neurodegenerative diseases (NDDs) are characterized by the dysfunction of different neuronal populations and consequent neuronal loss throughout the central nervous system (CNS). It is not clear what causes NDDs, however, genetic mutations and ageing are associated with the development of NDDs. Among these diseases, Spinocerebellar ataxia type 1 (SCA1), is an autosomal dominant, adult-onset, motor-associated neurodegenerative disease characterized by atrophy in cerebellum. The neurons mainly affected by the disease are the Purkinje cells (PC). SCA1 is caused by the expansion of a polyglutamine repeat within the ubiquitously expressed Ataxin-1 protein. The exact cause of this premature degeneration of PCs is still unknown. Unpublished findings from our group show that within the cerebellar cortex there is an enhanced PV expression in Molecular Layer Interneuron (MLIN), potentially leading to enhanced inhibition onto the PCs. Furthermore, we previously shown an imbalance in the excitatory-inhibitory balance within the cerebellar cortex leading to PCs degeneration. The primary objective of this thesis is to investigate the pathogenic role of Molecular Layer Interneuron (MLIN). For our experiments, we used *SCA1* $^{154Q/2Q}$ and *WT* mice model and iPSCs model from SCA1 patient. Firstly, an increase in PV expression, as a marker of neuronal activity in MLINs,was observed from the cerebellar cortex of *SCA1* $^{154Q/2Q}$ than *WT* . The PV expression increased with the increasing age of the mice. We hypothesized that the MLIN might be more active therefore impacting PC physiology, we further evaluate synaptic connectivity onto MLIN and PCs. Moreover, ther results from proteomics analysis of MLINs was validated revealing multiple synaptic proteins downregulated in *SCA1*$^{154Q/2Q}$ compared to *WT*. We focused our attention on characterizing Synaptotagmin 1 (Synt 1), a calcium sensor protein involved in neurotransmitter release.Further its role in mouse and human model of SCA1, was validated confirming its downregulation in both human and mouse models of SCA1. Finally, our findings suggests that the MLINs are important modulators of PCs physiology in SCA1, potentially contributing to PCs degeneration.

2. INTRODUCTION

2.1 Neurodegenerative diseases

Neurodegenerative diseases (NDDs) are characterized by the dysfunctions of different neuronal populations and the consequent neuronal loss throughout the central nervous system (CNS) (Leng et al., 2021).

Ageing is one of the major risk factors for NDDs as its occurrence increases with ageing. The life expectancy in our society is increasing, thanks to the availability of new medical resources and technology. As a consequence, there is an increase in the worldwide ageing populations and of age-related health disorders which are cause of financial burden for the society (Hou et al., 2019).Unfortunately, no effective treatments that can stop or slow down disease progression are available for ageing related NDDs.

The most common neurodegenerative diseases in the increasing aging populations are Alzheimer's disease (AD), Parkinson's disease (PD), Amyotrophic lateral sclerosis (ALS), and Polyglutamine (PolyQ) disorders such as Huntington's disease (HD), Spinocerebellar Ataxias (SCAs). Further, NDDs can be classified as cognitive disorders or movement disorders or both accordingly to symptoms and pathology manifestation.

(i) Cognitive disorders, such as AD, Frontotemporal Dementia, are neurological disorders wherein there is an impairment of cognitive processes such as memory loss, learning abilities, speech impairments or neuropsychological deficits.

(ii) Movement disorders, such as ALS, PD and Spinocerebellar ataxia (SCA); are associated with motor function, in which the cerebellar cortex, spinal cord, and the basal ganglia are involved.

(iii) At times both cognitive and movement disorders can be concomitantly present such as in the case of Lewy Body Dementia (Kovacs, 2016).

One of the major features of neurodegeneration-related symptoms is movement disorders. According to Bach 2011, movement disorders will likely increase considerably between 2010 and 2050 (Bach, 2011). Based on the ''status-quo model'', by 2050, diseases involving ageing as a decisive factor will have a faster rise with the increase in life expectancy. Therefore, NDDs with

increasing aging populations represent a major burden to both patients and the healthcare system (Bach, 2011).

There are common pathological hallmarks that characterize NDDs, for example, the accumulation of misfolded proteins, that forms aggregates within the neurons. For instance, studies on post-mortem brain tissues from patients have reported abnormal deposits of misfolded proteins such as hyperphosphorylated tau (p-tau), amyloid-β (Aβ), α-synuclein (Kovacs, 2016). There are common hallmarks between NDDs and aging. Nine 'hallmarks of aging have been identified and categorized as primary, antagonistic, and integrative (Lopez-Otin, 2013). For example, primary hallmarks of aging are genomic instability, telomere attrition, epigenetic alterations, loss of proteostasis, mitochondrial dysfunction, cellular senescence and deregulated nutrient sensing as depicted in **Figure 1**.

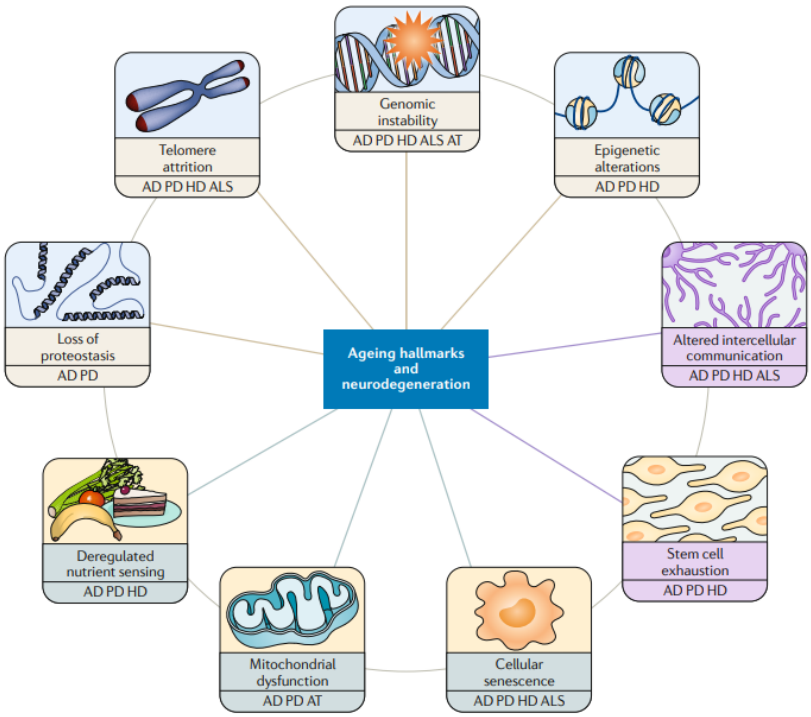

Fig. 2 | **Hallmarks of ageing.** Nine hallmarks of ageing — genomic instability, telomere attrition, epigenetic alterations, mitochondrial dysfunction, deregulated nutrient sensing, loss of proteostasis, cellular senescence, stem cell exhaustion and altered intercellular communication — seen in the main neurodegenerative diseases. AD, Alzheimer disease; ALS, amyotrophic lateral sclerosis; AT, ataxia telangiectasia; HD, Huntington disease; PD, Parkinson disease.

Figure 1: Hallmarks of aging such as genomic instability, telomere attrition, epigenetic alterations, loss of proteostasis, mitochondrial dysfunction, cellular senescence, deregulated nutrient sensing, stem cell exhaustion and altered intercellular communication correlate with susceptibility to neurodegenerative disease, Source: (Hou et al., 2019).

Genomic instability, cellular senescence, protein aggregation, mitophagy, and inflammation are also considered as potential therapeutic targets for NDDs. For instance, NAD+ deficiency is a major biomarker for mitochondrial dysfunction. Elevation of intracellular NAD+ have shown promising results against neurodegeneration through induction of mitophagy, promotion of DNA repair via sirtuins (SIRTs), senescence and inflammation. (Hou et al., 2019).

Studies have shown how targeting endogenous pathways that degrade misfolded proteins improves clearance of toxic species (Lieberman et al., 2019). For example, in HD (the expanded repeat polyQ–containing proteins or mRNAs, or both), and different strategies have been proposed to target the mutant protein (Lieberman et al., 2019). For instance, activating either macroautophagy or chaperone-dependent pathways to enhance cell-clearance machinery is essential for maintaining neuronal homeostasis (Lieberman et al., 2019).

Movement disorders are frequent neurological disorders that have a profound impact on patients' quality of life. This thesis work focuses on movement-related neurological disorders, in particular Spinocerebellar ataxia type 1 (SCA1), a polyglutamine (PolyQ) disorder. Along with SCA1, the PolyQ diseases cover a wide range of movement disorders which are explained in the ensuing chapters.

2.2 Polyglutamine (polyQ) diseases

PolyQ diseases are caused by expanded cytosine–adenine–guanine (CAG) repeats encoding a long polyQ tract in the respective encoded protein (Hughes & Olson, 2001). The mutated gene translates proteins carrying an abnormally expanded polyQ tract that tends to aggregate, forming insoluble protein aggregates (Nóbrega, 2018). There are nine PolyQ diseases identified: HD, Spinobulbar Muscular Atrophy (SBMA), Dentatorubral- Palidoluisiana Atrophy (DRPLA), and the Spinocerebellar Ataxias (SCAs) type 1, 2, 3, 6, 7 and 17. (Nóbrega, 2018).

The most common feature of the PolyQ diseases is the nuclear localization of the mutant protein that interfere with gene expression and translation (Dickson, 2011).Moreover, proteins carrying abnormal PolyQ tract can aggregate within the cytosol of neurons forming insoluble aggregates (Liu & Fang, 2019). The role of these inclusions in the pathogenesis of PolyQ diseases is still debated (Liu & Fang, 2019). However, common features of PolyQ disease include:

(i) The direct relation between the severity and precocity of symptoms and the variable CAG repeat number.

(ii) The instability in CAG repeats number transmission.

(iii) Protein aggregation and intracellular multiprotein inclusions detected in patient neuronal tissue (Nóbrega, 2018).

Though they share common pathogenic features, the symptoms and the patterns of neurodegeneration can differ between disorders. For example, post-translational modification can contribute to pathogenesis as in SCA1, where phosphorylation of mutant ataxin1 (*ATXN1*) at specific sites enhances the progression of the disease (Emamian et al., 2003). The abnormal aggregation or misfolding of the mutant proteins may interfere with the proteasomal processing of these proteins. Moreover, protein aggregation directly impairs the function of the ubiquitin-proteasome system. In a study performed by Bench et al, transient expression of two unrelated aggregation-prone proteins, a huntingtin fragment in HD model caused inhibition of the ubiquitin-proteasome system (Bence et al., 2001). SCA12 is characterized by an expansion in the 5' - untranslated region of the gene that codes for a regulatory subunit of protein phosphatase 2A resulting in haplo-deficiency. Most patients present upper extremity tremors, gait ataxia, and dysmetria, with disease progression (over several decades) patients manifest head tremors, dysdiadochokinesishyperreflexia, paucity of movement, abnormal eye movements and, in some cases, dementia. The study also highlighted both cortical and cerebellar atrophy (Holmes et al., 1999).Similarly, SCA8 and myotonic dystrophies result from RNA-mediated dysfunctions where mRNA is transcribed but not translated. The message contains untranslated CUG repeats, which conceals the splicing factors, thus altering the expression of other non-mutated proteins (RS Daughters et al., 2009).

Finally, research for common disease mechanisms will provide putative therapeutic strategies that can be applied to different PolyQ diseases (Dickson, 2011).

2.2.1 Huntington's disease (HD)

HD is a neurological disease genetically heritable in an autosomal-dominant manner and it is caused by a CAG trinucleotide expansion resulting in a long PolyQ tract, in the huntingtin (Htt) protein (Orr and Zoghbi, 2007).

The prevalence of HD is 5 – 10 per 100,000 in Western countries (Walker, 2007). In other parts of the world, the prevalence is lower (Walker 2007). Among the patients who develop symptoms before the age of 20 (6% of all cases), termed as juvenile HD (JHD), 75% have inherited the mutation

from their father, and the CAG repeat is usually over 55 repeats (Ghosh & Tabrizi, 2013). HD patients experience chorea and dystonia, incoordination, cognitive decline, and behavioural changes. It is generally characterized by a triad of progressive motor, cognitive and psychiatric symptoms (Ghosh & Tabrizi, 2013).

HD (IT15) gene is polymorphic with healthy individuals carrying 17 – 20 CAG repeats. In pathogenic condition, HD patients have CAG repeats of 40 or more, with repeat lengths of 36 – 39 characterized by incomplete penetrance (Lee et al., 2019). HD gene is 185 kb and contains 67 exons out of which two mRNA transcripts (10.5 and 13.5 kb) encode for the protein htt, a 348 kDa protein comprised of multiple repeated units of 50 amino acids (Lu et al., 2020).The CAG repeat is in the coding region of the gene (exon 1) and the expansion leads to production of abnormal huntingtin that contains an expanded polyglutamine stretch near the N terminus of the protein. The toxic gain of function is caused by this tail (Ghosh & Tabrizi, 2013).

Mutated htt protein interacts (often differently) with numerous other proteins (htt – associated proteins). For example, the CREB-binding protein (CBP) affects transcriptional dysregulation (Steffan et al., 2000). Compared to the wild-type protein, the mutant protein contains an expanded polyglutamine stretch starting at residue 18. Neuronal inclusions are formed fragments of abnormal htt containing the expanded glutamine repeat together with ubiquitin and other proteins(Dickson, 2011).

Imaging studies describe significant atrophy of basal ganglia and cerebral cortex even in asymptomatic individuals a decade or more before the predicted onset of clinical signs (Dickson, 2011). Clinical neurophysiological studies reveal reduced amplitudes of early cortical somatosensory evoked potentials and latency (Dickson, 2011).

Normally HD patients, are treated with dopamine receptor as a blocking and depleting agent that reduce symptoms of involuntary movements. A major challenge for this approach is the development of a suitable and effective way for the delivery of the siRNA.(Walker, 2007). Of note, one of the milestones is the first ASO Clinical Trial in HD was the drug called ISIS-HTTRx developed by Ionis/Roche. (Kordasiewicz et al, 2012).

2.2.2 Spinobulbar Muscular Atrophy (SBMA)

SBMA, is a late-onset motor neuron disease characterized by slowly progressive muscle weakness and atrophy (Katsuno et al., 2012). It is also known as bulbospinal neuronopathy and bulbospinal muscular atrophy.

SBMA exclusively affects adult men, whereas females homozygous for the AR mutation do not manifest neurological symptoms (Katsuno et al., 2012). The prevalence of this disease is estimated to be 1 – 2 per 100,000 (Fischbeck, 1997). The CAG trinucleotide expansion encodes a polyQ tract within the first exon of the androgen receptor (AR) gene. The major histopathological characteristic of SBMA is the loss of lower motor neurons in the anterior horns of the spinal cord as well as in the brainstem and motor nuclei except for the IIIrd, IVth, and Vith cranial nerves (Katsuno et al., 2012). In contrast, the sensory neurons are less affected. One of the major pathological hallmarks of polyQ diseases is the presence of nuclear inclusions (Nis). In SBMA, Nis contain the pathogenic AR. They are found in the residual motor neurons in the brainstem and spinal cord, as well as in non-neuronal tissues including the prostate, testes, and skin (Ogura et al., 2022).

The polyglutamine-expanded AR causes transcriptional dysregulation, axonal transport disruption, and mitochondrial dysfunction (Ogura et al., 2022), which together play a role in SBMA pathogenesis and neurodegeneration. One important feature is that the ligand-dependent nuclear accumulation of the polyglutamine-expanded AR protein is central to the gender-specific pathogenesis of SBMA. Even though recent studies have shown that DNA binding, inter-domain interactions, and post-translational modification of AR, have different toxicity modalities. Studies conducted on preclinical mice models have shown that the pathogenic AR-mediated neurodegeneration is suppressed by androgen inactivation (Ogura et al., 2022).

Pharmacological activation of cellular defence machineries, such as molecular chaperones, ubiquitin-proteasome system, and autophagy, exert neuroprotective effects in experimental models of SBMA. Moreover, the efficacy of androgen inactivation in preclinical models has been also tested in clinical trials (Ogura et al., 2022).

2.2.3 The Cerebellar Ataxia

The term ‘ataxia’ was originally derived from a Greek word that means “lack of order”. From clinical symptoms perspective, the symptom ataxia can be linked to disorders of heartbeat, gait, and movement, caused by different factors such as neurodegeneration, stroke, disease, brain tumours, trauma, multiple sclerosis (MS).

Eventually, ataxia is more specifically used to affirm the incoordination of movement because of damage to the sensory and/or cerebellar system (Bastian AJ, 1997). In particular, cerebellar ataxia is a clinically heterogeneous group of neurological disorders, which includes several well-characterized genetic diseases as well as sporadic forms of ataxia resulting in uncontrolled voluntary limb movement or gait, and high amplitude tremor that accompanies movement (Bastian AJ, 1997).

Cerebellar ataxia has a large overlap between different pathologies, heterogeneity, and clinical presentations. In 1954, Greenfield J G, based on pathoanatomical findings, was the first to propose a global classification for this group of disorders which was followed by Harding's classification in 1983 (Greenfied J.G., 1955). They regrouped the ataxias according to the age of onset, as a proxy for the mode of inheritance, and clinical findings. Since then, more than 40 genes have been linked to each of the recessively and dominantly inherited ataxias (Beaudin et al., 2017). The different groups of cerebellar ataxias are summarized in the **Table 1**.

Sporadic SCAs

- cerebellar cortical atrophy (CCA) (pure cerebellar ataxia, idiopathic cerebellar ataxia)
- multiple system atrophy (MSA)
- olivopontocerebellar atrophy (OPCA) (MSA-c)
- striatonigral degeneration (SND) (MSA-p)
- Shy–Drager syndrome (SDS)

Hereditary SCAs

Autosomal dominant

- spinocerebellar ataxia type 1 (SCA1) 6p22-23, ataxin 1
- spinocerebellar ataxia type 2 (SCA2) 12q23-24.1, ataxin 2
- spinocerebellar ataxia type 3 (MJD/SCA3) 14q24.3-32, ataxin 3
- spinocerebellar ataxia type 4 (SCA4) 16q24-ter
- spinocerebellar ataxia type 5 (SCA5) 11ctr, SPTBN2
- spinocerebellar ataxia type 6 (SCA6) 19p13, CACNA1A
- spinocerebellar ataxia type 7 (SCA7) 3p14.1-21.3, ataxin 7
- spinocerebellar ataxia type 8 (SCA8) 13q21, ataxin 8 opposite strand
- spinocerebellar ataxia type 10 (SCA10) 22q13, ataxin 10
- spinocerebellar ataxia type 11 (SCA11) 15q14-21.3, TTBK2
- spinocerebellar ataxia type 12 (SCA12) 5q31-33, PPP2R2B
- spinocerebellar ataxia type 13 (SCA13) 19q13.3-13.4, KCNC3
- spinocerebellar ataxia type 14 (SCA14) 19q13.4-ter, PRKCG
- spinocerebellar ataxia type 15 (SCA15) 3q26-25.3, ITPR1 (SCA16)
- spinocerebellar ataxia type 17 (SCA17) 6q27, TBP
- spinocerebellar ataxia type 18 (SCA18) 7q22-32
- spinocerebellar ataxia type 19 (SCA19) 1p21-q21 (SCA22)
- spinocerebellar ataxia type 20 (SCA20) 11p13-q11
- spinocerebellar ataxia type 21 (SCA21) 7p21.3-15.1
- spinocerebellar ataxia type 23 (SCA23) 20p13-12.3
- spinocerebellar ataxia type 25 (SCA25) 2p21-13
- spinocerebellar ataxia type 26 (SCA26) 13p13.3
- spinocerebellar ataxia type 27 (SCA27) 13q34, FGF14
- spinocerebellar ataxia type 28 (SCA28) 18p11, AFG3L2
- spinocerebellar ataxia type 29 (SCA29) 3p26
- spinocerebellar ataxia type 30 (SCA30) 4q34.3-35.1, ODZ3?
- spinocerebellar ataxia type 31 (SCA31) 16q22.1, BEAN
- dentatorubropallidoluysian atrophy (DRPLA) 12q12-ter, atrophin
- episodic ataxia type 1 (EA1) 12p, KCNA1
- episodic ataxia type 2 (EA2) 19p13, CACNA1A

Autosomal and X-linked recessive

- Friedreich's ataxia (FRDA) 9q13-21.1, frataxin
- ataxia with isolated vitamin E deficiency (AVED) 8q13.1-13.3, TTPA
- early-onset ataxia with oculomotor apraxia and hypoalbuminemia (EOAH)
- (ataxia oculomotor apraxia 1 (AOA1)) 9q13, aprataxin
- autosomal recessive spastic ataxia of Charlevoix-Saguenay(ARSACS) 13q12, sacsin
- spinocerebellar ataxia, autosomal recessive 1 (SCAR1) 9q34, senataxin
- ataxia-telangiectasia (AT1) 11q22.3, ATM
- fragile X tremor/ataxia syndrome (FXTAS) Xq27.3, FMR1

Besides SCA28 and FRDA, some mitochondrial encephaloneuromyopathies, which are not included in the box, show ataxia due to the involvement of the cerebellum, spinal cord and peripheral nervous system. In addition to those listed here, there are many autosomal recessive spinocerebellar ataxias (SCAR2–9), most of which affect children. Spastic paraplegias (SPG1–39) are also not included in this box.

Table 1: General Classification of different types of Cerebellar Ataxia, Source: (Mizusawa et al., 2011).

Hereditary ataxias are a large and heterogeneous group of cerebellar ataxias affecting the cerebellum. They are characterized by the development of ataxia as an early and dominant feature of the disease. The overall occurrence of ataxia has been estimated at the rate of 26/ 100,000 in children. The frequency of dominant hereditary cerebellar ataxia has an occurrence rate of 2.7/ 100,000, and the frequency of recessive hereditary cerebellar ataxia is 3.3/ 100,000 (Pilotto & Saxena, 2018).

The genetic, pathophysiological, clinical, and neuropathological features of these diseases are varied. Most of the hereditary ataxias are transmitted as an autosomal dominant or autosomal recessive trait, whereas episodic ataxias (EAs) have an autosomal dominant inheritance pattern (Mizusawa et al., 2011; Pilotto & Saxena, 2018). EAs have been subclassified into eight subtypes based

on genetic mutations and clinical characteristics. X-linked ataxias are rare. The most common in this group of X-linked ataxias is Fragile X-associated tremor/ataxia syndrome (Pilotto & Saxena, 2018).

The neurodegenerative process affects the cerebellum, brainstem, and spinal cord, the brain, including basal ganglia. Moreover, in some cases, the peripheral and autonomic nervous systems are also affected. The diagnosis of cerebellar ataxias requires an initial neurological examination (eye, hand, finger movements), family history, and non-genetic causes (Jayadev & Bird, 2013). The most common hereditary ataxia i.e. autosomal dominant cerebellar ataxia (ADCA) and autosomal recessive cerebellar ataxia (ARCA) are described below.

2.2.3.1 Autosomal recessive cerebellar ataxias (ARCA)

ARCA is a heterogeneous group of rare degenerative and metabolic genetic NNDs that share the hallmark of progressive damage of the cerebellum and its associated tracts (Pilotto & Saxena, 2018). Several additional neurologic systems (e.g., retina, cerebral cortex, basal ganglia, corticospinal tracts, and peripheral nerves) as well as non-neurologic tissues (e.g., heart, pancreas, muscle), are also affected leading to severe and complex multisystemic phenotypes, often starting before the age of 40.

Examples of recessive ataxia include Ataxia with oculomotor apraxia type 1 (APA1), Ataxia - telangiectasia (ATM), Cerebrotendinous xanthomatosis (CTX), and Friedreich ataxia (FRDA), being the most common in this category with an incidence of 1:29,000-50,000 (Mazzara et al., 2020). Similarly, the Autosomal recessive spastic ataxia of Charlevoix Saguenay (ARSACS) is considered the second most common recessive ataxia with onset at childhood, presenting cerebellar ataxia, pyramidal spasticity, and peripheral neuropathy (Pilotto & Saxena, 2018).

Three common pathways have been identified as responsible for ARCAs: mitochondrial dysfunction, impaired DNA repair, and complex lipid homeostasis (Ilg et al., 2010; Synofzik et al., 2019), caused by gene mutation. Most ARCAs have symptom onset during childhood or adolescent years, but variability is considerable and is inversely dependent on the expansion size.

This genetic pleiotropy is further expanded as the growing number of autosomal-dominant ataxia genes is also one of the major factors for the cause of autosomal-recessive ataxia in case of biallelic inheritance, often giving rise to very severe, early-onset recessive ataxia syndromes (e.g., AFG3L2/SCA 28, SPTBN2/ SCA5, ITPR1/SCA29, OPA1) (Synofzik and Ne´ meth, 2018 , Synofzik et al., 2019).

Novel ARCA treatments might target common hubs in pathogenesis by modulation of gene expression, stem cell transplantation, viral gene transfer, or interventions in different metabolic pathways (Synofzik and Ne´ meth, 2018).

2.2.3.2 Autosomal dominant cerebellar ataxias (ADCA)

ADCAs are defined as a group of inherited NDDs that consists of more than 40 diseases linked to 39 genes (M. Huang & Verbeek, 2019; Pilotto & Saxena, 2018). SCAs are a heterogeneous group of diseases and diverse clinical criteria for their classification are still debated. The frequency distribution is 1 with an incidence of 3 per 100,000 in the European population (Paulson et al., 2017).The cerebellum, brainstem, and spinal cord are the major regions involved in the neurodegenerative process. The brain, basal ganglia, as well as peripheral and autonomic nervous systems, are also affected by some disorders forms. Ataxic speech, nystagmus, and ataxic gait as well as other symptoms, including parkinsonism, uncontrolled involuntary movements, dysautonomia, cognitive impairment, motor weakness, and sensory impairments are also observed (Pilotto & Saxena, 2018).

Polyglutamine SCAs have been extensively described and known to cover more than half of characterized SCAs. The principal cause of the most common SCAs (SCA1, 2, 3, 6, 7, and 17) is a CAG trinucleotide repeat expansion in specific genes, causing an expanded polyglutamine tract (Poly Q) in the encoded proteins. These long Poly Q repeats cause misfolding of proteins, which aggregate, forming inclusions in the cytoplasm or nucleus of vulnerable neurons, invariably contributing to the progression of the pathology, neuronal dysfunctions, and subsequent neuronal degeneration. From a genetic point of view, they share a common pool of expanded CAG repeats, expansion in non-coding proteins caused by conventional mutations either duplication, deletion, insertion, and missense (Duenas, 2006; Paulson, 2009). The formation of misfolded proteins that tend to aggregate, forming inclusions in the cytoplasm or in the nucleus of vulnerable neurons eventually contributes to the pathological progression in SCAs (Pilotto & Saxena, 2018; Sandford & Burmeister, 2014).

Six other ataxias—SCA8, 10, 12, 31, 36, and 37—are also caused by nucleotide repeat expansions as shown in **Figure 2**. However, these repeats do not occur in the coding region of the gene. The pathogenic mechanism is due to the toxic RNA species or a peptide product that results from a non-canonical form of translation known as repeat-associated non-ATG initiated translation (RAN translation) (Durr, 2010). The remaining SCAs are caused by conventional mutations which include

point mutations or deletions in the coding regions of the genes, resulting in abnormal protein products (Brooker et al., 2021).

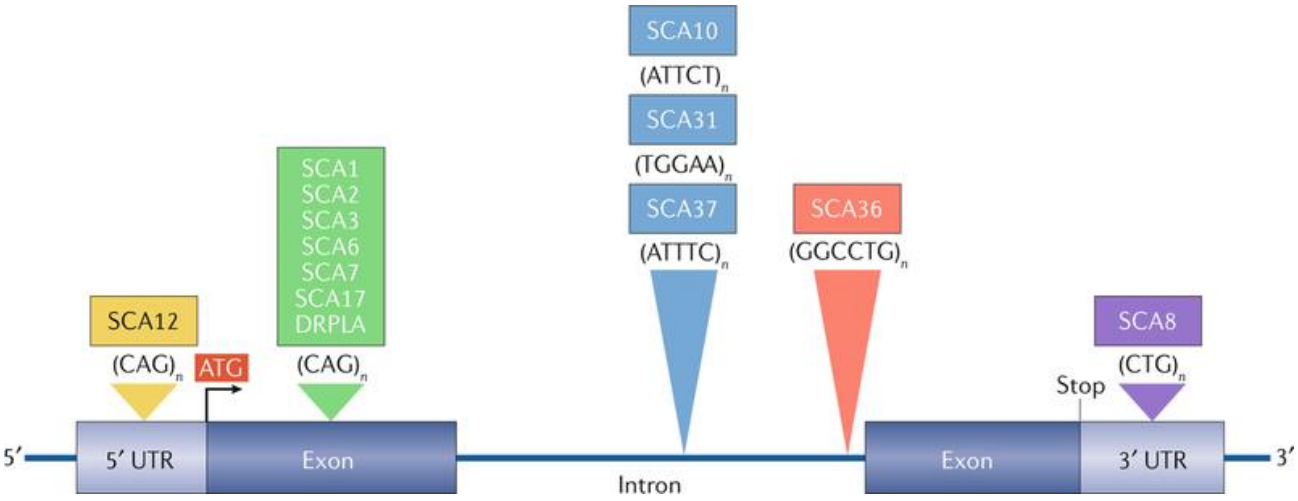

Figure 2: Hereditary degenerate ataxias caused by the expanded micro satellite repeats, Source: (Ashizawa, 2018)

However, certain SCAs have specific features. As shown in the **Figure 3**, different spinocerebellar ataxias (SCAs), SCA1, SCA2, SCA3 and SCA6 have similar disease etiology but the patterns of pathological involvement are not identical. For instance, SCA3 (Machado–Joseph disease), neuropathology differs from that of SCA1 and SCA2. The cerebellar cortex and olivary nuclei are relatively less affected in SCA3, whereas the deep cerebellar nuclei and basis pontis are usually more severely affected in SCA3 (Sequeiros & Coutinho, 1993). Combined atrophy of the basis pontis and cerebellum in hereditary ataxia, "olivopontocerebellar atrophy" (OPCA) was thought to be equivalent to autosomal dominant ataxia, multiple system atrophy (MSA), being the most common cause of OPCA. This was well proved by SCA1, SCA2, and SCA7 show OPCA pathology (Schöls et al., 2004, Rüb et al., 2013). In contrast, SCA6 and SCA31 belong to a group in which "pure cerebellar" or "cerebellum - olivary" atrophy is observed (Menzel P., 1861). In addition to this, SCA6 is specific to the cerebellum in which only the PC degenerate, while patients affected by SCA7 present also retinal degeneration, and SCA10 patients show epilepsy (Paulson, 2009).

Though the neuropathology and symptoms are unique to a particular group of SCA, they are governed by some similarity. In a nutshell, study by Paulson et al.,2009, the degeneration of Purkinje

neurons (PC) in the cerebellum, atrophy of the brainstem, and spinocerebellar tract in the preclinical mice models (Paulson, 2009).

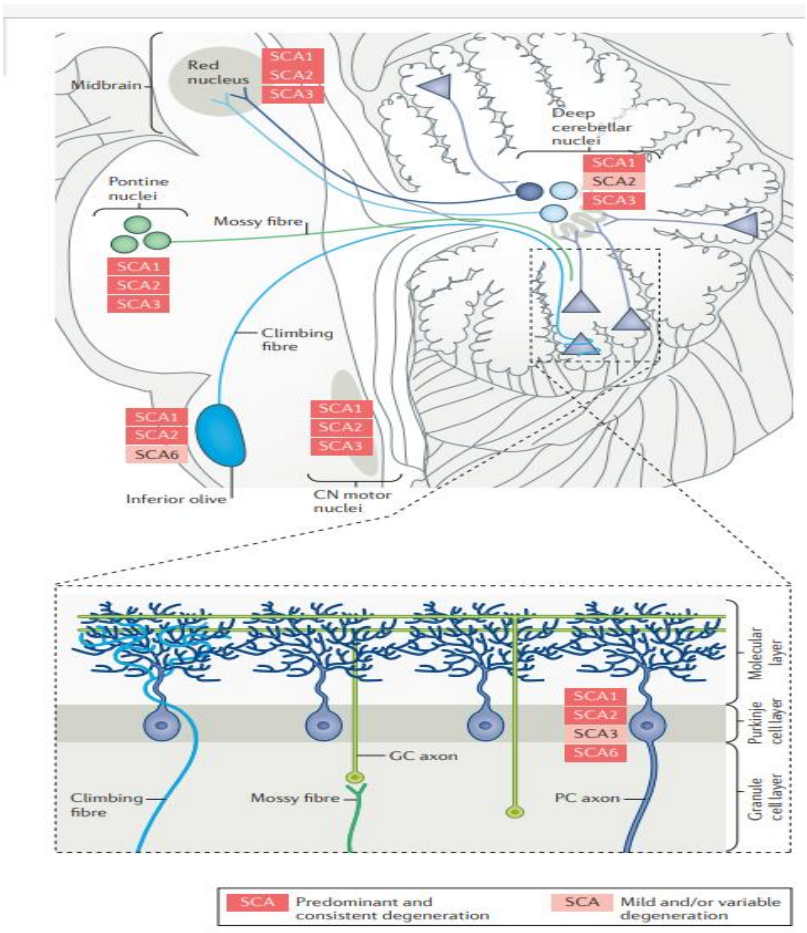

Figure 3: Components of the cerebellar circuitry showing degeneration in the polyglutamine spinocerebellar ataxias. The areas and cell types affected include the cerebellar cortex particularly Purkinje cells (PCs), the cell bodies which are depicted by triangles in the cerebellum, the inferior olive and the climbing fibres, the pontine nuclei and the mossy fibres, the deep cerebellar nuclei, the red nucleus, the cranial nerve (CN) motor nuclei and the, cerebellar granule cell (GC) , Source: (Paulson et al., 2017)**.**

Another feature of SCAs is the correlation between the length of the repeat expansion and the age of onset and severity of the disease (Paulson, 2009). Patients carrying short CAG expansions show symptoms at later ages and are characterized by the manifestation of mild symptoms, unlike those with larger expansions, such as in SCA 3 (Paulson, 2009).

Some of the major SCA classified are highlighted in the **Table 2**.

SCA	Gene	Type of mutation	Symptoms
SCA1	ATXN1	(CAG)*n*	Pyramidal features, active reflexes, peripheral neuropathy, and ophthalmoparesis
SCA2	ATXN2	(CAG)*n*	Motor neuron involvement, peripheral neuropathy, slow saccades, parkinsonian features, myoclonus, and dementia
SCA3	ATXN3	(CAG)*n*	Pyramidal features, motor neuron involvement, peripheral neuropathy, eyelid retraction, and parkinsonian features
SCA4	16q21.1	Unknown	Peripheral neuropathy and pyramidal signs
SCA5	SPTBN2	Point mutations	Tremor and facial myokymia
SCA6	CACNA1A	(CAG)*n*	Dysphagia, tremor, and somatosensory deficits
SCA7	ATXN7	(CAG)*n*	Slow saccades, retinal macular degeneration, and dementia
SCA8	ATXN8	(CTG*CAG)*n*	Pyramidal signs
SCA10	ATXN10	(ATTCT)*n*	Dysphagia, seizures, and cognitive impairments
SCA11	TTBK2	Point mutations	Pyramidal signs
SCA12	PPP2R2B	(CAG)*n*	Peripheral neuropathy, tremor, and parkinsonian features
SCA13	KCNC3	Point mutations	Pyramidal signs and intellectual disability
SCA14	PRKCG	Point mutations	Dystonia and myoclonus
SCA15, 16 and 29	ITPR1	Point mutations, large deletions	Tremor and dystonia
SCA17	TBP	(CAG)n	Parkinsonian features and dementia
SCA18	IFRD1	Point mutations	Peripheral neuropathy
SCA19/22	KCND3	Point mutations, small deletions	Myoclonus and dysphagia (SCA22)
SCA20	Unknown	Genomic duplication	Dysphonia and palatal tremor
SCA21	Unknown	Unknown	Parkinsonian features and mild cognitive impairment
SCA23	PDYN	Point mutations	Pyramidal features
SCA25	Unknown	Unknown	Peripheral neuropathy
SCA26	EEF2	Point mutations	Dysarthria and eye movement abnormalities
SCA27	FGF14	Point mutations	Tremor and dystonia
SCA28	AFG3L2	Point mutations	Pyramidal features and ophthalmoparesis
SCA31	BEAN1	(TGGAA)*n*	Dystonia
SCA35	TGM6	Point mutations	Tremor and ocular dysmetria
SCA36	NOP56	$(GGCCTG)_n$	Motor neuron involvement
DRPLA	ATN-1	(CAG)*n*	Myoclonus, epilepsy, and dementia
SCA37	DAB1	ATTTC(*n*)	Gait instability, dysarthria, and eye movement abnormalities
SCA38	ELOVL5	Point mutations	Nystagmus and dysarthria
SCA40	CCDC88C	Point mutations	Ocular dysmetria and tremor
SCA41	TRPC3	Point mutations	Imbalance and gait instability
SCA42	CACNA1G	Point mutations	Gait instability, dysarthria, and nystagmus
SCA43	MME	Point mutations	Peripheral neuropathy, dysarthria, and tremor
SCA44	GRM1	Point mutations	Dysarthria, dysphagia, and dysmetria
SCA45	FAT2	Point mutations	Dysarthria and nystagmus
SCA46	PLD3	Point mutations	Eye movement abnormalities

SCA: spinocerebellar ataxia.
[a]Violet: SCAs with classical PolyQ expansions in the coding region of the gene; blue: SCAs with repeat expansions in the non-coding region of the gene; black: SCAs arising due to point mutations or deletions; green: SCAs arising due to as of yet unidentified mutations

Table 2: Genetic and clinical features of autosomal dominant spinocerebellar ataxias. SCAs are named according to the gene they are linked to and have a specific type of mutation leading to certain symptoms, Source: (Pilotto & Saxena, 2018).

There are currently no disease-modifying treatments for any of the SCAs and many challenges to be overcome in clinical trial development. One of the proposed strategies is reducing the accumulation of the toxic mutant protein (Ashizawa, 2018). Moreover, several high-throughput small molecule screens have revealed promising candidates that may lower levels of the mutant protein as shown in **Table 3** (Ashizawa, 2018, Yang et al., 2016).

Type of SCA	Molecular candidates	Scientific Premise	Status/Results	Comments
SCAs 1, 2, 3, 6, 7, 8 & 10	BHV-4157 (trigriluzole)	Riluzole prodrug.	Ongoing but enrollment has been completed.	
Heterogeneous cerebellar ataxia including SCAs	Acetyl-DL-leucine (ALCAT trial)	Previous clinical studiesS57	PlannedS58	
SCA38	Docosahexanoic acid	The SCA38 gene encodes an enzyme involved in omega-3 fatty acid biosynthesis	Ongoing	
SCAs	Exercise		Ongoing open-label trial	
SCAs	Transcranial magnetic stimulation	Based on earlier studiesS59	Completed	No results available
SCAs	Whole body vibration	Proprioceptive modulation	Completed	Significant improvements in SCAs1, 2, 3 and 6 reported by another groupS60
Spinocerebellar degeneration	KPS-0373	Thyrotropin releasing hormone	Completed Phase 3 trial	No results available
Spinocerebellar degeneration	Intravenous immunoglobulin	Inflammation	Completed	No efficacy data available
Hereditary cerebellar ataxias	Mesenchymal stem cell infusion	Based on one study on SCA2 animal model S62 and a prior clinical studies S63	Phase 2 trial (unknown status)	Phase 1/2a trial from another groupS64 reported safety and tolerability.
Polyglutamine SCAs	Stemchymal®	Standardized stem cells product isolated from human adipose tissue	Ongoing Phase 2 trial	

SCA3	Weight in lower limbs		Completed	No efficacy data available

Table 3 Treatments of SCAs in ongoing or recently completed clinical trials Source: (from clinicaltrials.gov, (Zesiewicz et al., 2018).

Recently, new approaches based on newer RNA depleting or DNA editing tools have been developed (Gustincich et al., 2017).These include small-interfering RNA (siRNA), micro-RNA (miRNA), or the most promising antisense oligonucleotide (ASO)-based approaches to target RNA species, that have been validated in preclinical animal models of SCAs (Coarelli et al., 2018).For instance, the *ATXN3*-targeting ASO was successful in the reduction of polyglutamine-expanded *ATXN3* up to 8 weeks after treatment and it prevented oligomeric and nuclear accumulation of *ATXN3* up to at least 14 weeks after treatment (McLoughlin et al., 2018).

In another study, use of antisense oligonucleotides helped to mask predicted exonic splicing signals, resulting in exon 10 skipping from *ATXN3* pre-mRNA (McLoughlin et al., 2018). Thus, there was a reduction of toxic polyQ expansion and truncated ataxin-3 protein, which retained its ubiquitin-binding and cleavage function. Finally, the repeated intracerebroventricular (ICV) injections of the antisense oligonucleotides in a SCA3 mouse model led to long-lasting exon skipping and formation of the modified ataxin-3 protein throughout the mouse brain, being detectable for at least 2.5 months (Toonen et al., 2017).

Since my thesis work is related to SCA1 disease, in the next section a more detailed introduction will be covered.

2.3. Spinocerebellar ataxias Type 1 (SCA 1)

SCA1 is an inherited autosomal progressive neurodegenerative disorder caused by a CAG repeat expansions in the *ATXN1* gene. Repeat expansions of about 39 or more CAG repeats result in the expression of a poly Q expansion in the Atxn1 protein. The SCA1 is a subset of heterogeneous hereditary cerebellar ataxias that are autosomal dominantly transmitted. Among the different heterogenous groups, SCA1 is the first characterized ADCA (Orr et al., 1993). SCA1 is characterized by the loss of cerebellar Purkinje cells (PCs), progressive dysfunction and degeneration of the cerebellum, brain stem and spinal cord due to the accumulation of the mutant *ATXN1* (Wagner et al., 2016).

2.3.1 Clinical features, Epidemiology and Pathogenicity

SCA1 symptom can be distinguished from other hereditary ataxias by the predominance of pyramidal symptoms in addition to myotrophy and sensory loss in affected individuals. SCA1 is characterized by progressive degeneration that is most severe in the cerebellum and brainstem but with the progression of the pathology spread to other brain regions. SCA1 patients experience deficits in motor coordination (i. e. ataxia), swallowing impairments, balance difficulty, brisk tendon reflexes, hypermetric saccades, nystagmus, mild dysphagia, and cognitive impairment like the speaking cognition and mood are seen. During the early stages of the disease, patients face difficulty in maintaining balance, manifest slurred speech and nystagmus. While in the advanced phases, symptoms include loss of proprioception, muscle atrophy, and dystonia (Adam et al., 1998). With progression of the disease the main cause of death for SCA 1 is respiratory failure (Subramony and Ashizawa, 1993). While extra-cerebellar pathology in SCA1 patients remains less understood, dysfunction in the brain stem, motor cortex, and hippocampus have been described and is thought to contribute to different spectrum of SCA1 symptoms such as cognitive deficits, mood disorders, difficulties in respiration and swallowing, and premature lethality (Brooker et al., 2021).

The prevalence of SCA1 is about 1-2 cases in 100,000 which represents 6% of the total patients diagnosed with ADCA worldwide.However, the frequency is varied and highly influenced by ethnic background as mostly seen in the western populations (Pilotto & Saxena, 2018). The age of onset of SCA1 ranges from childhood (4 years) to late adult life (74 years), with a mean onset in the fourth decade of life. Fast disease progression is observed with earlier age of onset and larger CAG expansions. Moreover, among the polyQ SCAs, the progression of SCA1 is the fastest (Schols et al.2004, Jacobi et al., 2011).

The neuropathology of SCA1 is also complex and varied. In SCA1, cerebellar and brainstem degeneration are nearly always prominent, whereas more anterior regions (such as the basal ganglia) and posterior regions (such as the spinal cord) exhibit a variable degree of degeneration (Paulson et al., 2017). The signature pathology of SCA1 is the degeneration of PCs in the cerebellum. In addition to this, the neurons of the dentate, basal pontine, and olivary nuclei and other brainstem areas, including the red nuclei, vestibular nuclei, and motor cranial nerve nuclei, are often affected, whereas the pars compacta of the substantia nigra are usually spared. The MRI/CT scans highlighted Olivopontocerebellar atrophy (Schöls et al., 2004).

2.3.2 The *ATXN1* Gene

The *ATXN1* gene encodes for the Atxn1 protein. It binds RNA and interacts with large protein complexes. It is involved in transcriptional repression and regulates the Notch pathway and Capicua (CIC), which are important for the cerebellar development and maturation (Bergeron et al., 2013). Normal translation of PolyQ repeats within normal repeat range produces normal protein transcript and protein folding. For instance, wild-type *ATXN 1* includes a polyQ tract that normally contains 6–34 glutamines. Wild-type *ATXN1*- shuttles between the cytoplasm and nucleus. A monopartite nuclear-localization signal (NLS) motif near the carboxyl terminus directs the localization of the protein to the nucleus (Klement et al., 1998).

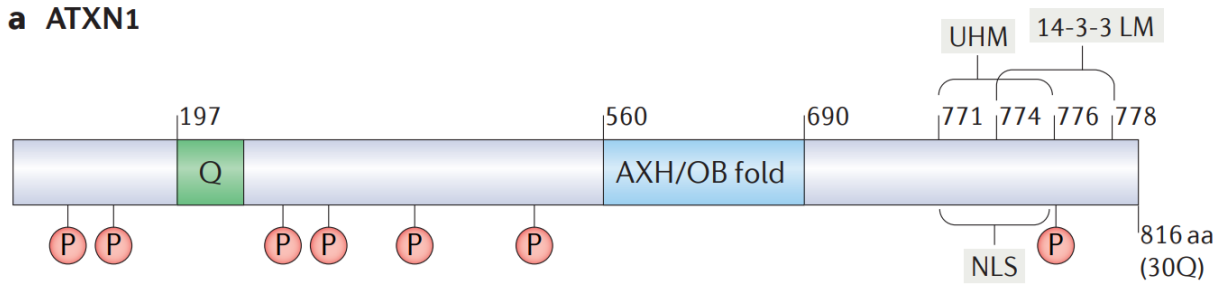

Figure 4: Functional motifs in ATXN1. The polyQ regions is denoted as 'Q', as well as the phosphorylation sites is denoted as 'P' and ubiquitylation sites ('Ub'). Here, ATXN1 has a 30Q polyQ region. The ATXN1 HBP1 (AXH) domain and the U2AF homology motif (UHM) of ATXN1 are interaction motifs for capicua (CIC) and RBM17, forming an oligonucleotide/ oligosaccharide-binding (OB) fold. Near the carboxyl terminus of the protein, localization to the nucleus and a

phosphorylation-dependent binding motif for the chaperone 14-3-3 (14-3-3LM) is shown, Source: (Paulson et al .,2017).

In contrast, *ATXN1* containing an expanded poly Q tract is transported to the nucleus but cannot be exported to the cytosol (Irwin et al., 2005). A single amino-acid substitution within its NLS prevents expanded *ATXN 1* from entering the nuclei of Purkinje cells and eliminates its toxicity (Tsai et al., 2004), suggesting that in these cells, disease pathogenesis may be linked to a function of *ATXN1* in the nucleus. Wild-type and expanded *ATXN1* interact with various nuclear components, as **in Figure 4** including RNA and, several regulators of transcription, SMRT30 (silencing mediator of retinoic acid and thyroid hormone receptor; also known as NCOR2), capicua (CIC), a transcriptional repressor containing a high mobility group (HMG) box ,the zinc finger protein GFI1 and the nuclear receptor-α (RORα)–60 kDa Tat-interactive protein (TIP60; also known as KAT5) complex3 (Tong et al., 2011; Tsai et al., 2004; Yue et al., 2001).

2.3.3 The mutant form of ATXN1

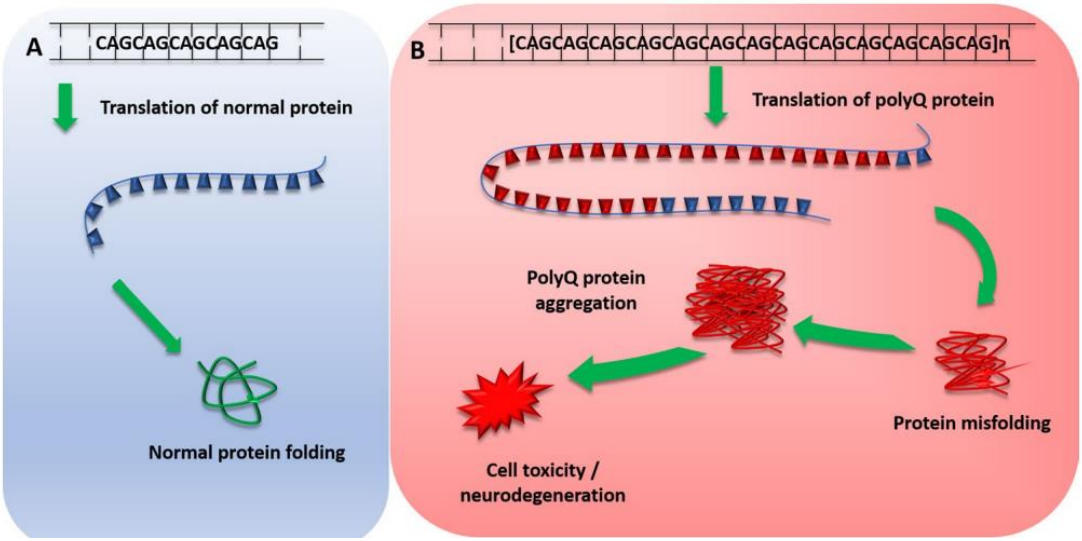

Figure 5: Mechanism of Polyglutamine expansion A) Translation of normal protein and folding and B) Pathogenic polyglutamine expansion repeat length leads showing the translation of expanded abnormal PolyQ repeat, which leads to protein misfolding , Source: (Sullivan et al., 2019).

The human normal poly Q- Atxn1 protein is mainly localized in the nucleus of neuronal cells but in PCs, it is found in both the cytoplasm and the nucleus, with high abundance of protein complexes such as CIC (Servadio et al., 1995). The presence of human mutant Atxn1(illustrated **in Figure 5**) disturbs the size distribution of these complexes and inhibits the repressor activity of CIC. In a study of Lam et al, overexpression of CIC in a fly model of SCA1 suppressed the morphologic changes induced by polyQ-Atxn1 (Lam et al., 2006). Additionally, Yue et al. 2001, found that Atxn1 binds RNA, and when the size of its polyQ tract is increased, its ability to bind RNA decreased. Thus, it was concluded that the expansion of the Atxn1 polyQ tract has a deleterious impact on RNA metabolism (Yue et al., 2001). PolyQ-Atxn1 also has impact in several RNA processing, cellular pathways, including transcription and signal transduction, disrupting normal cell function and leading to cell death (Kang and Hong, 2009; Wagner et al., 2016).

Phosphorylation contributes to the regulation of Atxn1 folding and distribution which is disturbed in the disease condition. The phosphorylation of Serine 776 (S776) is one of seven phosphorylation sites in Atxn1 near the C-terminus of Atxn1, just downstream of the NLS. In a study performed by Emamian et al, mutating S776 to alanine altered the intracellular deposition of polyQ-Atxn1 and prevented nuclear inclusions from forming. The S776 and A776 forms of polyQ-Atxn1 were expressed in PCs in mice (Emamian et al., 2003). It was found that polyQ-Atxn1- A776 was substantially less toxic than expanded/ mutant-Atxn1-S776. Thus, the phosphorylation of this serine residue contributes significantly to the harmful effects of the mutant protein (Emamian et al., 2003).

Interestingly, the toxicity arises from expanded polyQ within- Atxn1 adversely affects the function of other proteins (Lam et al., 2006). One of the cAMP-dependent kinase responsible for the phosphorylation in the S776 of Atxn1, is Protein Kinase A (PKA) (Chen et al., 2003; Jorgensen et al., 2009). In a model of SCA1 pathogenesis the crucial nuclear interactions and functions of Atxn1 was incorporated in which the Ser776 phosphorylation leads to a reduction in the proteolytic clearance of Atxn1 (Lim et al.,2008).

Proteomic approaches have indicated that changes in the mechanistic target of rapamycin (mTOR) signalling is involved in SCA1 cerebellar pathogenesis (Vierra-Green et al., 2005). Moreover, analysis of synaptic proteins in disease-susceptible PCs in the *Sca1*$^{154Q/2Q}$ knock-in mice showed that the levels of Homer-3, a synaptic scaffold protein enriched in Purkinje cells, was dramatically reduced at pre symptomatic stages. Importantly, deletion of mTORC1 led to reduced Homer-3 levels and

accelerated disease while restoring Homer-3 increased pathology showing PC susceptibility in SCA1 pathology (Ruegsegger et al., 2016).

2.3.4 Diagnosis and Treatment

Initial diagnosis of SCA1 on molecular genetic tests like methylation analysis and targeted mutation analysis is used for the detection of the PolyQ repeats (Tan & Ashizawa, 2001,;Adam et al., 1998).

The European Molecular Genetics Quality Network (EMQN) has published best practice guidelines for the genetic testing of the spinocerebellar ataxias including SCA1. The guidelines improve the accuracy of genetic testing with different repeats (Ramos et al 2016).

Molecular genetic testing approaches can include single-gene testing or the use of a multigene panel:

(i) Single-gene testing includes targeted analysis for the heterozygous CAG repeat number in *ATXN1* and should be performed first.

(ii) A multigene testing panel that includes *ATXN1* and other genes of interest may also be considered. Multigene panels are most likely to identify the genetic cause of the condition while limiting the identification of variants of uncertain significance, identify pathogenic variants in genes that do not explain the underlying phenotype, custom phenotype-focused exome analysis in the gene, sequence analysis, deletion/duplication analysis, and/or other non-sequencing-based tests vary (Ramos et al 2016).

To date, there are no efficient therapies that have been identified for the cure of SCA1 (Whaley et al., 2011). Nevertheless, its symptoms may be eased (Adam et al., 1998). Intensive rehabilitation (or coordinative physiotherapy) improves motor function in a heterogeneous group of individuals with various types of cerebellar degeneration(Ilg et al., 2010; Ma et al., 2014).

As SCA1 is a monogenic disease, gene therapy might be considered ad treatment approach. Different therapeutic options available from pharmacological medicines to stem cells and genetic therapies in preclinical models of SCA1 are summarized in **Table 4**. Nevertheless, further investigations are necessary to identify potential treatment options (Wagner et al., 2016).

	Treatment	Animal model	Route	Outcome
Cvetanovic et al., 2011	VEGF	154Q/2Q mice	Pharmacologic: intraventricular infusion Transgenic: gene over-expression	Improved pathological hallmarks and motor function
Hearst et al., 2014a	PKA inhibitory polypeptide (Synb1-ELP-PK)	B05 mice	Intraperitoneal/intranasal	Decreased intranucelar inclusions, improved PC morphology
Hourez et al., 2011	3,4-diaminopyridine	B05 mice	Subcutaneous injection	Normalized PC firing rate, reduced PC atrophy, improved motor function
Hearst et al., 2014b	Focused Laser Light Hyperthermia	B05 mice	Cerebellar	Hsp70 production, suppressed PC loss, improved motor function
Watase et al., 2002	Lithium	154Q/2Q	Dietary	Improved motor coordination, learning, and memory. Increased Dendritic branching in hippocampal pyramidal neurons
Perroud et al., 2013	Lithium	154/2Q	Dietary	Increased metabolic processes, specifically higher purine levels
Iizuka et al., 2015	Memantine	154Q/2Q	Dietary	Attenuated PC loss and vagus motor neuron loss. Extended life span and reduced weight loss

	Mouse model	Type of stem cells	Route	Histology results	Functional results
Chen et al., 2011	SCA1 154Q/2Q mice	BMDC (genetically modified using AAV7 to carry SCA 1 modifier genes)	Right retro-orbital sinus injection	Diminished nuclear inclusions, increased number of surviving PC	Not assessed
Chintawar et al., 2009	B05 transgenic mice	Subventricular zone derived NPCs	Stereotactic cerebellar white matter microinjection	Thicker molecular layer. Diminished PC loss	Improved motor skills Normalized behavior
Matsuura et al., 2014	B05 transgenic mice	Bone marrow derived MSC	Intrathecal injections	Suppression of PC dendrites atrophy Thicker molecular layer	Improved motor coordination

	Treatment/vector	Animal model	Route	Outcome
Keiser et al., 2013	(1) miRNA/AAV serotype 2/1 (2) Atxn1 Like/AAV serotype 2/1	B05 mice	DCN injection	Widespread PC transduction Improved histology and behavioral profiles
Xia et al., 2004	siRNA/AAV2	B05 mice	Direct injection into the cerebellar lobules	Cerebellar morphology restoration, PC inclusions resolution, improved motor coordination
Keiser et al., 2014	RNAi/AAV serotype 2/5	SCA1 154Q/2Q knock-in mice	Deep cerebellar nuclei (DCN)	Preserved neurohistology and rotarod performance
Venkatraman et al., 2014	HDAC 3 depletion	(1) PC-specific HDAC3 null knock-in mice (2) SCA1 154Q/2Q mice (heterozygous HDAC3+/− mice)	N/A	(1) No improvement in cognitive and cerebellar function (2) Deleterious effects both behaviorally and histologically

Table 4: Overview of pharmacological, stem cell, and gene therapy of SCA1, Source: (Wagner et al., 2016)

2.3.5 Animal models of SCA1

Animal models are employed in the study of human disease because of their similarity to humans in terms of genetics, anatomy, and physiology.

An important approach to understanding spinocerebellar ataxia (SCA) pathogenesis has been to model disease features in mice. According to the Centers for Disease Control and Prevention (CDC), the protein-coding regions of the mouse and human genomes are 85 percent identical on average. SCA1 is an adult-onset neurodegenerative disease from 40 years that progresses very slowly, this issue can be resolved in the short lifespan of a mouse, which is typically 2 years. The approaches used are for example knock-in strategies to insert an expanded pPolyQ-encoding region into the mouse gene with its endogenous transcriptional regulator elements or transgenic strategies using vectors capable of carrying an entire human gene, including its regulatory elements. Thus, the resulting model is arguably more genetically precise because it reflects the molecular genetic features of the human disease. (Paulson et al., 2017).

There are numerous transgenic animals generated over the years to recapitulate the disease, from Drosophila to mice. Fly transgenic lines expressing either SCA1-30Q (the wild-type human isoform) or SCA1-82Q (an expanded isoform) were generated ((Fernandez-Funez et al., 2000).According to this model, a certain percentage of even the normal protein is prone to misfolding (Fernandez Funez et al., 2000; Chen et al., 2003).

One of the most fruitful approaches to studying polyglutamine diseases has been to generate transgenic mouse models expressing truncated or full-length cDNAs encoding the mutant protein in neurons (review; Lin et al., 1999; Gusella and MacDonald, 2000). Most of these transgenic mice overexpress the mutant protein under either neuron-specific or ubiquitous promoters, which is enough to reproduce various aspects of the human neurological phenotypes, including aggregate formation in neurons. To study the effect of mutant ataxin-1 expression under the control of its endogenous promoter, a knock-in model was generated by inserting an expanded CAG trinucleotide repeat into the mouse Atxn1 locus. The original model, Sca 78Q/2Q, expressed endogenous levels of expanded ataxin-1 in the expected temporal and spatial patterns. However, the mice lacked any ataxic phenotype or neuropathological abnormalities(Lorenzetti, 2000).

Burright et al. (1995) generated B05 transgenic mouse model (B05) (**Figure 6**) in which the human SCA 1 cDNA was modified to contain 82 CAG repeats and expressed under the control of the Purkinje

cell protein 2 (pcp2). The 5' regulatory sequences of pcp2 are sufficient to restrict transgene expression to PCs (Oberdick et al., 1990; Vandaele et al., 1991). It expresses a full-length mutant ataxin-1 mRNA with 82 (82Q) at around 50–100 times endogenous levels only in the PCs after postnatal day (P)10 that develops the ataxia symptoms similarly to human SCA1. B05 transgenic mice overexpress polyQ ATXN1, which leads to the loss of PCs from the cerebellum and thus present the neurological phenotype of ataxia.

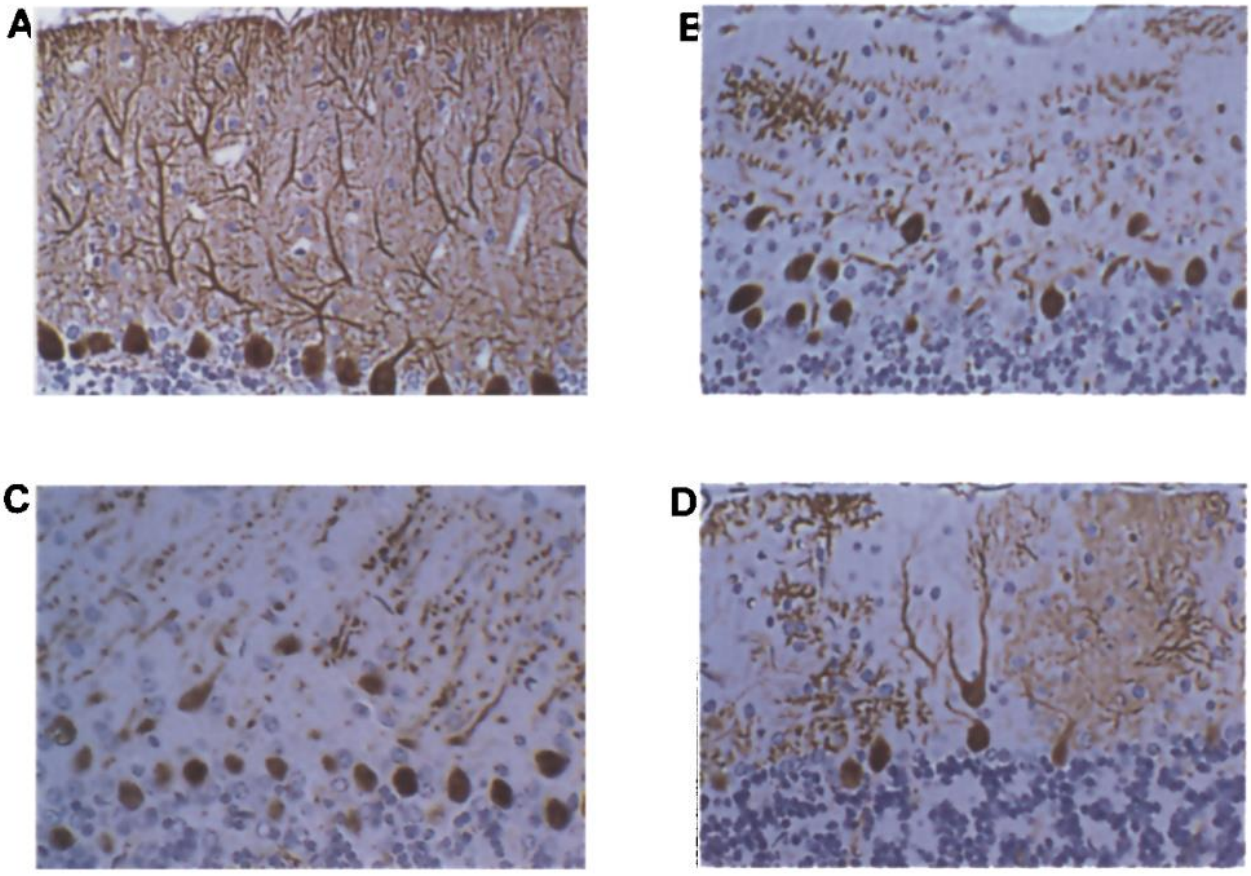

Figure 6: Immunohistochemical Staining for Calbindin to Illustrate Purkinje Cell Morphology

A. Nontransgenic animal at 17 weeks of age displaying the normal appearance of the cerebellar cortex. B. B04 transgenic mouse at 17 weeks of age with ectopic Purkinje cells and disorganization of the Purkinje cell layer.C. B05 transgenic mouse at 16 weeks of age with changes similar to those described in (B). D. B06 transgenic mouse at 26 weeks of age with ectopic Purkinje cells and some Purkinje cell loss is seen focally in Iobule IX. (Magnification, 165 x), Source: (Burright et al., 1995).

For the examination of the role of the aggregates and cellular localization in SCA1, two additional transgenic models were developed. Using the SCA1[82Q] transgene, a lysine- to-threonine

substitution at amino acid residue 772 disrupted the nuclear localization signal (NLS) function. A second model, Ataxin-1 was developed by deleting the self-association region of ataxin-1. SCA1K772T transgenic animals express ataxin-1 primarily in the cytoplasm of PCs in contrast to control SCA1[82Q] mice that expressed significant levels in both the cytoplasm and nucleus. Importantly, SCA1K772T mice did not develop ataxia, as measured by rotating-rod deficits or ataxic cage behaviour and no cerebellar pathology was found (Ingram et al., 2012; Lorenzetti, 2000).

To faithfully recreate the features of the human neurodegenerative disease spinocerebellar ataxia type 1, 154 CAG repeats were targeted within exon 8 of the targeted endogenous mouse locus. The knock-in Sca1 $^{154Q/2Q}$ mice (**Figure 7**) develop progressive neurological deficits that resembles human SCA1, featuring motor incoordination. However, the role of repeats in pathogenesis remains unclear, and many cognitive deficits, muscle wasting, and premature death, with Purkinje cell loss and age-related hippocampal synaptic dysfunction (Watase et al., 2002). Moreover, mutant ataxin-1 solubility decreased as the mice aged so the aggregates did not form until the advanced stage of the disease making it a reliable preclinical model (Watase et al., 2002).

In general, the two important mouse models are summarized in the table below (**Table 5)**.

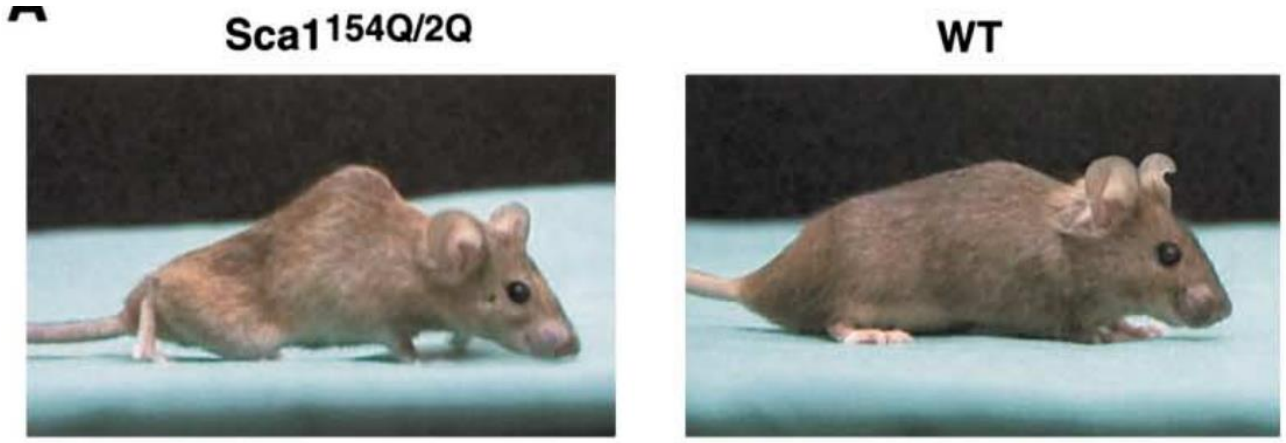

Figure 7: The phenotype of Sca1$^{154Q/2Q}$ Mice representing, 28-week-old Sca1$^{154Q/2Q}$ mice and their wild-type littermates, Source: (Watase et al.,2002).

	B05 transgenic mice (B05)	*Sca1 154Q/2Q* mice (154Q/2Q)
Phenotype	Motor incoordination, ataxia (12 weeks), no cognitive impairment	motor incoordination, muscle wasting, cognitive impairment, memory deficits
Physical Onset	5 weeks	7–8 weeks
Course of the disease	Normal life span	Premature, 35–45 weeks
Neuropathology	PC loss, Bergmann glial proliferation, shrinkage and gliosis of molecular layer	Reduced dendritic arborization of PCs (early stage)
		Neuronal intranuclear inclusions and PC loss (advanced disease)
	Purkinje neuron dendritic and somatic atrophy	Hypocampal synaptic dysfunction but no significant loss
Mechanism	Overexpression of polyQ-ATXN1 (82 CAG repeats) under the control of Purkinje Cell pcp2 promoter	Expanded repeat of 154 CAGs was inserted into the mouse Sca 1 locus (knock-in)
References	Burright et al., 1995; Clark et al., 1997	Watase et al., 2002

Table 5: Overview of mouse models for SCA 1, Source: (Wagner et al., 2016).

2.4 The Cerebellum

The central nervous system of the vertebrate comprises the brain and the spinal cord. The brain is further divided into cerebrum, cerebellum, and brainstem. The cerebellum represents 10% of the brain size (Purves D et al., 2001). The **cerebellum** ("little brain") is a structure that is located at the back of the brain, underlying the occipital and temporal lobes of the cerebral cortex (Knierim, 2020). It consists of two hemispheres connected by the vermis which holds more than half of the total neurons found in the brain (Knierim, 2020). Classically, thought to control movement coordination (Flourens 1824; Luicani 1891) and motor learning but recent experimental evidence suggests that the cerebellum also has a key role in cognition and emotions (Schmahmann, 2004; Schmahmann and Caplan,2006; Ito 2008; D'Angelo & Casali, 2013).

2.4.1 Cerebellar circuit

Anatomically, cerebellar neurons with distinct cytological and neurochemical properties reside in specific layers and sites of the cerebellum. They are connected with each other and also with specific brain regions outside the cerebellum forming a dense network known as the cerebellar circuit as depicted in **Figure 8**. The cerebellum consists of the cortex and the centrally located deep cerebellar nuclei (DCN) connected by the white matter tract.

The major source of excitation is the subthalamic nucleus within the basal ganglia, which projects directly to the pontine nuclei, providing a pathway for basal ganglia circuits to deliver reward-related information to the cerebellar cortex via the mossy fibers (MF) (Bostan et al., 2010). Afferent inputs

to the inferior olive from the forebrain also arise from a variety of sources including direct projections from the neocortex as well as signals relayed via the meso-diencephalic junction (De Zeeuw et al., 1998; Garden et al., 2017; Ten Brinke et al., 2019; Wang et al., 2021) and then to the climbing fibers in the cerebellar cortex. The cerebellar cortex exhibits a characteristic trilaminar structure composed of the Molecular Cell layer (ML), Purkinje cell layer (PCL), and Granular layer (GL) described below (Binda et al., 2020).

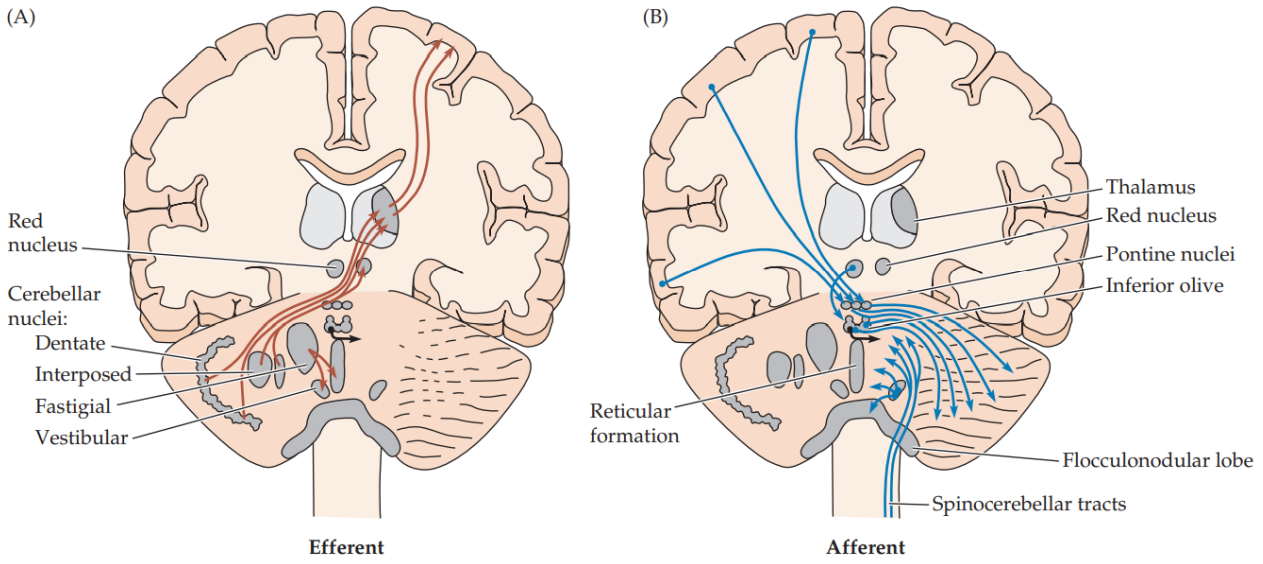

Figure 8: Efferent and Afferent Pathways of the Cerebellum shown in relation to the underlying nuclei, cerebral hemispheres, brainstem and spinal cord. (A) Outputs from the cerebellum (red) are through the dentate, interposed, and fastigial nuclei. Fibers from the dentate nucleus supply the contralateral motor cortex through the ventrolateral nuclei and parts of the ventro posterolateral nuclei of the thalamus. The interposed nuclei project to the contralateral red nucleus. The fastigial nucleus projects to the vestibular nucleus and the pontine and medullary reticular formations, contributing to the medial motor system.

(B) Inputs (blue) to the lateral hemispheres of the cerebellum are from wide areas of the cerebral cortex, through the pontine nuclei. Afferent input from the red nucleus is relayed through the inferior olive. More medially, the cerebellum receives extensive input from the spinocerebellar tracts. The flocculonodular lobe is supplied by the vestibular nucleus, Source : (Nicholls J G. et al.,2011).

2.4.1.1 The cerebellar cortex

The cerebellar cortex consists of only seven types of neurons, Purkinje cells (PC), Granular cells (GC), basket cell (BC), stellate cell (SC), Golgi cell, Lugaro cell (LC), and unipolar brush cell (UBC). The cerebellar cortex is the most superficial structure and is organized into three layers, molecular cell layer (ML), Purkinje Cell layer(PCL) and granular cell layer (GCL).

(i) Molecular Cell Layer (ML)

The ML accommodates the complex and ramified dendritic tree of PCs together with two types of GABAergic interneurons: BCs, that inhibit through synapse onto PC soma. Also, BC inhibits the initial axonal segment of PC forming a characteristic structure known as pinceau (Ango et al., 2004; Blot and Barbour, 2014). SCs innervate PC dendrites. MLIs receive two distinct glutamatergic excitatory inputs, climbing fibers (CFs) and parallel fibers (PFs) (Palay and Chan-Palay, 1974). They provide feed-forward inhibition, which modulates PC spike output (Mittmann et al., 2005; Brown et al., 2019), calcium influx, and long-term plasticity (Binda et al., 2016). These two afferent fibers are explained below in detail.

- **Climbing fibers (CF)**

The CF forms hundreds of synapses through twist around the proximal dendritic compartment of the PC. Activation of CFs causes strong depolarization of PC dendrites. It triggers "Ca^{2+} spikes" due to the activation of voltage-dependent Ca^{2+} channels (VDCCs) in PC dendrites (Miyakawa et al., 1992), and generates characteristic "complex spikes" in the PC soma (Eccles et al., 1966). Each complex spike is composed of a fast somatic Na^{+} action potential followed by slow dendritic Ca^{2+} spikes. They also predictive signals carry sensory/motor error signals along with predictive signals (Ohmae and Medina, 2015; Heffley et al., 2018; Kostadinov et al., 2019; Larry et al., 2019).

Parallel Fibers (PF)

The MFs originate from several pre-cerebellar nuclei in the brainstem and spinal cord. They carry motor, sensory, vestibular, and proprioceptive information passed by the GCs. They form PFs through bifurcation of axons. They excite PC by exciting granule cells which ascend to the molecule layer forming PF (Ito et al., 1982).

(ii) Purkinje cell layer (PCL)

The main cells of PCL are the PCs, the represent the only output of the cerebellar cortex. PCs extend well-arborized dendrites in the molecular layer and project g-aminobutyric acid (GABA)ergic axons to the DCN and vestibular nuclei (Binda et a.l,2020). PC receive two main excitatory input, parallel and climbing fibers. The simultaneous activation of CF and PFs leads to long-term depression at the PF to PC synapses (Ito et al., 1982).

Each PC receives up to 105–106 excitatory PF synaptic contacts, however, one PF makes only one to two synapses onto a single PC (Napper and Harvey, 1988). PF activity induces simple spike discharge in PCs; the dendritic trees of the PC overlap with the PF forming synapses at 90 degrees with simple spikes in regular intervals. Each climbing fiber wraps the dendrites of the PC forming hundreds of synapses causing a broad atypical spike followed by a silent phase known as simple spikes. The PCL also include the small pear-shaped soma of Candelabrum cells (CaCs) which have one or two long dendrites that enter the ML, and several short dendrites localized below the GCL (Laine and Axelrad, 1994).

(iii) Granule cell layer (GCL):

It is the deepest cerebellar layer with white matter underneath comprising cell bodies of the excitatory granule cells, inhibitory Golgi neurons, LCs and the glutamatergic interneurons UBC. GCL are densely packed, small neurons that account for the huge majority of neurons in the cerebellum. Moreover, more than half of the neurons in the entire brain are represented by the cerebellar granule cells. These cells receive input from mossy fibers and project to the Purkinje cells through extensions of its axons to forms the PFs into the molecular layer (ML) (Knierim, 2020).

2.4.1.2 The Deep Cerebellar Nuclei:

The DCN can be divided in 3 anatomical parts: the medial (fastigial), interpositus (globose and emboliform), and lateral (dentate) nuclei, each of which is connected topographically with the vermis, paravermis, and hemisphere, respectively (Binda et al., 2020).The deep cerebellar nuclei receive an excitatory signal from the climbing and mossy fibers. The only inhibitory signal the DCN receives is from the cerebellar cortex via PC. The DCN also engage with other elements of the basal ganglia: the dentate nucleus (DN) has a disynaptic connection with the striatum (Hoshi et al., 2005; Ichinohe et al., 2000). Cerebellar output also influences cortical reward circuits via the dense reciprocal connectivity with the prefrontal cortex (Kelly and Strick, 2003; Middleton and Strick, 1994,

2001), via thalamic relays. The output of the DCN is primarily to the thalamus and then to the premotor cortex and motor cortex altering motor coordination. Thus, the overall circuit completes from the motor cortex and spinal cord (Inferior olivary nucleus) then to the cerebellum(mossy/climbing-PC)-thalamus-and again motor cortex.

In summary, there is evidence both for direct connections between cerebellar circuits and midbrain dopaminergic neurons (Carta et al., 2019; Fallon et al., 1984; Watabe-Uchida et al., 2012). These pathways as illustrated in **Figure 9**, therefore, provide opportunities for the reward system to directly influence cerebellar function, as well as for higher-level processing to manipulate reward signals before transmission to the cerebellum.

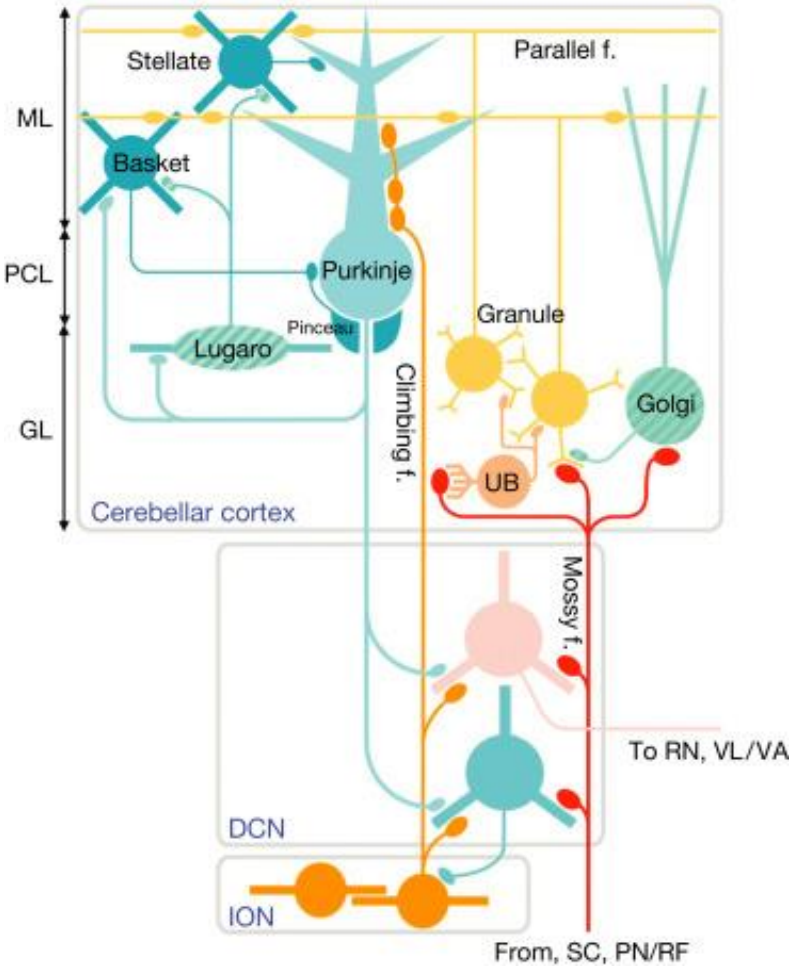

Figure 9: Neuronal circuit of the cerebellum. Neurons painted with warm colors (yellow, orange, and pink) represent excitatory neurons, while those with cold colours (blue, light blue, and green) represent inhibitory neurons. DCN, deep cerebellar nuclei; GL, granular layer; ION, inferior olivary nucleus; ML, molecular layer; PCL, Purkinje cell layer; UB, unipolar brush cell, spinal cord SC, Source: (Kano & Watanabe, 2020).

2.4.2 Interneurons of the cerebellar circuit

The interneurons in the cerebellar circuit are classified based on multiple factors such as morphology and location (**Figure 10**). They are divided into excitatory (Glutamatergic) interneurons: GC and UBC and inhibitory (GABAergic) interneurons: BC, SC, GoCs, and LC (Barmack & Yakhnitsa, 2008). GC are the smallest interneurons; smaller than six micrometers found in the GCL (Barmack & Yakhnitsa, 2008). The feature of these interneurons is their activation by serotonin, which induces firing in an otherwise silent cell (Dieudonne and Dumoulin, 2000; Dumoulin et al., 2001). The interneurons involved in the cerebellar circuit are found in the molecular and the granular layer, described below.

- The molecular layer incorporates GABAergic inhibitory synapses from the basket and stellate cells are targeted to the PC soma and dendrites, respectively. The GABAA receptors appear to be crucial for activity-dependent regulation of the density of inhibitory synapses on PCs(Kano & Watanabe, 2020).
- GC receive input from the mossy fibers. These are the afferent branches of the pontocerebellar tract forming glomerulus together. Axons of GC form parallel fibers. Many granule cells are in contact with one PC.
- GoCs are inhibitory interneurons. Each GoC receives the signal from the granule cells but in turn, innervates the granule cells via feed-forward and feedback inhibitory loops (Kanichay and Silver, 2008).
- LCs have spindle-shaped cell bodies (Laine and Axelrad, 1996) and they innervate the MLIs (Laine and Axelrad, 1998), GoCs (Dieudonne and Dumoulin, 2000; Dumoulin et al., 2001), and PCs (Dean et al., 2003).
- UBCs are the glutamatergic interneurons, that establish excitatory inputs onto GCs and on other UBCs (Nunzi et al., 2001). They mainly receive excitatory inputs from a single MF carrying vestibular information and are particularly enriched in the posterior cerebellum and flocculus (Rossi et al., 1995). UBCs also receive inhibitory synaptic inputs from GoC (Dugue et al., 2005).

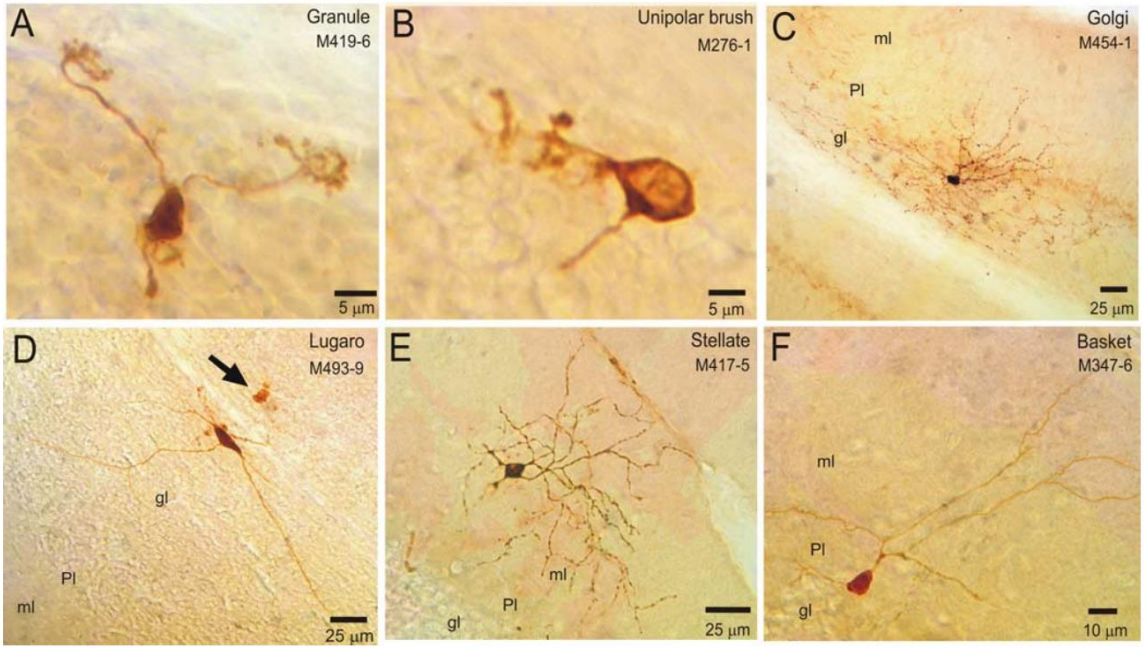

Figure 10 : Six interneurons, A, Granule cell (GC). B, Unipolar brush cell (UBC). C, Golgi cell(GoC). D, Lugaro cell (LC). E, Stellate cell (SC). F, Basket cell (BC). G, Granule cell layer(GCL); Molecular layer (ML); Pl, Purkinje cell layer(PCL), Source: (Barmack & Yakhnitsa, 2008).

2.5 Cerebellar circuit dysfunction

The cerebellar circuitry contributes to of execution of movements, motor learning, and motor behaviour prediction.

Mutations linked to SCA directly or indirectly affect not only the PC activity but also, calcium dynamics, and dendrite development within the cerebellar circuit. This has resulted in an alteration to cerebellar compartmentation, wiring, and efferent organization (**Figure 11**). The profound changes in PC neurophysiology precede PC loss and are likely to lead to cerebellar circuit dysfunction that explains behavioural signs of ataxia characteristic of the disease observed in various transgenic models that recapitulate human SCA1 (Meera et al., 2016).

Kasumu and Bezprozvanny (Kasumu and Bezprozvanny, 2012) described the dysfunction of PC and cerebellar circuitry as the eliciting hallmark of pathogenic mechanisms across SCA diseases. The resulting loss was more than 75% of the total Purkinje cell population in SCA2 (Kasumu and Bezprozvanny, 2012). The underlying cause of PC neurodegeneration is still not understood. It was hypothesized due to increased susceptibility to genetic or functional insults than makes PCs more vulnerable compared to other neuronal cell types (Hekman and Gomez, 2015).

Healthy Purkinje cells display autonomous pacemaker activity. The firing occurs without synaptic input and also with very little variability between spiking intervals (Heiney et al., 2014; Meera et al., 2016; Paulson et al., 2017; Huang and Verbeek, 2019,Tanaka-Yamamoto et al., 2020). PC firing defects in SCA mouse models have also shown that the expression of the mutant ATXN1 in SCA1 PCs, might impaired PCs pacemaker firing (Hansen et al., 2011; Dell'Orco et al., 2015). The increase in PC firing variability in the SCA2 mouse model was also found to be responsible for the expression of PC degeneration (Kasumu et al., 2012). Furthermore, the PolyQ expansion alters Cav2.1 physiology via decreased channel expression in PCs, reducing P/Q type calcium channel-mediated currents in SCA6 knock-in mice model (Watase et al., 2008).

Another early pathophysiological mechanism in SCAs cerebellar circuit is the altered metabotropic glutamate receptor (mGluR) signalling and disrupted calcium homeostasis in PCs. Together these findings indicate that aberrant calcium signalling and profound changes in PC neurophysiology precede PC loss and are likely to lead to cerebellar circuit dysfunction that explains behavioural signs of ataxia characteristic of the disease (Meera et al., 2016).

The major cerebellar circuit damages are described under the following subheadings.

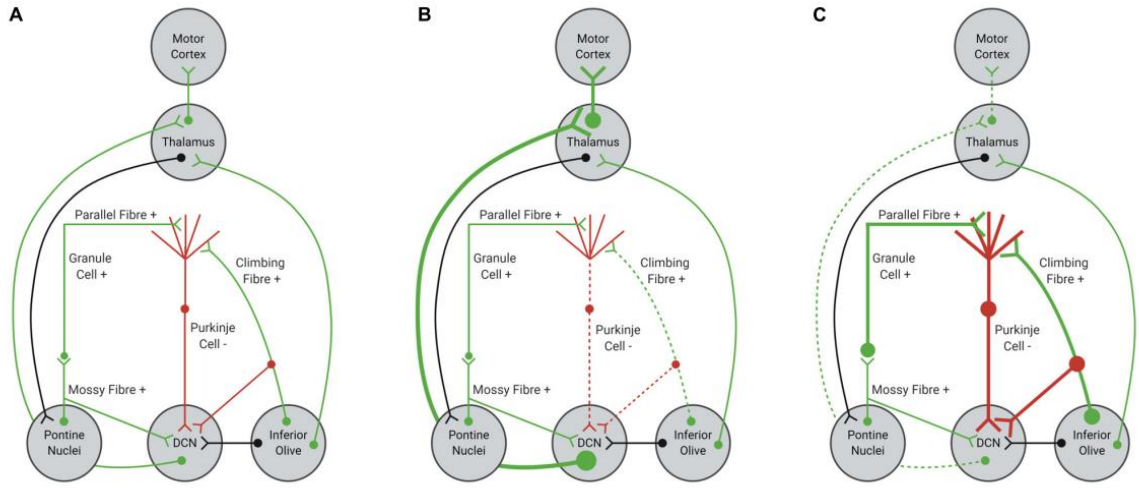

Figure 11: Schematic representation of cerebellar afferents and efferents where excitatory inputs are highlighted in green, with inhibitory inputs highlighted in red. Black inputs are both, inhibitory or excitatory. (A) The normal function of Purkinje cells shown by balanced excitation and inhibition in cerebellar circuitry. (B) Reduced excitatory input from glutamatergic climbing fibers, decreasing Purkinje cell firing, that results in lack of inhibition of the DCN-thalamus-motor cortex circuit. (C)

Increased excitatory input from parallel and climbing fibers, increasing Purkinje cell firing, that results in inhibition of the DCN-thalamus-motor cortex circuit (Source: Robinson et al . 2020).

2.5.1 Impairments in the cerebellar excitatory system

PCs are GABAergic neurons that directly contact the DCN and the only output to the cerebellar cortex. If the firing of Purkinje cells is impaired or dysfunctional, DCN neurons could not be inhibited, increasing excitatory tone within the cerebellum as shown in Figure 11 (B)(Meera et al., 2016).

Analysis of the process of CF synapse elimination during cerebellar development is one of the main reasons for defects in CF wiring and function in SCA1.The CF mono-innervation on PCs requires extensive removal of other synapses. CF polyinnervation in young adult PCs and the impaired somatic CF synapse had been identified in SCA1 (Ebner et al., 2013).

PC fire at approximately 40 Hz(50-100Hz) with striking, almost metronomic regularity (Raman & Bean, 1999). The synaptic transmission through impaired climbing fibers can lead to impairment in the PCs functionality, impacting crucial pathways for neuronal survival and physiological metabolism (Ruegsegger et al., 2016). It was found that mice lacking mGluR1 or any of its downstream effectors such as PKCγ and PLC-β4 show signs of defective CF synapse elimination (Binda et al., 2020; K. Hashimoto et al., 2000; Kano et al., 1995). When the regular PC firing is degraded in at least six mouse models of SCA2 and in a number of other non-SCA-related transgenic mouse models, they exhibited behavioural ataxia. In a PC-specific, human transgene model of SCA2 (pcp2- Atxn2127Q), the severity of behavioural ataxia is linked to the reduction of PC firing rates over an 8-month time course of disease progression (Hansen et al. 2013).

Decreased inhibition of DCN neurons because of PC degeneration, would result in increased excitatory input from the DCN to cortical motor centers, causing impairments in motor performance (Meera et al., 2016). Thus, reduced excitatory input from glutamatergic climbing fibers, due to shortened length or impaired functionality, can decrease Purkinje cell firing, resulting in lack of inhibition of the DCN-thalamus-motor cortex circuit.

2.5.2 Impairments in the cerebellar inhibitory system

PCs are inhibitory projection neurons (Ito, 1984) and they are spontaneously active at unusually high firing rates in vivo (50 –100 Hz; Thach, 1968). It was also suggested early on that PCs could exert control by transiently reducing their firing rate (i.e., generating a brief "pause") and activating motor areas via disinhibition of the DCN (Ito et al, 2001).

Furthermore, in vivo recordings have shown that the high spontaneous activity of PCs is occasionally interrupted by a brief pause, which are in coordination with nearby cells (De Zeeuw et al., 2011). Although the "disinhibition hypothesis" provides the foundation for many current models of cerebellar function (Houk et al., 1996; Medina and Mauk, 2000), it has not been possible to establish a link between suppression of PC firing, disinhibition of DCN neurons, and the movement coordination as there was no way to inactivate PCs precisely and selectively on behaviorally relevant timescales in vivo. The optogenetic strategy performed by Heiny et al. 2014, reviewed to inhibit PCs while simultaneously examining the PCs demonstrates that the amount, duration, and spatial extent of PC firing suppression can be used as an effective control. These signals can be used to correlate the timing and kinematic properties of motor output via graded disinhibition of neurons in the DCN (Heiney et al., 2014).

Though the involvement of altered glutamatergic transmission in SCAs is well illustrated than the role of GABAergic transmission in SCAs, research conducted in the past with inhibitory signals by GABA transporter 1 (GAT1) KO mouse (Chiu et al., 2005) and the vesicular GABA transporter (VGAT) KO mouse (Kayakabe et al., 2013) display an ataxic gait and poor motor coordination (Binda et al.,2020). In addition to this, the AxJ cerebellar ataxia mouse model also had high levels of PCs expressing the ionotropic GABAA receptor (GABAAR) and enlarged IPSCs (Lappe-Siefke et al., 2009).

These findings therefore support a possible role of GABAergic transmission in ataxia onset and in disease progression. There is a strong correlation between the PC loss and BC plexus density. This was demonstrated in a study by Lee et al. 2018, where they quantified empty baskets across a spectrum of cerebellar degenerative disorders characterized by variable degrees of PC loss (SCA types 1, 2,and 6).The marked loss of PC drew conclusion that they are all part of the same pathophysiological cascade (Lee et al., 2018). The percentage of empty baskets in SCA types 1, 2, and 6 were 1.8, 2.3, and 2.6 times that of controls, respectively (Rüb et al., 2013). The neurodegenerative processes of these SCA types cause a marked and widespread neuronal loss in

the cerebellar PC layer, while at the same time there was a maintaince of the inhibitory connectivity coming from the MLIs (Rüb et al., 2013).

Moreover, Edakamanti et al.2018, demonstrated increased basket cell plexus density in both human SCA1 subjects and disease mouse model, supporting a pathogenic role for increased GABAergic inhibition in disrupting PC function. Indeed, postmortem analysis of brain tissue from SCA1 patients revealed a prominent increase in the BC to PC synapses (Edamakanti et al., 2018). As per study by Edamakanti et al., in both knock in and transgenic models of SCA1, defects in PC synaptic connectivity precede ataxia, and gene expression changes appear within the first few weeks of life. In addition to this, SCA1 model mice in the fifth postnatal weeks have shown the number of BC exceeds that of physiological conditions while the number of synapses on PC formed by CF decreases, eventually leading to PC degeneration at six months of age (Edamakanti et al., 2018).

2.5.3 Calcium Dysregulation and Synaptic Deficits in SCA1

The homeostatic control of intracellular calcium release is an important function for cellular activity. Ca^{2+} can act as an intracellular messenger initiating other processes such as synaptic neurotransmission and transcriptional regulation (Berridge and Irvine, 1984; Taylor and Traynor, 1995).

There are two specific mechanisms by which Purkinje cells manage supraphysiological calcium levels; calcium-binding proteins and mitochondrial uptake of excess Ca^{2+} (Llano et al., 1994). Generally, the excess of intracellular Ca^{2+} can be buffered by calcium-binding proteins such as calbindin and parvalbumin (Llano et al., 1994; Bastianelli, 2003). The calcium-binding proteins (CaBP) are found exclusively within GABAergic interneurons. It has been proposed that CaBP consist of two groups: those regulating calcium concentration and the calcium-modulated proteins (Yáñez et al., 2012). CaBP such as calbindin is expressed within Purkinje cells, while parvalbumin is expressed within PC, BC, SC, and GoC (Bastianelli, 2003). It is hypothesized that the relatively high expression levels of calcium-binding proteins within PC may accommodate large Ca^{2+} influxes resulting from repetitive neuronal spiking and the increased metabolic load of PC (Bushart et al., 2016). The important neuroprotective role of endogenous calcium-binding proteins is highlighted in transgenic calbindin knockout mice, which present with mild ataxic symptoms and impaired PC physiology (Airaksinen et al., 1997; Bastianelli, 2003; Kasumu and Bezprozvanny, 2012; Bushart et al., 2016).

Under normal conditions, due to homeostasis, increase in intracellular Ca^{2+} are well tolerated, however more prolonged increases can be harmful (Kasumu and Bezprozvanny, 2012). When there is excessive intracellular calcium, it can induce toxicity and decrease neuronal cell survival (Kasumu and Bezprozvanny, 2012). The dysregulation of this homeostasis mechanism is commonly prevalent and disrupted in transgenic animal models and human SCA1 patients (Kasumu and Bezprozvanny, 2012; Vig et al., 2012; Bushart et al., 2016; König et al., 2016; Prestori et al., 2019). Furthermore, knockout of both calbindin and parvalbumin in ataxin-1- expressing mice resulted in severe ataxia and altered Purkinje cell morphology with altered phenotype (Vig et al., 2012). Moreover, some excess Ca^{2+} is stored by PC mitochondria (Kasumu and Bezprozvanny, 2012).

Increased Ca^{2+} influx triggers activation of the PKC signaling pathway (Berridge and Irvine, 1984). Batchelor and Garthwaite (1997) showed that increased intracellular Ca^{2+} results in the potentiation of Metabotropic glutamate receptor 1 (mGluR)-mediated signals. Activation of mGluRs via binding with glutamate, activates a signalling cascade, ending with the release of Ca^{2+} from the endoplasmic reticulum via activation of IP3R1. This initial release of Ca^{2+} into the cytosol can be further amplified via the activation of ryanodine receptors (RyanR), an intracellular Ca^{2+} release channel (Berridge and Irvine, 1984; Llano et al., 1994; Taylor and Traynor, 1995). In addition to this, endoplasmic reticulum calcium stores decrease. Therefore, any imbalance in calcium signalling may initiate cellular processes, that leads to cerebellar PC death (Kasumu and Bezprozvanny, 2012; Matilla-Dueñas et al., 2014; Bushart et al., 2016; Hisatsune et al., 2018; Prestori et al., 2019). The central role for mGluR dysregulation in cerebellar ataxia is supported by abundant evidence from mouse and human genetics, implicating each of the signalling proteins in the cascade from mGluR1 to the IP3R as shown in **Figure 12** (Robinson et al., 2020).

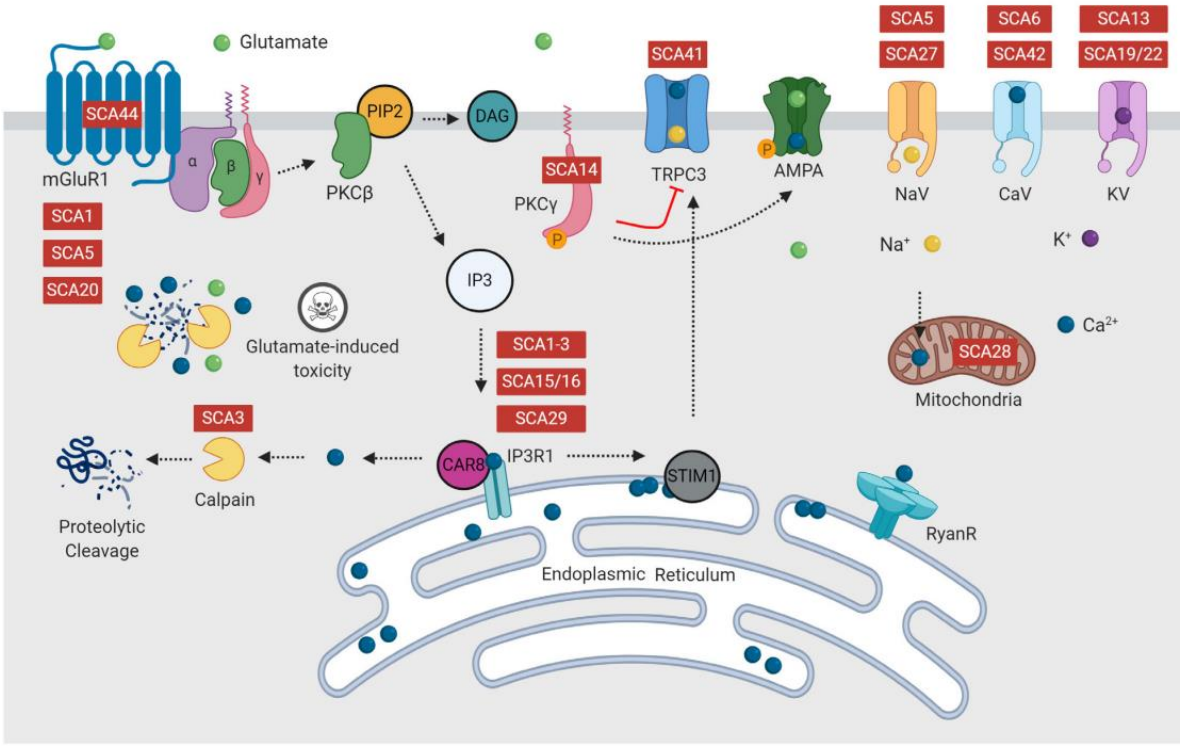

Figure 12: Different forms of Spinocerebellar ataxias attributed to mutations in intracellular calcium signaling, glutamate release or the PKC pathway, which form multiple positive feedback loops. Diseases indicated in red are reported to have dysfunction of this component of the signaling pathway. Source: (Robinson et al, 2020).

Synapse formation is the key step for neuronal networks. Nascent synapse and subsequent maturation involve the assembly of pre-synaptic and post-synaptic signalling machinery, which is mediated by synaptic cell/adhesion molecules (Yamagata et al., 2020). PC synapses have known to undergo activity-dependent plasticity, which brings changes in Purkinje cell physiology (Smeets and Verbeek, 2016; Bushart et al., 2016; Huang and Verbeek, 2019). Reduced number of climbing fiber-PC synapses in the distal segment of the PC dendritic arbour has been observed in *ATXN1* mice (Barnes et al., 2011), therefore, contributing to dysfunctional PC signalling in SCA1 (Ebner et al., 2013).

The influx of Ca^{2+} into neurons during membrane depolarization is regulated by the voltage-gated calcium channels. Voltage-gated calcium channels can trigger calcium-dependent processes including the release of neurotransmitters, modulate neuronal excitability synaptic plasticity, and gene transcription. High-voltage P/Q-type (Cav2.1), N-type (Cav2.2), and R-type (Cav2.3) channels are considered the primary driver of evoked synaptic transmission (Cain and Snutch, 2011). Cav2.1

channels are functionally more critical to the regulation of spiking properties. They contribute to calcium spikes triggered by increased activity of cerebellar climbing fibers. However, T-type voltage-gated calcium channels (Cav3.1, Cav3.2, and Cav3.3) are known to exhibit a hyperpolarised range of activation and inactivation to regulate neuronal activity (Zamponi et al., 2015; Hashiguchi et al., 2019). Upon membrane depolarization, voltage-gated calcium channels (mainly Cav2.1 and Cav3 family members) also become activated, allowing external calcium entry into Purkinje neurons. PC firing defects have been described in several SCA models such as expression of the mutant ATXN1 in SCA1 PCs. Also, ATXN2 in SCA2 PCs reduced their firing frequency (Hansen et al., 2011; Dell'Orco et al., 2015). This decrease was also associated with an increase in PC firing variability in the SCA2 mouse model (Kasumu et al., 2012). SCA6 is caused by a PolyQ tract expansion in the alternatively spliced exon 47 of the CACNA1A gene encoding for the α1A subunit of Cav2.1 voltage gated calcium channels (Zhuchenko et al., 1997).

These voltage-gated calcium channels are tightly coupled to calcium activated potassium channels (KCa channels), so that the net effect of calcium entry is an outward potassium current, which hyperpolarizes the membrane potential. In addition to this, voltage-gated calcium channels have also been found to functionally interact with large conductance calcium-activated potassium (BK) channels. These channels mainly provide additional modulation of neuronal excitability (Zamponi et al., 2015). In a mouse model of SCA1, disrupted Purkinje neuron membrane excitability is associated with reduced expression and function of two potassium channels, BK and the G-protein coupled inwardly-rectifying potassium (GIRK1) channel. In an early stage of disease, Purkinje neurons from *ATXN1*[82Q] mice show depolarized somatic membrane potential and a reduced fast afterhyperpolarization (AHP) amplitude. This resulted to a large proportion of non-firing cells. As disease progressed, it was found that the dendritic degeneration reduced the size of *ATXN1[*82Q]. Purkinje neurons, thereby increasing the current density of remaining BK and GIRK1 channels to restore spontaneous firing, although at a reduced frequency (Dell'orco et al., 2015).

The role for calcium entry also regulates KCa channel activity. The correlation of the SCA and different channel pathways is highlighted in **Figure 13**. One of the channels is SK channel activators, improve both Purkinje neuron spike regularity and motor performance. Additionally, the spiking of neurons of the deep cerebellar nuclei, which receive input from Purkinje neurons and act as the output of cerebellar motor processing, is also dependent upon KCa activity. This suggests that there is a direct link between ion-channel function, Purkinje neuron spiking, and motor output from the

cerebellum, and that pharmacologic agents which target ion-channel dysfunction may have therapeutic potential(Walter et al., 2006; Bushart & Shakkottai, 2019).

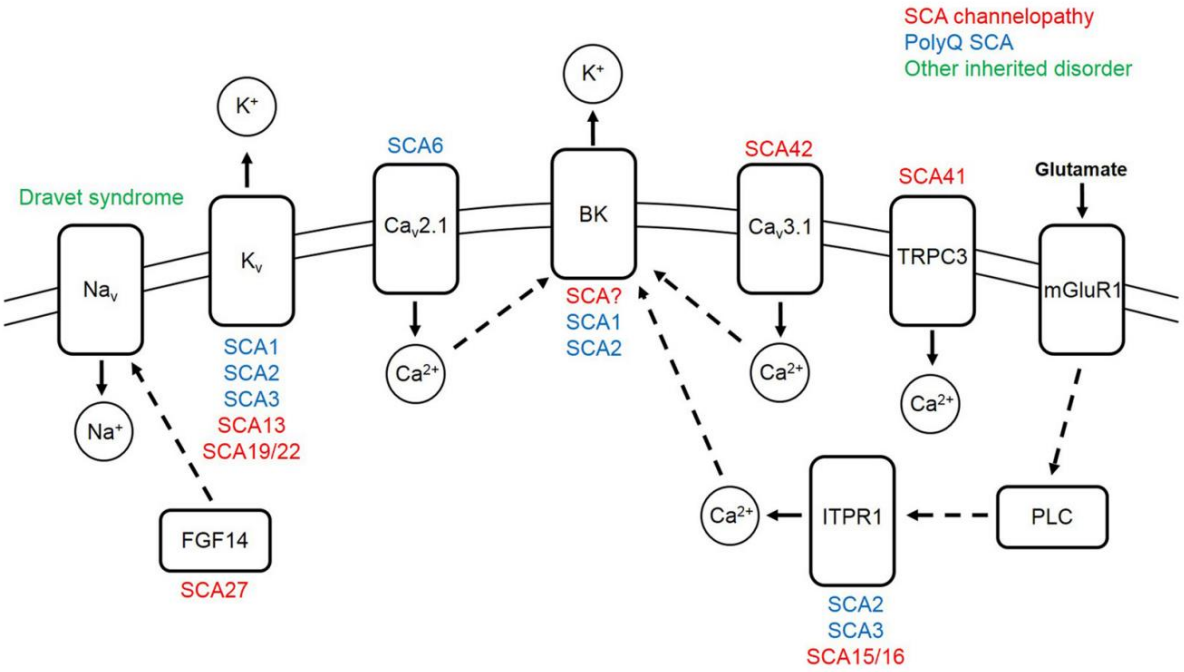

Figure 13: Ion-channel dysfunction is associated with spinocerebellar ataxia in humans and rodent models. Mutations which result in an SCA channelopathy are listed in red. Ion-channel dysfunction in mouse models of polyQ SCA are listed in blue. Dashed arrows signify a protein–protein interaction. Solid arrows signify the direction of ion movement upon channel activation.

Nav, voltage-gated sodium channel; Kv, voltage gated potassium channel; Cav, voltage-gated calcium channel; BK, large conductance calcium-activated potassium channel; TRPC3, transient receptor potential cation channel type 3; mGluR1, metabotropic glutamate receptor type 1; FGF14, fibroblast growth factor 14; ITPR1, inositol 1,4,5 trisphosphate receptor type 1; PLC, phospholipase C; Na+, sodium ion; K+, potassium ion; Ca2+, calcium ion. Source: (Bushart & Shakkottai, 2019).

Molecular pathways responsible for CF strengthening and synaptic refinement are also susceptible to SCA-causing molecules/mutations. Several studies have identified problems in CF to PC synaptic transmission (Smeets and Verbeek, 2016). Moreover, in a study by Ruegsegger et al., the molecular alterations in mutant PCs and the relationship with respect to impaired synaptic inputs and dysfunctional PC excitation in SCA1 was determined. Analysis of synaptic proteins in disease and

susceptible PCs in the *SCA1*$^{154Q/2Q}$ knock-in mice was correlated with that the levels of HOMER3, a synaptic scaffold protein enriched in Purkinje cells according to the proteomic results. These proteins were found to be dramatically reduced at pre symptomatic stages. In contrast, the restoration of Homer-3 alleviated pathology in SCA1 mice models. These finding establishes the vulnerability of the PCs (Ruegsegger et al., 2016).Physiological, morphological, and developmental abnormalities of these synaptic inputs can precede PC degeneration (Duvick et al., 2010; Barnes et al., 2011; Ebner et al., 2013; Ruegsegger et al., 2016). Furthermore, this mechanism of rising calcium overload contributes to degeneration of PC in different forms of SCA (Meera et al., 2016). Hence, it can be concluded that the high metabolic activity, large cell size, and expansive dendritic arbor of Purkinje cells may leave them more susceptible to changes in the cellular environment (Hekman and Gomez, 2015).

2.6 Aims and Objectives

To discover possible therapeutical targets for disease conditions, the target-based research is essential to uncover the early pathological hallmarks (Davis, 2020; Emmerich et al., 2021). Based on the previous study of cerebellar circuit alterations by our group on the excitatory-inhibitory balance within the cerebellar circuit of the *SCA*$^{154Q/2Q}$ mouse model (Ruegsegger et al., 2016), we aim to focus on the molecular layer interneurons (MLIN) as a important players in maintaining the physiological excitatory-inhibitory balance in the cerebellar cortex. To validate this, we use proteomics and immunofluorescence approaches on two different preclinical models of SCA1 disease: the *SCA*$^{154Q/2Q}$ mouse model GABArgic neurons deriving from human induced pluripotent stem cells. We found alteration in synaptic proteins involved in neurotransmitter release such as Synaptotagmin 1 (Synt 1), as well as altered calcium binding proteins such as PV, responsible for maintaining calcium homeostasis in the MLIN. This alteration might potentially alter excitatory inhibitory balance within the cerebellar cortex and causally drive PC degeneration.

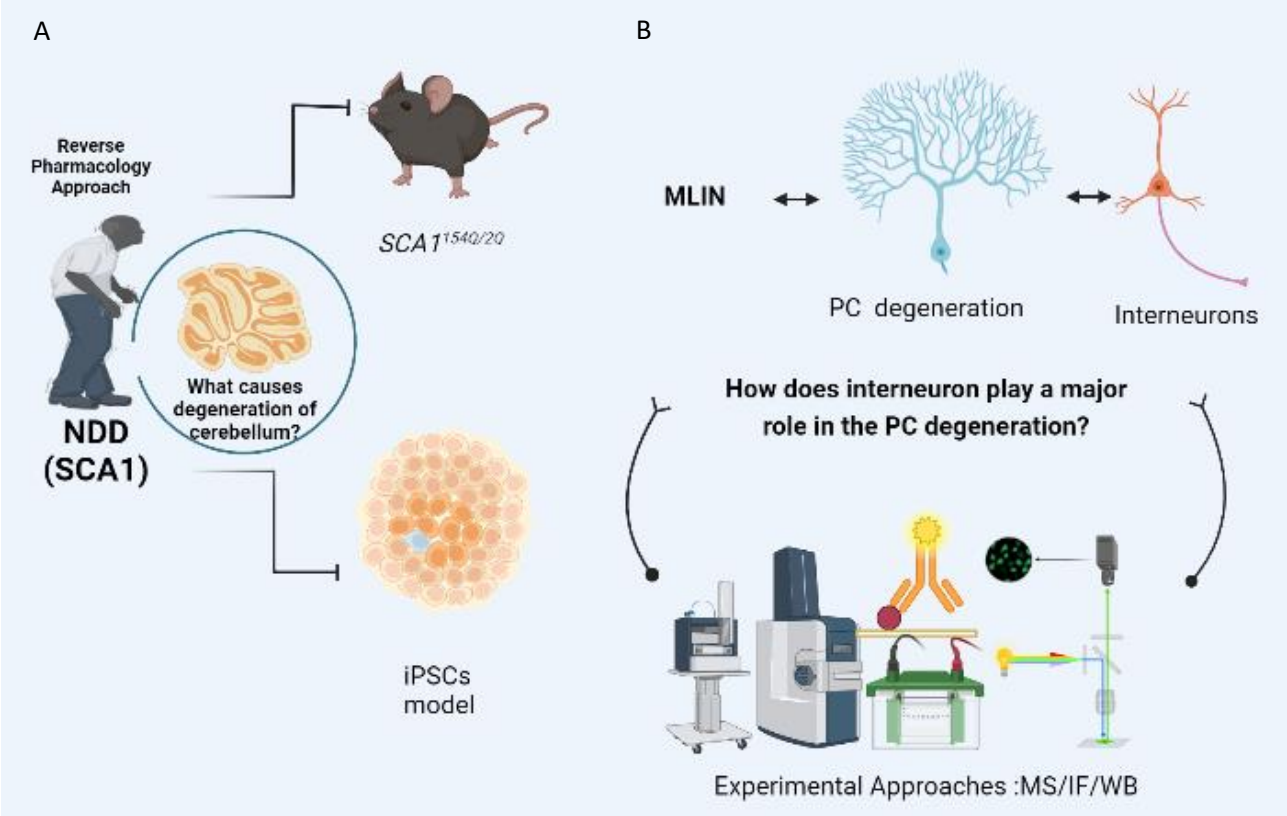

Figure 14: Schematic representation of the Project's aims. A. Animal and iPSc Model used for answering questions of cerebellar atrophy in NDD $S^{CA}1$, B. Establishing role of interneurons in degeneration of PC using different experimental approaches such as MS/IF/WB.

3.RESULTS

3.1 Alteration of PV expression in MLIN and dysregulation in synaptic connectivity in *SCA$^{154Q/2Q}$*

PC are the most vulnerable neurons in SCA1 nevertheless other neurons within the cerebellar cortex might play a role in disease manifestation and contribute to circuit dysfunctions, ultimately leading to PC degeneration (Meera et al., 2016). As previously shown by Edamakanti et al., 2018, molecular layer interneurons (MLIN) are also involved in cerebellar dysfunction in *SCA1*. Therefore, we hypothesize that the MLIN might be more active therefore impacting PC physiology. To this end we investigated PV expression as a marker of neuronal activity in MLINs, from the cerebellar cortex of *WT* and *SCA1$^{154Q/2Q}$* mice through immunofluorescent staining. Our data revealed that PV expression levels were increased in the MLIN of *SCA1$^{154Q/2Q}$* at postnatal days (P) 30, 90, and 200 (Figure 1A-B). Further, there is an increment in the percentage of neurons expressing high levels of PV with the increasing age of *SCA1$^{154Q/2Q}$* mice, therefore directly correlating with pathology development.

The PC are the vulnerable degenerating neurons in SCA1 (Sullivan et al., 2019). It has been shown that *SCA1$^{154Q/2Q}$* animals present PC degeneration, starting from its dendritic arborization (Watase et al., 2002). Therefore, we wanted to investigate if the number of PV-positive interneurons in the molecular layer of the cerebellum also degenerates. Counting the number of positive PV interneurons we found no significant difference in end-stage *SCA 1 $^{154Q/2Q}$* animals (p200) (Figure 1A and 1C).

As we found increased expression in PV interneurons we wondered if this was due because of impaired excitatory connectivity. We measured synaptic excitatory input onto PV positive MLIN using as a marker the vesicular glutamate transport 1 (VGluT1) at P200. Immunostaining of the marker VGluT1 on the PV-positive interneurons and measurement of puncta per cell revealed a significant increase in the number of VGluT1 synapse (Figure 1D, 1E), nevertheless the volume of VGluT1 synapses is smaller in *SCA1$^{154Q/2Q}$* compared to *WT* (Figure 1 H). We further investigate the connectivity between MLIN and PC using the vesicular GABA transporter (VGAT) as a marker of inhibitory synapses. Surprisingly, we found decreased number but no difference in volume of VGAT synapses coming from the MLIN onto the PC, probably because at P200 many PC are already degenerated (Figure 1F,1G and 1I).

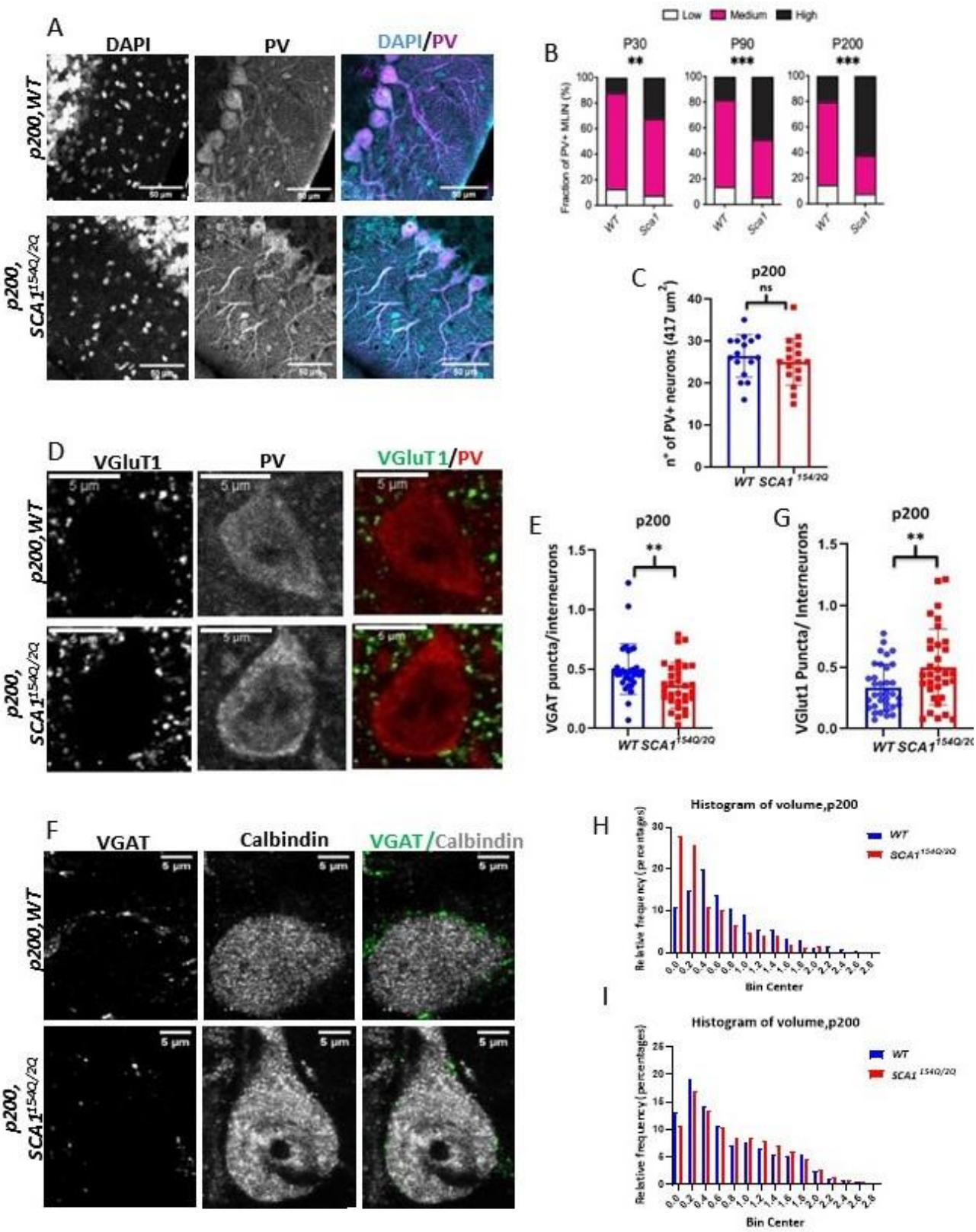

Figure 1. *Alteration in the PV and the excitatory-inhibitory balance in the molecular layer of SCA$^{154Q/2Q}$* ***(A)*** *Representative confocal images of WT and SCA1$^{154Q/2Q}$ cerebellar cortex stained for parvalbumin.* ***(B)*** *Quantitative analysis (Q.A) of expression of PV in SCA1$^{154Q/2Q}$ and WT MLIN at P30, P90, and P200, **P<0.01, ***P<0.001.* ***(C)*** *Q.A. of number of PV positive interneurons* ***(D)*** *Representative confocal images showing reduced VGluT1 puncta on PV positive interneurons in SCA1$^{154Q/2Q}$ versus WT at P200.* ***(E)*** *Q.A of density of*

*synapsis of VGluT 1 on PV- interneurons between SCA1$^{154Q/2Q}$ versus WT at P200, P -value = 0.0099**, Mean of SCA1 =0.5023 and Mean of WT=0.3366, Mean difference (SCA1 – WT) = -0.1658 ± SEM 0.06236.* ***(F)*** *Representative confocal images showing reduced VGAT puncta on calbindin-PC in SCA1$^{154Q/2Q}$ versus WT at P200.* ***(H)*** *Histogram for the distribution of volume of density of synapse of VGluT1 for WT and SCA1$^{154Q/2Q}$at P200, horizontal axis represents the bin center for volume.* ***(G)*** *Q.A of density of synapsis of VGAT 1 on calbindin-PC between SCA1$^{154Q/2Q}$ versus WT at P200, P -value = 0.0091**, Mean of SCA1= 0.3636 and Mean of WT=0.4990, Mean difference (SCA1 - WT = -0.1355) ± SEM ± 0.05028.* ***(I)*** *Histogram for the distribution of volume of density of synapse of VGAT volumes for WT and SCA1$^{154Q/2Q}$at P200, horizontal axis represents the bin center for volume. 3 mice/ genotype. Scale Bar, Figure 1A (50 µm) and Figure 1 D and 1F (5 µm).*

3.2 Proteomic profiling of *WT* and *SCA1$^{154Q/2Q}$* MLIN.

To gain insights onto the molecular signature that characterized MLIN in *SCA1$^{154Q/2Q}$* mouse model, we have specifically targeted the MLIN crossing the *SCA1$^{154Q/2Q}$* animals with the Parvalbumin CRE reporter line and performed stereotaxic injection to label the MLIN of the cerebellar cortex at P30. We subsequently FACS sorted the MLIN and perform proteomic profiling (Figure 2A).

Mass spectrometry analysis revealed multiple downregulated proteins in *SCA1$^{154Q/2Q}$* compared to *WT* (Figure 2B). PANTHER analysis revealed that most of the proteins downregulated belong to RNA metabolisms, Transporter, Metabolite interconversion enzyme and membrane trafficking proteins classes (Figure 2C). Of interest, among the membrane-associated trafficking proteins class different proteins involved in synaptic transmission and GABA recycling were downregulated, such as Synaptotagmin 1 (Synt1), Synaptotagmin 2 (Synt 2), Synapsin 25 (SYNAP 25) (Figure 2C).

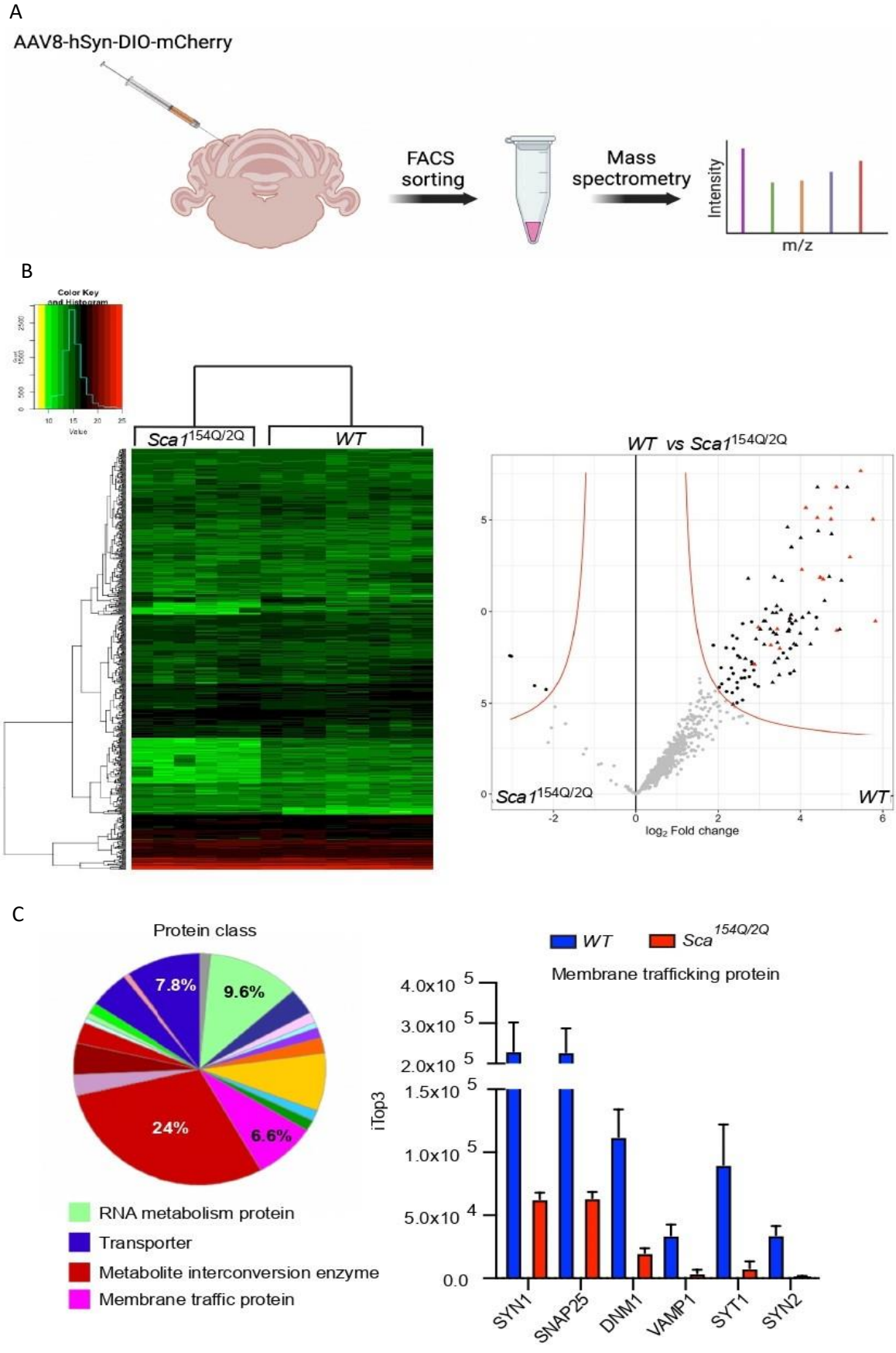

Figure 2 *Proteomic profiling of WT and SCA1$^{154Q/2Q}$ MLIN* ***(A)*** *Experimental timeline for FACS sorting and MS analysis of MLIN from WT and SCA1$^{154Q/2Q}$.* ***(B)*** *Hierarchical clustering accordingly to protein*

expression profile. Right: Volcano plot: proteins over-expressed in SCA1$^{154Q/2Q}$ compared to WT are shown on the left, proteins over-expressed in WT compared to SCA1$^{154Q/2Q}$ on the right-hand side of the plot, ***(C)*** *Panther protein class analysis of downregulated proteins in SCA1$^{154Q/2Q}$, and iTop3 (sum of the three most intense peptide intensities) plot values of membrane trafficking protein involved in synaptic neurotransmitter release. (Results previously generated in the lab)*

3.3 Downregulation of Synaptotagmin 1 protein in molecular layer interneurons of *SCA1$^{154Q/2Q}$*

Based on the proteomic profiling results, we focused our attention on Synt 1 as it is the most downregulated calcium sensor protein. Using immunofluorescence staining we saw decreased expression of Syt1 in *SCA1*$^{154Q/2Q}$ mice compared to *WT* (Figure 3A,3D, and 3G). We measured the density of Synt 1 puncta within the MLIN of the cerebellar cortex. Our data revealed downregulation of the Synt 1 (Figure 3B, 3C,3E,3F,3H and 3I) in *SCA1*$^{154Q/2Q}$ mice at different pathological stages (p60, p100 and p 200) compared to *WT*. Nevertheless, no significant difference was detected in the volume of Syt1 puncta between genotypes.

Furthermore, the downregulation of Synt 1 in *SCA1*$^{154Q/2Q}$ was also confirmed by western blots at P60 (Figure J-K). Further confirming our proteomics data.

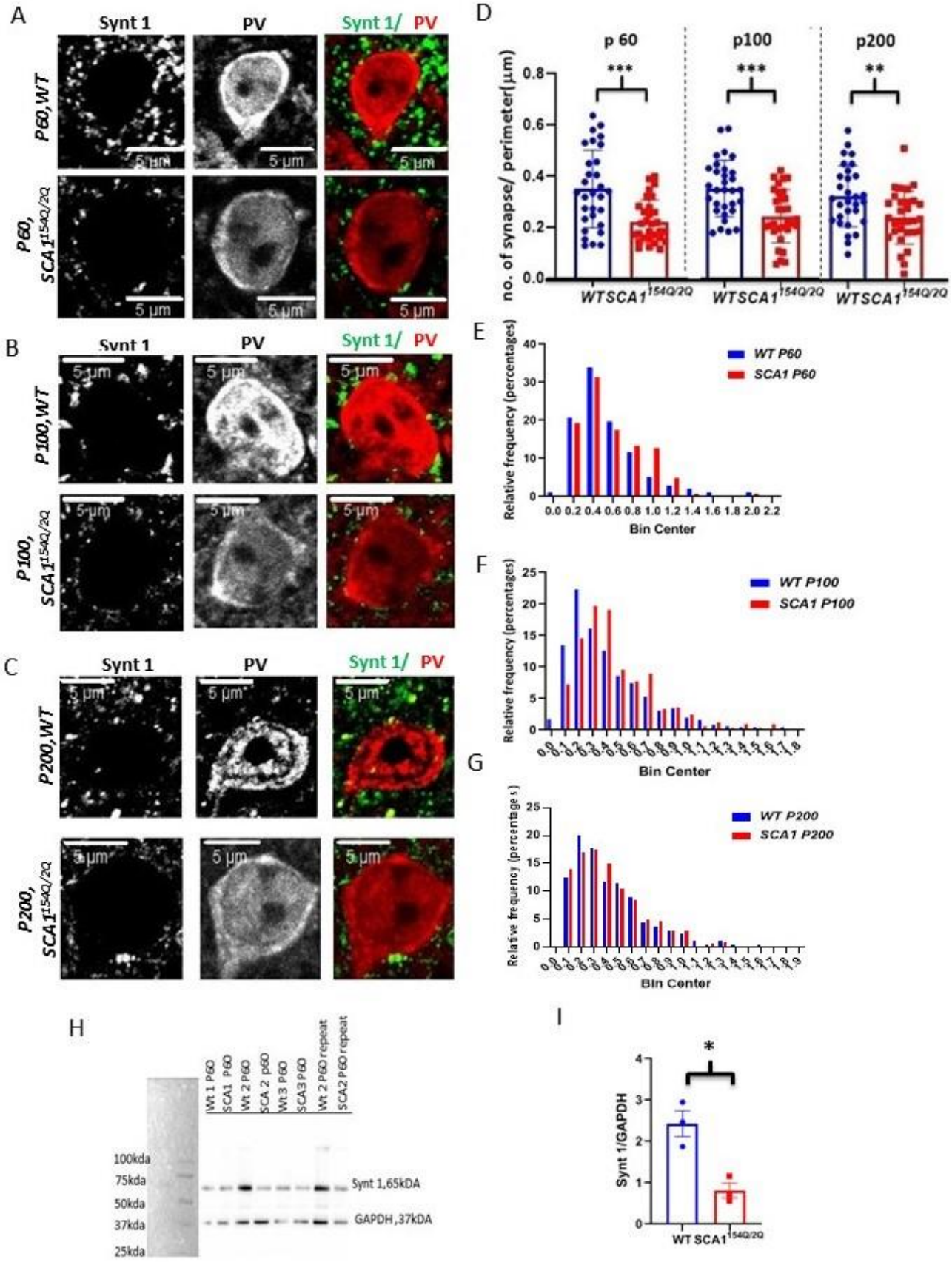
A
Synt 1
PV
Synt 1/ PV
P60,WT
P60, SCA1154Q/2Q
5 µm
B
P100,WT
P100, SCA1154Q/2Q
C
P200,WT
P200, SCA1154Q/2Q
D
p 60
p100
p200
***
***
**
no. of synapse/ perimeter(µm)
0.0
0.2
0.4
0.6
0.8
WTSCA1154Q/2Q
WTSCA1154Q/2Q
WTSCA1154Q/2Q
E
WT P60
SCA1 P60
Relative frequency (percentages)
0.0 0.2 0.4 0.6 0.8 1.0 1.2 1.4 1.6 1.8 2.0 2.2
Bin Center
F
WT P100
SCA1 P100
Relative frequency (percentages)
Bin Center
G
WT P200
SCA1 P200
Relative frequency (percentages)
Bin Center
H
Wt 1 P60
SCA1 P60
Wt 2 P60
SCA 2 p60
Wt 3 P60
SCA3 P60
Wt 2 P60 repeat
SCA2 P60 repeat
100kda
75kda
50kda
37kda
25kda
Synt 1,65kDA
GAPDH,37kDA
I
*
Synt 1/GAPDH
WT SCA1154Q/2Q

Figure 3: *Downregulation of Synaptotagmin 1 protein in molecular layer interneurons of SCA1$^{154Q/2Q.}$* ***(A)*** *Representative confocal image of Synt 1 puncta on PV positive interneurons in Sca1$^{154Q/2Q}$ and WT at p60.* ***(B)*** *Representative confocal image of Synt 1 puncta on PV positive interneurons between Sca1$^{154Q/2Q}$ versus WT at p100.****(C)*** *Representative image of Synt 1 puncta on PV positive interneurons between Sca1$^{154Q/2Q}$ versus WT at p200.* ***(D)*** *Q.A of the density of synapsis of Synt 1 on PV positive interneurons between Sca1$^{154Q/2Q}$ versus WT at p60, P value = 0.0002***,Mean of SCA1=0.2225 and Mean of WT=0.3493, Mean difference (SCA1 - WT = -0.1268) ± SEM ± 0.03172, p100: P value = 0.0002***, Mean of SCA1= 0.4600 and Mean of WT=0.6618 ,Mean difference (SCA1 - WT = -0.2018) ± SEM ± 0.05084 and p 200: P value = 0.0013**, Mean of SCA1 = 0.4848-Mean of WT =0.6739,Mean difference (SCA1 - WT = -0.1892) ± SEM± 0.05575****.*** ***(E)*** *Histogram for the distribution of volume of density of synapsis for WT and SCA1$^{154Q/2Q}$at p60, horizontal axis represents the bin center volume.* ***(F)*** *Histogram for the distribution of volume of density of synapsis for WT and SCA1$^{154Q/2Q}$at p100, horizontal axis of density of synapsis represents the bin center for volume.* ***(G)*** *Histogram for the distribution of volume of density of synapsis for WT and Sca1$^{154Q/2Q}$at p200, horizontal axis represents the bin center for volume.****(H)****Western blots of the Synaptotagmin1 at P60.* ***(I)****Q.A. of western blot with Synt1 and molecular marker GAPDH between SCA1$^{154Q/2Q}$ versus WT, P value = 0.0109*, Mean difference (SCA1 - WT = -1.617) ± SEM ± 0.3598, 3 mice/ genotype. Scale Bar, Figure 3 A, B, and C (5 µm).*

3.4 Proteomic Profiling of the iGABergic neurons of SCA1 iGNs

As in our lab we used different translational approaches to eventually identify new putative molecular targets for future therapies we generated GABAergic neurons from *SCA1* patients and unaffected siblings as control and perform proteomics profiling.

Mass spectrometry analysis revealed multiple downregulated proteins in human *SCA1* compared to control (Figure 4A). PANTHER analysis revealed that most of the proteins downregulated belong to RNA metabolisms, Transporter, Metabolite interconversion enzyme, and membrane trafficking proteins classes (Figure 4B). Of interest, among the membrane-associated trafficking proteins class different proteins involved in synaptic transmission and GABA recycling were downregulated, such as Synaptotagmin 1 (Synt1), Synaptotagmin 2 (SYNT 2), Synapsin 25 (SYNAP 25). Finally, we compared the proteomics profile of *SCA1* iGNs with the one obtained from *Sca1* mice, and we identify a conserved proteomic signature between human and rodent interneurons (Figure 4C).

A

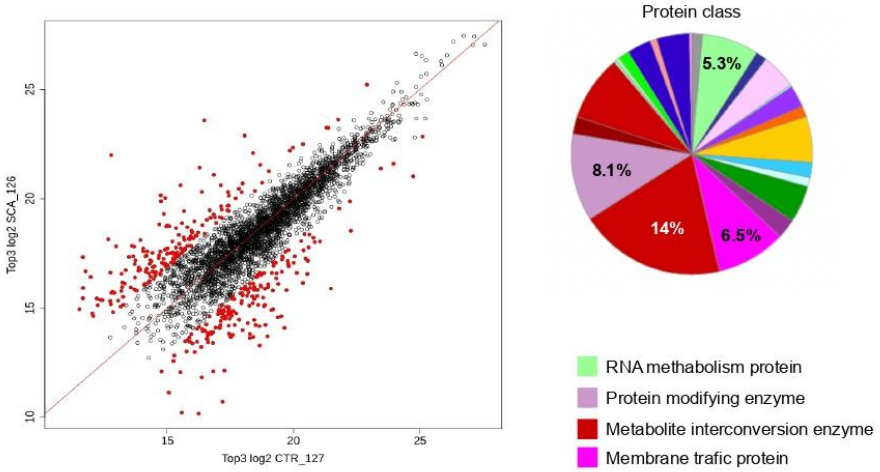

B

GABA synthesis release, reuptake and degradation (human reactom pathways)

ABAT	4-aminobutyrate aminotransferase, mitochondrial;ABAT;ortholog	transaminase(PC00216)
STX1A	Syntaxin-1A;STX1A;ortholog	SNARE protein(PC00034)
RAB3A	Ras-related protein Rab-3A;RAB3A;ortholog	
HSPA8	Heat shock cognate 71 kDa protein;HSPA8;ortholog	Hsp70 family chaperone(PC00027)
RIMS1	Regulating synaptic membrane exocytosis protein 1;RIMS1;ortholog	membrane traffic protein(PC00150)
ALDH5A1	Succinate-semialdehyde dehydrogenase, mitochondrial;ALDH5A1;ortholog	dehydrogenase(PC00092)
VAMP2	Vesicle-associated membrane protein 2;VAMP2;ortholog	membrane traffic protein(PC00150)
SYT1	Synaptotagmin-1;SYT1;ortholog	membrane trafficking regulatory protein(PC00151)
DNAJC5	DnaJ homolog subfamily C member 5;DNAJC5;ortholog	chaperone(PC00072)
SNAP25	Synaptosomal-associated protein 25;SNAP25;ortholog	SNARE protein(PC00034)

GABA synthesis release, reuptake and degradation (mouse reactome pathways)

RAB3A	Ras-related protein Rab-3A;Rab3a;ortholog	membrane trafficking regulatory protein(PC00151)
STXBP1	Syntaxin-binding protein 1;Stxbp1;ortholog	transaminase(PC00216)
ABAT	4-aminobutyrate aminotransferase, mitochondrial;Abat;ortholog	membrane trafficking regulatory protein(PC00151)
SYT1	Synaptotagmin-1;Syt1;ortholog	SNARE protein(PC00034)
SNAP25	Synaptosomal-associated protein 25;Snap25;ortholog	

C

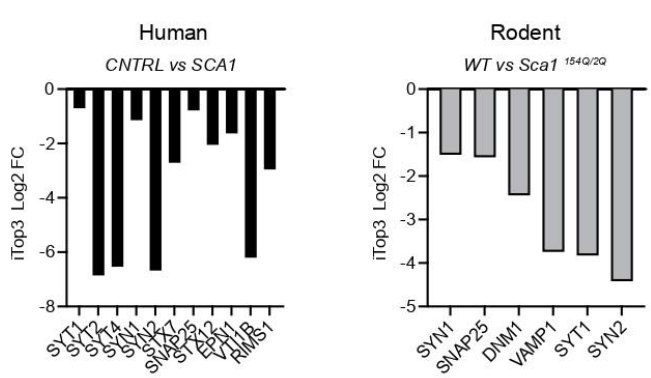

Figure 4 *Proteomic profiling of iGABergic neurons of SCA1 and control.* ***(A)*** *MS analysis of SCA1and Control, Volcano plot: proteins over-expressed in iGABergic neuron and panther protein class of iGABergic neurons,* ***(B)*** *Comparative analysis of Panther protein class analysis of downregulated*

proteins in mouse and human reactome pathways. ***(C)*** *Comparison of downregulation of proteins between human iGABergic neurons with the rodent model with iTop3 (sum of the three most intense peptide intensities) plot values of membrane trafficking protein involved in synaptic neurotransmitter release. (Results previously generated in the lab).*

3.5 Expression of PV, Synt 1 and ATP1 2A in iGABAergic Neurons of SCA1 and control.

To further validate our proteomics results on iGNs, we performed immunostaining on different candidates, such as Synt1 and ATP1-2a.

Immunostaining of eleven days old iGNs revealed higher expressions of PV (Figure 5A and 5B), similarly on what we previously observed in Sca1 mouse model. Synt1 is a crucial molecule belonging to the SNARE complex involved in neurotransmitter release, similarly to our data obtain in MLI of the Sca1 mouse model also human SCA1 iGNs express low Synt 1 levels (Figure 5A and 5C) compared to healthy control. The expression of ATP1-2a, that belongs to the family of P-type cation transport ATPases, was found increased in SCA1 iGNs compared to control iGNs, highlighting possible dysfunction in excitability (Figure 5D and 5E).

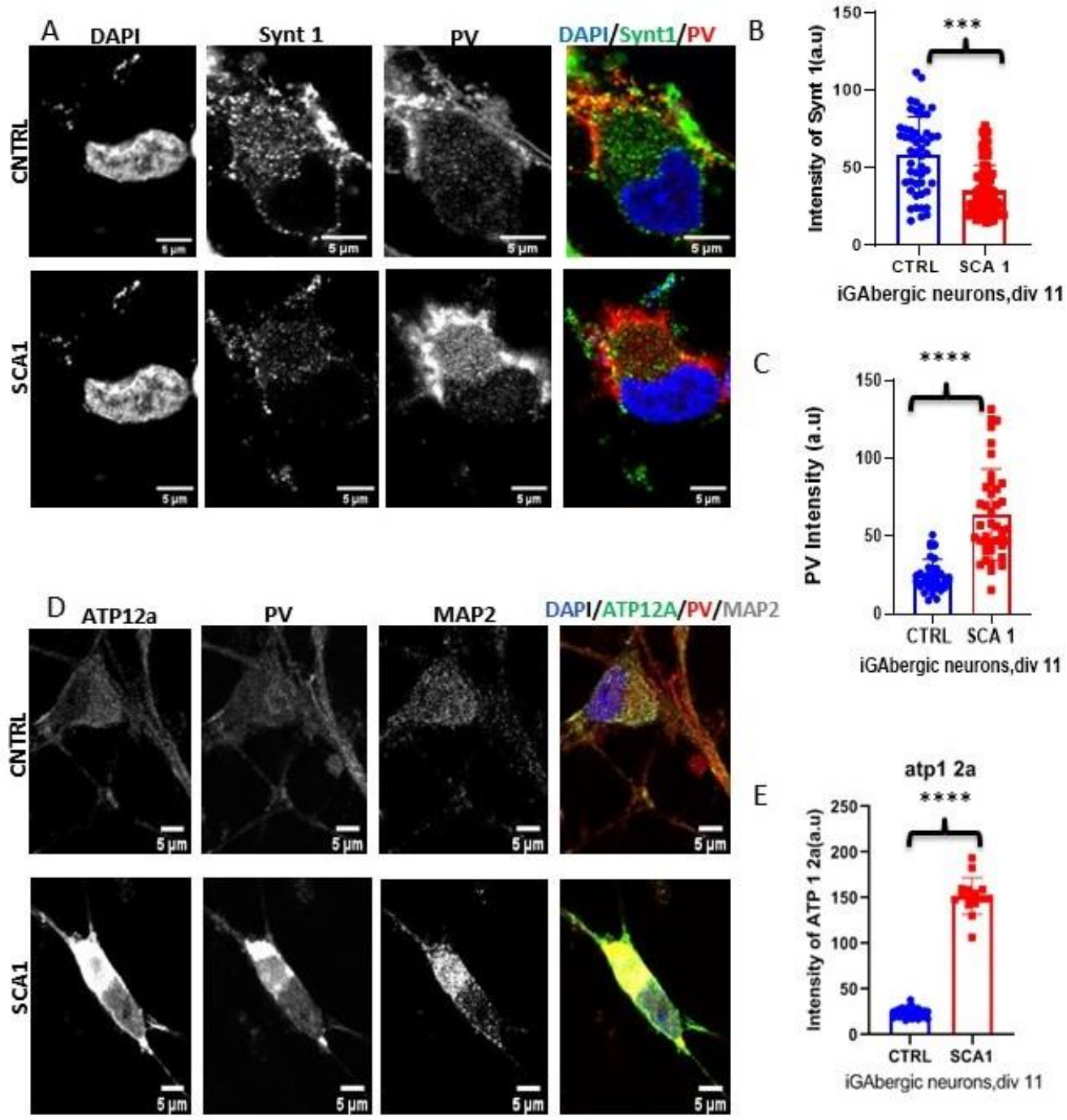

Figure 5: *Expression of PV, Synt 1 and ATP1 2A in iGNs of SCA1 and control.* ***(A)*** *Representative confocal image of expression of Synt 1 and PV on iGNs (SCA1 and Control) at day 11.* ***(B)*** *Q.A showing expression of intensity of Synt 1 protein between the iGNs (SCA1 and Control), P -value <0.0001,****Mean of SCA1=34.91 and Mean of Control=58.40 , Mean difference (SCA1 -Control = -23.49) ± SEM ± 3.572* ***(C)*** *Q.A showing expression of intensity of PV between the iGNs (SCA1 and Control), P -value <0.0001 ****,Mean of SCA1= 63.89 and Mean of Control= 24.81, Mean difference (SCA1 - Control =± 39.07) ± SEM ± 5.036* ***(D)*** *Representative confocal image of expression of ATP1 2a*

on iGNs (SCA1 and Control) at day 11. ***(E)*** *Q.A showing expression of intensity of ATP1-2a between the iGNs (SCA1 and Control), P -value <0.0001****, Mean of SCA1=152.0 and Mean of control= 24.04. Mean difference (SCA1 - Control = 127.9) ± SEM± 4.051. Unpaired t-test *P<0.05 , 3 mice/ genotype*. *Scale Bar, Figure 5A and 5D (5 µm).*

4. DISCUSSION

NDDs are characterized by alterations in intracellular calcium dynamics, impaired intrinsic neuronal excitability and neuronal circuits dysfunctions (Bezprozvanny, 2010; Roselli and Caroni, 2015). In this context, it is important not only to identify the molecular basis of these alterations at the cellular and neuronal circuit level but also to understand their role during disease progression (Lin et al., 2000; Serra et al., 2004).

The underlying cause of PC neurodegeneration in SCA1 is still debated. Nevertheless because of PC increase susceptibility to genetic and functional insults they are more vulnerable to degeneration compared to other neuronal cell types (Hekman and Gomez, 2015). In SCA1, profound changes in PC neurophysiology precede PC loss and contribute to cerebellar circuit dysfunction that characterize SCA1 pathological manifestation (Meera et al., 2016).

Our group focus on the early circuit and molecular changes underpinning the degeneration of Purkinje cells (PCs) in SCA1. Unpublished data from our group reviled early alterations in the MLIN within the cerebellar circuit. Proteomics analysis of mutant MLIN highlighted widespread synaptic alterations, that might count for increase expression of PV and in turn disrupting excitatory/inhibitory balance of the cerebellar cortex in pathological conditions. Furthermore, we compared the proteomics signature of SCA1 mice MLIN with human iGABAergic neurons, highlighting a conserved synaptic dysfunction between rodent and human preclinical model of SCA1.

4.1 Alteration of PV expression and the excitatory-inhibitory imbalance in *SCA$^{154Q/2Q}$* MLIN

We investigated PV expression in the MLIN of *WT* and *SCA1$^{154Q/2Q}$* mice through immunofluorescent staining that revealed an increase in its level in *SCA1$^{154Q/2Q}$* postnatal days (P) 30, 90, and more prominently at P200 (Figure 1B). PV positive interneurons are distributed in different regions of the brain and shape the output of other neurons (Brown et al., 2015; Nahar et al., 2021). The dysfunction of PV-positive interneurons in different parts of the brain is implicated in several neurological condition as well as NDDs (Murray et al., 2015). For instance, PV interneurons are dysfunctional in the prefrontal cortex (PFC) of patients affected by schizophrenia (Hanada et al., 1987; Lewis et al.,

2005; Murray et al., 2015). Similarly, another study on autism spectrum disorder (ASD) used shank mouse model in which they found a significant reduction in the intensity of PV in the prefrontal cortex (Filice et al., 2016). Additionally, the expression of PV is enhanced in neurons of the anterior olfactory nucleus of PD patients (Ubeda-Bañon et al., 2017).

We also investigated if there was loss in the number of PV-positive interneurons in the MLIN of the cerebellum along with the PC degeneration. Differently from PCs, we found no significant difference in p200, *WT,* and *SCA1*$^{154Q/2Q}$ (Figures 1A and 1C).

In a study, environmental enrichment promotes the emergence of large fractions of low-differentiation (low PV and GAD67 expression) basket cells with low excitatory-to-inhibitory synaptic-density ratios, and Pavlovian contextual fear conditioning leads to large fractions of high-differentiation (high PV and GAD67 expression) basket cells with high excitatory-to-inhibitory synaptic-density ratios thereby highlighting the importance of PV expression in network plasticity (Donato et al., 2013). We further investigated if excitatory/inhibitory balance is disrupted in SCA1 within the MLIN population by measuring the density of excitatory synapsis onto PV positive interneurons and found a significant increase in VGluT1positive synapse at P200 (Figure 1D 1E and 1H).

The increase in VGlut1 expression coincides with late phase of CF synapse elimination, a process critically dependent on normal PF-PC synapse formation (Kano et al., 2018). vGlut 1 dysregulation may also disrupt CF maturation, distal CF extension and Ca^{2+} signalling (Catterall, 2000; Miyazaki et al., 2004). Moreover, the C-terminal tail of the channel functions as a transcription factor, coordinating the expression of genes involved in PC development (Du et al., 2013).

A study on SCA23, revealed that VGlut1 protein levels were significantly increased in mutant animals at different pathological stages, suggesting an increased number of synapses onto the PC dendritic tree (Smeets et al., 2021).

Moreover, this study highlighted alterations in the maturation and number of CF-PC synapses, the number of BC-PC synapses and the expression of VGlut2 and VGlut1; supporting our hypothesis that deficits in synaptic wiring contribute to motor dysfunction and ataxia (Smeets et al., 2021).

In contrast to VGluT1, when we measured VGAT positive synapses on the calbindin-positive PC we found a significant decrease in the VGAT- PC synapse (Figure 1F,1G, and 1I). Probably due to PC loss as the animals analysed were already end stage of the pathology.

In accordance with data from our group, showing increase MLIN-PC connectivity at early symptomatic stage (data not shown), the study from Edamakanti et al, found that mutant ATXN1 stimulates the proliferation of postnatal cerebellar stem cells in SCA1 mice into GABAergic inhibitory interneurons rather than astrocytes. This phenomena significantly increased the MLIN-PC connectivity, disrupting cerebellar Purkinje cell function in a non–cell autonomous manner. Pattern observed in human post-mortem tissue from SCA1 patients (Edamakanti et al., 2018).

All in all, our findings may uncover the fact that the profound alterations in inhibitory and excitatory transmission within the cerebellar circuit may count as possibly contributing to the vulnerability of cerebellar PCs in SCA1.

4.2 Alteration in the proteome of *SCA1*$^{154Q/2Q}$ MLI and SCA1 iGABAergic neurons.

To gain insights into the molecular signature that characterized MLIN in *SCA1*$^{154Q/2Q}$ mouse model we used a proteomic approach. Mass spectrometry analysis revealed multiple downregulated proteins in *SCA1*$^{154Q/2Q}$ compared to *WT* (Figure 2B). PANTHER analysis revealed that most of the proteins downregulated belong to RNA metabolisms, Transporter, Metabolite interconversion enzyme and membrane trafficking proteins classes. Of interest, among the membrane-associated trafficking proteins class different proteins involved in synaptic transmission and GABA recycling were downregulated, such as Synaptotagmin 1 (Synt1), Synaptotagmin 2 (SYNT 2), Synapsin 25 (SYNAP 25) (Figure 2C).

Previous study from our group focused on identifying early alterations in PC proteomic profile. Ruegsegger et al., 2016 had compared the total cerebellar proteome of *WT* and *SCA1*$^{154Q/2Q}$ mice at post-natal day P35 by MS. A total of 675 proteins were detected and shared between both genotypes. This semiquantitative analysis revealed an altered proteome in which 68 proteins were upregulated and 32 were downregulated. PANTHER analysis revealed an enrichment for proteins belonging to diverse classes such as oxidoreductases, membrane-associated trafficking proteins, calcium-binding proteins and chaperones. Some candidates such as Homer-3 were validated with immunostaining and it was discovered that interlinked pre- and postsynaptic deficits contribute to

SCA1 pathogenesis. This included a reduced Homer-3 expression and impaired mTORC1 signalling in PC (Ruegsegger et al., 2016).

Based on the proteomic profiling results, we focused on Synt 1, because it is an important calcium sensor involved in synaptic transmission. We therefore validated our proteomics data using immunofluorescence for Synt 1 (Figure 3) in *SCA1*$^{154Q/2Q}$ mice at different pathological stages (p60, p100 and p200), confirming its downregulation throughout disease progression.

Synt1 is a calcium sensor for fast, synchronous synaptic vesicle exocytosis (Glavan et al., 2009),essential in neurons and neuroendocrine cells (Su¨ dhof and Rizo, 1996). Syt1 participate in the rapid adaptation of subsequent transmitter release (Fukuda, 2006 ; Courtney et al., 2019). Therefore, the downregulation of Synt 1 might suggest its adaptation to the high neurotransmitter release and neuropathogenicity. In support with our findings, few studies have proposed the involvement of Synaptotagmin 1 protein in the neuropathology of NDDs (Glavan et al., 2009)

In 2009, a correlation was found between synaptic loss and severity of dementia, which suggest a close relationship between synaptic pathology and the cognitive decline in AD (Davidsson & Blennow, 1998, Sze et al., 2000; Glavan et al., 2009). The synaptic vesicle proteins rab3a, Synt, and synaptophysin, the presynaptic protein GAP43 and the post-synaptic protein neurogranin have all been found to be reduced in the frontal, temporal, parietal cortex and hippocampus from patients with AD and age-matched control subjects (Bogdanovic et al., 2000).

Further, loss of presynaptic vesicle proteins such as Syt 1 and postsynaptic proteins was found in all frontal and parietal cortices of specimens from patients with AD compared to those from age-matched control subjects (Masliah et al., 2001; Reddy et al., 2005). Syt1 was found to be downregulated also in the neurons of the nucleus basalis that are known to be selectively vulnerable and, in the cerebellum, thalamus, and hippocampus of patients with AD (Sze et al., 2000; Yoo et al., 2001; Mufson et al., 2002).

Since the neuropathology of Synaptotagmin 1 downregulation can be linked with calcium homeostasis, Professor Bezprozvanny summarized the results demonstrating impaired calcium signaling in AD, PD, HD, ALS, and SCAs (Bezprozvanny, 2009).

Calcium binding proteins, ion exchangers, transcriptional networks and G protein coupled receptors are the checkpoints which regulate the calcium in plasma membrane, mitochondria and

endoplasmic reticulum. Generally, the regulatory mechanism of the calcium is weakened in NDD resulting the diminished neuroplasticity, synaptic function and neuronal death. The major role players for this cause could be disrupted energy metabolism, change in the disease related proteins and stress (Zü and Reiser, 2011).

Similar to SCA1, the neuropathology of SCA23 corresponds with an elevated intracellular Ca^{2+} (Smeets et al.,2015). In a study by Smeet et al., 2015, SCA23-mutant PDYN-R212W ($PDYNR^{212W}$) displayed elevated levels of mutant dynorphin A. This increased level of mutant dynorphin A were confirmed with radioimmunoassay and visualized by IHC which is associated to activate the NMDA-R, very likely mimicking the actions of glutamate which are associated with climber fibre retraction and Purkinje cell loss. Thus the high levels of mutant dynorphin A in Parallel fiber-PC synapse in cerebellum of $PDYNR^{212W}$ suffer from pathologically uncontrolled intracellular calcium levels, which may lead to transcriptional dysregulation, and eventually neuronal cell death (Smeets et al., 2015).

In addition, in a study of in SCA23 transgenic mice, altered expression of several critical Ca^{2+} channel subunits were detected, potentially contributing to altered Ca^{2+} transients in $PDYNR^{212W}$ cerebella (Smeets et al., 2021).

4.3 Expression of PV, Synt 1, and ATP1 2A in iGABAergic Neurons of SCA1 and control.

The iPSCs-based models allow for the studying of both hereditary and sporadic cases of pathologies including molecular mechanisms underlying neurodegeneration (Grekhnev et al., 2022).To correlate our previous findings on the SCA1 mouse model with a translational approach we generated iGABergic neurons (iGNs). Similarly of what we observed in rodent Sca1 MLIN, immunostaining of eleven days old iGNs revealed higher expressions of PV (Figures 4A and 4B) whereas lower expression of Synt 1 (Figures 4A and 4C) in SCA1 than compared to healthy control. Similarly, the ATP1-2a expression was higher in the SCA1 iGNs than in control iGNs (Figures 4D and 4E).

The study from Edakimanti et al,2018, demonstrate that in SCA1, stem cells are hyperproliferative and preferably differentiate into GABAergic interneurons leading to increased inhibitory connections with PCs and non-cell autonomous PC dysfunction (Edamakanti et al., 2018).

Since the interaction between expanded ATXN1 and CIC acts in a gain-of-function manner in SCA1, Rousseaux et al. investigated the transcriptional profile in SCA1 hiPSC-derived neurons and found that genes involved in glutamatergic neurotransmission were downregulated (Rousseaux et al., 2018).

Using SCA-iPSCs as an *in vitro* disease modelling platform another study, found that neuronal cell death and polyQ aggregation were also one of the phenotypic hallmarks in SCA2 and SCA3(Chuang et al., 2019).

A recent study has demonstrated aberrant calcium signalling in iPSCs-based models of polyglutamine ataxias, including SCA1, SCA2, SCA3, SCA7, and SCA17. For instance, an increase in calcium entry through voltage-gated calcium channel in SCA17 GABAergic striatal medium spiny neurons (MSN) was shown. In contrast, was observed a decrease in the store-operated calcium entry and no changes in the functioning of voltage-gated calcium channels in SCA1 GABAergic neurons (Grekhnev et al., 2022).

5. CONCLUSION

The primary objective of this thesis to investigate the pathogenic role of molecular layer interneuron in causing the alterations in the degeneration of PC in SCA1. For our experiments, we used *SCA1* $^{154Q/2Q}$ and *WT* mice model and the iPSCs model from the SCA1 patient. Further, we validated the results from proteomics and immunofluorescence i.e. observing the expression and downregulation of membrane proteins such as PV and Synt 1, with these models.

Firstly, we observed an increase in PV expression, as a marker of neuronal activity in MLINs, from the cerebellar cortex of *SCA1* $^{154Q/2Q}$ than *WT* through immunostaining based on the previous findings of the group. The PV expression increased with the increasing age of the mice. We also investigated if the number of PV-positive interneurons in the molecular layer of the cerebellum also degenerated. To our knowledge, counting the number of positive PV interneurons we found no significant difference in end-stage *SCA 1* $^{154Q/2Q}$ animals (p200). Therefore, we hypothesize that the MLIN might be more active therefore impacting PC physiology.

Further, immunostaining of the marker VGluT1-PV positive interneurons and VGAT-PC measurement of puncta per cell revealed a significant increase in the number of VGluT1 -PV positive interneurons synapses than the PC- VGAT as a marker of inhibitory synapses in *SCA1*$^{154Q/2Q}$ compared to *WT*. Surprisingly, we found decreased number but no difference in the volume of VGAT synapses coming from the MLIN onto the PC, probably because at P200 many PC are already degenerated. Our findings may uncover the fact that the profound alterations in inhibitory and excitatory transmission within the cerebellar circuit may count as possibly contributing to the vulnerability of cerebellar PCs in SCA1, also hypothesized by Meera et al., 2016. Secondly, based on the previous findings of SCA1 pathology in the MLINs is reflected, an altered expression of the calcium-binding protein, parvalbumin only, or other calcium buffers as well, is reflected as was shown previously by Ruegsegger et al., 2016 in the PCs. MS analysis revealed multiple downregulated proteins in *SCA1*$^{154Q/2Q}$ compared to *WT*. We focused our attention to Synt 1, a calcium sensor protein to uncover the fact about the alteration in calcium homeostasis. We therefore, validated our proteomics data using immunofluorescence for Synt 1 in *SCA1*$^{154Q/2Q}$ mice at different pathological stages (p60, p100 and p200), confirming its downregulation throughout disease progression.To this end, we investigated PV, Synt 1 and ATP1a expression through immunofluorescent staining in the iGABergic neurons as well.

6. OUTLOOK

The cerebellum, originally known to establish as motor control function is now related in cognitive functions too (Beuriat et al., 2022) thereby establishing cerebellar cortex as a huge arena for research. Different SCA-linked mutations are directly or indirectly associated with the PC activity, calcium dynamics and impairments in dendrites development (Binda et al.,2020). Our findings also support these dynamics, potentially known to harm the cerebellar wiring and function, establishing MLIN layer as an important player in cerebellar atrophy. Moreover, our results in the mouse model correlated with the iGABergic neurons. This can be correlated with a glimpse of different stem cell-based replacement therapies. Various studies with embryonic, neural, and mesenchymal stem cells in SCA1, SCA2, and SCA3 mouse models, but to date, no hiPSC-based replacement studies have been reported in the SCA field. A persisting challenge in hiPSC technology is the high level of interindividual variability, especially in clinical trials (Buijsen et al., 2019). Until now, only SCA36 hiPSC-derived motor neurons have been treated with antisense oligonucleotides, but several animal and cell models for SCA1, SCA2, SCA3, and SCA7 have been highly instrumental to test different AONs with variable success rates (Bushart et al., 2021; Evers et al., 2011). Moreover, the rapid development of genome editing strategies by CRISPR/Cas makes it possible to correct causative genetic variation, which is of ultimate importance in personalized medicine.

7. MATERIALS AND METHODS

7.1 Sample Preparation

WT and SCA1$^{154Q/2Q}$ Animals were acquired from Jackson Laboratory. Animal care, handling, and protocols were performed in accordance with the Swiss Veterinary Law guidelines.

Perfusion and Section Preparation

The mice were transcardially perfused with PBS 1X followed by 4 % PFA. Tissue was kept in the fixative solution overnight (ON), followed by cryopreservation in 30% sucrose until use. Cerebellar samples were cut sagittal (50um) using a cryostat and placed in 1x PBS + 0.8% NaN_3.

7.2 Immunofluorescent Staining of the Tissue

The sections were blocked with blocking solution (Table 2) for 2 hours in PBS containing 10% NDS + 0.5% Triton X 100 (Table 1). Afterwards, primary antibodies were diluted in PBS containing 3% NDS + 0.5% Triton X and sections were incubated ON at 4°. The sections were washed with PBS for 10 minutes at room temperature (RT) on a shaker (3 times). Secondary antibodies were diluted in PBS containing 3% NDS + 0.5% Triton X and sections were incubated for 2h at RT shaking in the dark, followed by three washes with PBS (10 minutes each). The sections were directly mounted on a glass slide with DAKO mounting medium. The slides were dried ON before imaging. Primary and secondary antibodies used for staining are listed in Table 3 and 4 respectively.

Table 1: Triton X100 for a total volume of 10mL

Reagents	Volume
Triton X100	1 mL
1xPBS	9 mL

Table 2: Normal Donkey Serum (NDS) antibody I/II reagent for a total volume of 9mL

Solutions	NDS	Triton X100(1:10 in PBS)	PBS 1X
Blocking solution (9ml) 10% NDS+ 0.5% Triton X 100 (1:10 in PBS)	900µl	450µl	7650µl
Ab I/II solution(9ml) 3% NDS + 0.5% Triton X (1:10 in PBS)	270µl	450µl	8280µl

Table 3: Primary antibodies used in Immunofluorescence staining in cerebellar sections.

Antibody	Species	Manufacturer	Catalogue No.	Dilution
PV	Goat	Swant	PVG213	1:1000
Calbindin	Rabbit	ABCAM	Ab62623	1:1000
Synaptotagmin 1	Mouse	Synaptic Systems	105 103	1:1000
VGaT (Vesicular GABA Transporter 1)	Rabbit	Synaptic Systems	131 003	1:1000
VGluT 1 (Vesicular Glutamate Transporter 1)	Rabbit	Synaptic Systems	135 303	1:1000

Table 4: Secondary antibodies used in Immunofluorescence staining.

Antibody	Manufacturer	Dilution
Alexa Fluor Donkey anti-rabbit 488	Invitrogen A21206	1:1000
Alexa Fluor Donkey antimouse 488	Invitrogen A21202	1:1000
Alexa Fluor Donkey antimouse 568	Invitrogen A10037	1:1000
Alexa Fluor Donkey anti-goat 647	Invitrogen A21447	1:1000
Alexa Fluor Donkey anti chicken 647	Invitrogen A78952	1: 1000

7.3 Immunofluorescent Staining on iGABAergic neurons

Neurons plated on coverslips were fixed using 4% PFA for 15 minutes. Coverslips were washed with PBS three times for 10 minutes. Then incubated with PBS containing 10% NDS + 0.5% Triton X 100 solution for 1 hour. The blocking solution was removed, and the primary Abs was added overnight at 4 degrees followed by washes with PBS three times for 10 minutes. Secondary fluorescent abs were added and left for one hour at room temperature. Coverslips were then washed with PBS and mounted with DAKO medium. The primary and secondary antibodies used for staining are listed in Table 5 and 4 respectively.

Table 5: Primary antibodies used in Immunofluorescence staining in the iGABergic neurons

Antibody	Species	Manufacturer	Catalogue No.	Dilution
Map2	Chicken	Sigma	AB15452	1:500
Stim2	Rabbit	abcam	AB59342	1;200
ATP1 2a	Rabbit	Invitrogen	PA5-49624	1:500
FRRS1L	Mouse	Santa Cruz Biotechnology	398692	1:100

Synaptotagmin 1	Mouse	Synaptic Systems	105 103	1:1000
PV	Goat	Swant	PVG213	1:1000

7.4 Western Blot

Protein extraction for the cerebellum

Cerebellum were mixed with Radio-Immunoprecipitation Assay (RIPA) buffer and protease and phosphatase Inhibitor (PPI) (10µl of PPI per 100mg of cerebellum). The tissue was homogenized and centrifuged at 20000 rcf at 4°C for 15 minutes. The protein concentration was measured with the BCA reagent with absorbance of 562nm. Next, the samples were boiled at 95°C for five minutes. In labelled Eppendorf tubes, a volume of the sample depending on the required protein amount to be loaded per well was added and 1x Laemmle Buffer was added to bring the final volume to 20 µl.

Gel Preparation

A casting frame from BioRad was used to prepare the used 10% SDS-PAGE (Table 6 and 7). The comb was removed and sample was loaded in the wells. A volume of 4 ul of Precision Plus Protein All Blue Protein Standards (BIO-RAD) was loaded as marker for molecular weight. Finally, the gel was run with 1x running buffer (Table 8 and 9) at 180 V, 350 A for 70minutes.

Table 6: **SDS-PAGE for two gels (10% acrylamide in running gel *1L)***

Reagent	**Running Gel (ml)**	**Stacking gel (ul)**
Distilled water	3.99ml	2.1ml
30% Acrylamide	3.3ml	800 µl
8 1.5M Tris Buffer (pH 8.8)	2.5ml	-
0.5M Tris Buffer (pH 6.80	-	1 ml
10% SDS	100 µl	40 µl
10% APS	100µl	40 µl
TEMED	10µl	4 µl

Table 7: 10%SDS for a total volume of 100mL

Reagents	Quantity
SDS	10 g
Distilled water	100 ml

Table 8: Preparation of 10X Running buffer for a total volume of 1L

Reagents	Quantity
Glycine	144g
Tris base	30g
20% SDS	50mL

Table 9: Preparation of 1X Running buffer for a total volume of 1L

Reagents	Volume
10x Running Buffer	100 mL
Distilled water	900 mL

Gel Transfer

PVDF membrane was placed in methanol for activation. The Sandwich was placed into an electrode assembly along with an ice pad. The buffer tank was filled with transfer buffer, 200ml of ethanol and 700ml of distilled water for 1000ml of 1x transfer buffer (Table 10 and 11) and allowed to transfer at 100V, 350mA for 1 hour.

Table 10: Preparation of 1x Transfer buffer for a total volume of 1L

Reagents	Volume
10xRunning Buffer	100 mL
Methanol	200 mL
Distilled water	700 mL

Table 11: The required components for 10X TBS for a total volume of 2L

Reagents	Quantity
Sodium chloride (NaCl)	173.5g
Tris base	48.5g

Distilled water	1000 mL

Note: pH must be adjusted to 7.5 before bringing volume to 1000 mL

After the transfer, the membrane was blocked with 5% skimmed milk for half an hour and washed with PBST (1X PBS + 0.1% Tween 20) as listed in Table 12, three times for 10min each. The primary antibodies (Table 14) were diluted in PBST and membrane were incubated ON at 4°C.

The next day, the blot was washed three times in PBST (10 minutes each) then incubated with a suitable Alexa Fluor ab (Table 14) at a dilution of 1:10000 for one hour at room temperature, followed by another set of washes.

Table 12: Preparation of 0.1% PBST using 1X PBS for a total volume of 1L

Reagents	Volume
1x PBS	990 mL
Tween 20	10 mL

The membrane was scanned with the parameters in Table 13.

Table 13: Parameters for Licor -Odyssey Imagers

Intensity for 700nm	**Intensity for 800nm**	**Scan Control**
4.0	2.0	Medium

After scanning, the membrane underwent another set of washes with 1x PBST, and was incubated with Glyceraldehyde 3-phosphate dehydrogenase (GAPDH) at a concentration of 1:10,000, followed by an anti-mouse fluorescent secondary antibody of a wavelength equal to 800um; each of the previous three incubations was done for one hour. This was followed by a last set of washes and scanned at a wavelength of 800nm.

Alternatively, the membranes were developed using ECL system using secondary antibody solution (1: 1000 conjugated to HRP) (Table 14) for 1 hour at room temperature with shaking. Membranes were washed for 10 minutes each.

Table 14: Antibodies used for Western blotting.

Antibody	Species	Company	Catalogue No.	Dilution
Tubulin	Mouse	Sigma	T5168	1:10000
FRRS1L	Mouse	Santa Cruz	398692	1.500
Synaptotagmin 1	Mouse	Santa Cruz	sc-393392	1:1000
GAPDH	Mouse	Acris	ACR001P	1:5000
Alexa Fluor 800	Mouse	Invitrogen	A32730	1:10000
Hrp antimouse	Mouse	Thermo Scientific	MA5-15367	1: 1000

7.5 Cell Culture

Two cell lines were used, SCA1 and Control from skin biopsy was obtained from a 43 year old male SCA1 patient and his 43 year old sister respectively (Buijsen et al., 2018).

7.5.1 Induced pluripotent stem cells (iPSCs) Culture

On the first day mTesr Basal Media (mTeser + mTeser basal media) was prepared and rho-associated protein kinase inhibitor (ROCK) was added.

Followed by Gel Trex preparation so as to prevent the adhesion of iPSCs to the plates. For this, 100ul Gel Trex (100x) into was diluted in 10mL DMEM media and then coated with 1.5 – 2 mL 5& 6cm plates. These were incubated for 30 min.

Finally, 3mL of mTser media was added into a falcon tube. 1 ml of thawed iPSCs was added. The tube was centrifuged at 250g for 5 min supernatant was discarded carefully. The residue was resuspended with 4 mL of mTser media. The plates were coated with the Gel Trex for about thirty minutes.

On the second day, defined clusters of iPSCs was observed. If the confluency is 70 – 80%, the cells were splitted. Ez-lift was used to allow cell detachment and incubated for 5 min and centrifuged at 200 g for 3 min. IPSCS were then resuspended in fresh mTesr media containing ROCK inhibitor.

7.5.2 Embryoid Bodies (EBs)

The media from the iPSCs plates were aspirated, and washed with sterile PBS (dPBS), 2 mL of Accutase was added and left at 37°C for 5 – 10 minutes and transferred to the falcon tubes. The Falcone tube was centrifuged at 300rcf for 3 minutes. The supernatant was discarded while the pellet was resuspended in warm differentiation (N2B27) media (Table 16) supplemented with growth factors for the specific day as reported in Table 15. The content of the Falcone tube was then transferred to a labeled 6cm plate and incubated at 37°C.

On ‘Day 1’, small EBs are formed and are visible under the microscope.

On ‘Day 14’ 24-well plates were filled with 1 coverslip per well. Then coated with 500 ul polyornithine (50mg/ml) diluted in autoclaved distilled water (1:1000) and left overnight at RT. On the next day, plates were washed once with autoclaved water and filled with 500 ul laminin (45 mg/ml) in distilled water (1:1000) and left overnight at room temperature. The wells were washed twice with autoclaved water right before use.

7.5.3 Dissociation of the EBs

EBs were collected into the corresponding labelled Falcon tubes and centrifuged at rcf 300 for 3 minutes. The supernatant was discarded, and the pellet was washed with dPBS twice. This was followed by the incubation of the pellet with trypsin inhibitor (10ml) and DNase (1:1000) for 15 minutes, the tube was vortexed at an interval of 3 minutes. 1ml of fetal porcine serum (FPS) was added to inactivate the trypsin and mixed well by pipetting. 2-3ml of dPBS was added and titration was performed by mixing through pipetting till no pellets are seen. Then the solution was centrifuged for 5min at 500 rcf and the pellet was resuspended with neuron feeding Media (NDM Table 17). Into an Eppendorf tube, cell suspension was prepared with Trypan Blue at a dilution of 1:1. In a hemocytometer, the chambers underneath the coverslip. Using a microscope, the gridlines of the hemocytometer were focused at with 10X objective. Only the viable, non-stained cells were counted using a manual counter. Counting took place into 2 opposite ends and not counting those touching the edges. The formula below was used to determine the concentration of viable cells.

$$Cell\ concentration\ (\ cell/ml\ ) = number\ of\ viable\ cells \times dilution\ factor \times 10{,}000$$

The NDM media was supplemented with growth factors: GDNF (1:1000), BDNF(1: 1000), CNTF(1:1000), h-IGF(1:100), Ara C(1:1000), GluF (1:10,000) AA (1: 1000), U/FDU (1:10,000),N2(1:100), B27 (1:50) and the required cell suspension was transferred into volume of NDM media (the volumes depend on the number of cells and the desired number of wells; 500ul of media/ well) and then plated on wells followed by incubation at 37 °C.

After 48 hours from dissociation, half of the media was replaced from the wells.NDM and growth factors as in day 16 were added but without growth factor, Ara C. The new neurons were fed with fresh media every 2 – 3 days.

7.5.4 Fixation

Media was aspirated from wells and washed with dPBS once. The coverslips were then incubated in 4% PFA at room temperature for 15 minutes followed by three washes with 1x dPBS . For SCA 1 lines iGABergic neurons, the fixation was done after 11-12 days of maturation.

Table 15 : Different growth factors added to N2B27 media according to the respective days .

Days	Growth Factors	Dilutions
	ROCK Inhibitor	1:1000
Day 0	bFGF	1:2000 (10ng/ml final)
	SB	1:500 (20uM final, 10mM stock)
	LDN	1:10000 (0.1uM final), 1:1000 (100uM stock)
	CHIR	1:1000 (3uM final)
	AA	1:1000 (10uM final)
	N2	1:100
	B27	1:50
Day 2	SB	1:500 (20uM final, 10mM stock)
	LDN	1:10000 (0.1uM final), 1:1000 (100uM stock)
	CHIR	1:1000 (3uM final)
	AA	1:1000 (10uM final)
	SAG	1:2000 (500 nM final)
	N2	1:100
	B27	1:50
Day 4	SB	1:500 (20uM final, 10mM stock)
	LDN	1:10000 (0.1uM final), 1:1000 (100uM stock)
	CHIR	1:1000 (3uM final)
	AA	1:1000 (10uM final)
	SAG	1:2000 (500 nM final)
	N2	1:100
	B27	1:50
Day 7		
	AA	1:1000 (10uM final)
	SAG	1:2000 (500 nM final)
	BDNF	1:1000 (1:1000 10ug/ mL)
	N2	1:100
	B27	1:50
Day 9	AA	1:1000 (10uM final)
	SAG	1:2000 (500 nM final)
	BDNF	1:1000 (1:1000 10ug/ mL)
	DAPT	1:1000 (10mM stock 1:1000)
	N2	1:100
	B27	1:50

Day 11	AA	1:1000 (10uM final)
	SAG	1:2000 (500 nM final)
	BDNF	1:1000 (1:1000 10ug/ mL)
	DAPT	1:1000 (10mM stock 1:1000)
	N2	1:100
	B27	1:50
Day 14	AA	1:1000 (10uM final)
	GDNF	1:1000 (10ug/ mL)
	BDNF	1:1000 (1:1000 10ug/ mL)
	DAPT	1:1000 (10mM stock 1:1000)
	N2	1:100
	B27	1:50

Table 16 : Component of N2B27 Differentiation Medium

The following was added into a sterile filter cup (500 mL)

Advanced DMED/ F12	250 mL
Neurobasal medium	250 mL
Pen/ Strep	5 mL
25mM Glutamax	5 mL
55mM B-ME	900ul

Store for up to 2 weeks, light-protected at 4°C

Table 17: Component of NDM Motor Neuron Feeding Medium

The following was added into a sterile filter cup (500 mL).

Neurobasal medium	480mL
Pen/ Strep	5 mL
25mM Glutamax	5 mL
NEAA	5 mL
55mM B-ME	900ul

Store for up to 2 weeks, light-protected at 4°C

7.6 Confocal Microscopy and Image analysis

Images were acquired for fluorescent using Olympus Fluoview 1000-BX61 (Olympus Tokyo) microscope, fitted with 20X, 40X, air objectives or 60X oil immersion objective.

Fiji (ImageJ) and Imaris software were used for cell counting, and morphological measurements like density of synapsis, perimeter, area, volume, and intensity.

7.7 Statistical Analysis

A minimum of three animal replicates were used for each age group per experiment. The analysis and significance were performed using GraphPad Prism 9 and presented as mean ± standard error of the mean (SEM). A P value <0.05 was considered as statistically significant (P<0.05*; P<0.005**; P<0.0001***).

ACKNOWLEDGEMENT

It is my pleasure to express my deep sense of indebtedness to my professors, Prof. Dr. Polverino, for her support and guidance thoroughly in my Master's degree, Prof. Dr. Saxena for giving me the opportunity to join her research group and be an active member of the team. I would like to express my sincere gratitude to my supervisor Dr. Federica Pilotto for her motivation, enthusiasm, kind mentorship, and support throughout my tenure. In addition, I am grateful to Dr. Saxena and Dr. Federica for their insightful suggestions, comments, and guidance in writing this thesis.

I would like to recognize Miss Rim Diab for her assistance and guidance in the development of the iGABAergic interneurons and western blots. I would also like to thank my lab mates from Dr. Saxena's group, Dr. Niran Maharjan, Maria Essers, Carla Pernaci, Eli, Dr. Mert Duman, Joao Filipe Pinheiro Marques, Alex Joseph Schmitz, and Irina Oertig for their support, insightful discussions, and the fun we had in my brief period.

Last but not least, I would like to express my heartfelt gratitude to my beloved parents, Mahesh Thapa and Meera Thapa for their faith and support in every possible way, my brother, Ayush Thapa for his trust in me, and my friend Ramesh KC for his support and humour on my tough days.

REFERENCES

Adam, M. P., Mirzaa, G. M., & Pagon, R. A. (1998). *Spinocerebellar Ataxia Type 1 Synonym: SCA1* (Vol. 1).

Amy J Bastian. (1997). *Mechanisms of Ataxia*. https://academic.oup.com/ptj/article/77/6/672/2633166

Ashizawa, T. , Ö. G. , & P. H. L. (2018). Spinocerebellar ataxias: prospects and challenges for therapy development. *Nature Reviews. Neurology, , 14*(10), 590–605.

Bach, J. P. , Z. U. , D. G. , D. R. , & D.-R. G. (2011). Projected numbers of people with movement disorders in the years 2030 and 2050. *Ovement Disorders : Official Journal of the Movement Disorder Society, 26(12), 2286–2290.*, *26*(12), 2286–2290.

Barmack, N. H., & Yakhnitsa, V. (2008). Functions of Interneurons in Mouse Cerebellum. *Journal of Neuroscience*, *28*(5), 1140–1152. https://doi.org/10.1523/JNEUROSCI.3942-07.2008

Beaudin, M., Klein, C. J., Rouleau, G. A., & Dupré, N. (2017). Systematic review of autosomal recessive ataxias and proposal for a classification. In *Cerebellum and Ataxias* (Vol. 4, Issue 1). BioMed Central Ltd. https://doi.org/10.1186/s40673-017-0061-y

Bence, N., Sampat, R., & Kopito, R. (2001). Bence NF, Sampat RM, Kopito RRImpairment of the ubiquitin-proteasome system by protein aggregation. Science 292:1552-1555. *Science (New York, N.Y.)*, *292*, 1552–1555. https://doi.org/10.1126/science.292.5521.1552

Bergeron, D., Lapointe, C., Bissonnette, C., Tremblay, G., Motard, J., & Roucou, X. (2013). An Out-of-frame Overlapping Reading Frame in the Ataxin-1 Coding Sequence Encodes a Novel Ataxin-1 Interacting Protein. *Journal of Biological Chemistry*, *288*(30), 21824–21835. https://doi.org/10.1074/jbc.M113.472654

Beuriat, P.-A., Cohen-Zimerman, S., L Smith, G. N., Krueger, F., Gordon, B., & Grafman, J. (123 C.E.). Evidence of the role of the cerebellum in cognitive theory of mind using voxel-based lesion mapping. *Scientific Reports |*, *12*, 4999. https://doi.org/10.1038/s41598-022-09104-0

Bezprozvanny, I. (2009). Calcium signaling and neurodegenerative diseases. *Trends in Molecular Medicine*, *15*(3), 89–100. https://doi.org/10.1016/j.molmed.2009.01.001

Binda, F., Pernaci, C., & Saxena, S. (2020). Cerebellar Development and Circuit Maturation: A Common Framework for Spinocerebellar Ataxias. *Frontiers in Neuroscience*, *14*. https://doi.org/10.3389/fnins.2020.00293

Bogdanovic, N., Davidsson, P., Volkmann, I., Winblad, B., & Blennow, K. (2000). Growth-associated protein GAP-43 in the frontal cortex and in the hippocampus in Alzheimer's disease: an immunohistochemical and quantitative study. In *J Neural Transm* (Vol. 107).

Brooker, S. M., Edamakanti, C. R., Akasha, S. M., Kuo, S., & Opal, P. (2021a). Spinocerebellar ataxia clinical trials: opportunities and challenges. *Annals of Clinical and Translational Neurology*, *8*(7), 1543–1556. https://doi.org/10.1002/acn3.51370

Brooker, S. M., Edamakanti, C. R., Akasha, S. M., Kuo, S., & Opal, P. (2021b). Spinocerebellar ataxia clinical trials: opportunities and challenges. *Annals of Clinical and Translational Neurology*, *8*(7), 1543–1556. https://doi.org/10.1002/acn3.51370

Buijsen, R. A. M., Gardiner, S. L., Bouma, M. J., van der Graaf, L. M., Boogaard, M. W., Pepers, B. A., Eussen, B., de Klein, A., Freund, C., & van Roon-Mom, W. M. C. (2018). Generation of 3 spinocerebellar ataxia type 1 (SCA1) patient-derived induced pluripotent stem cell lines LUMCi002-A, B, and C and 2

unaffected sibling control induced pluripotent stem cell lines LUMCi003-A and B. *Stem Cell Research*, *29*, 125–128. https://doi.org/10.1016/j.scr.2018.03.018

Buijsen, R. A. M., Toonen, L. J. A., Gardiner, S. L., & van Roon-Mom, W. M. C. (2019). Genetics, Mechanisms, and Therapeutic Progress in Polyglutamine Spinocerebellar Ataxias. *Neurotherapeutics*, *16*(2), 263–286. https://doi.org/10.1007/s13311-018-00696-y

Burright, E. N., Brent Clark, H., Servadio, A., Matilla, T., Feddersen, R. M., Yunis, W. S., Duvick, L. A., Zoghbi, H. Y., & Orr, H. T. (1995). SCA1 transgenic mice: A model for neurodegeneration caused by an expanded CAG trinucleotide repeat. *Cell*, *82*(6), 937–948. https://doi.org/10.1016/0092-8674(95)90273-2

Bushart, D. D., & Shakkottai, V. G. (2019). Ion channel dysfunction in cerebellar ataxia. In *Neuroscience Letters* (Vol. 688, pp. 41–48). Elsevier Ireland Ltd. https://doi.org/10.1016/j.neulet.2018.02.005

Bushart, D. D., Zalon, A. J., Zhang, H., Morrison, L. M., Guan, Y., Paulson, H. L., Shakkottai, V. G., & McLoughlin, H. S. (2021). Antisense Oligonucleotide Therapy Targeted Against ATXN3 Improves Potassium Channel–Mediated Purkinje Neuron Dysfunction in Spinocerebellar Ataxia Type 3. *The Cerebellum*, *20*(1), 41–53. https://doi.org/10.1007/s12311-020-01179-7

Catterall, W. A. (2000). Structure and regulation of voltage-gated Ca^{2+} channels. *Annual Review of Cell and Developmental Biology*, *16*, 521–555. https://doi.org/10.1146/ANNUREV.CELLBIO.16.1.521

Chuang, C.-Y., Yang, C.-C., Soong, B.-W., Yu, C.-Y., Chen, S.-H., Huang, H.-P., & Kuo, H.-C. (n.d.). *Modeling spinocerebellar ataxias 2 and 3 with iPSCs reveals a role for glutamate in disease pathology Spinocerebellar ataxias 2 and 3 (SCA2 and SCA3) are dominantly inherited neurodegenerative diseases caused by expansion of polyglutamine-encoding CAG repeats in the*. https://doi.org/10.1038/s41598-018-37774-2

Coarelli, G., Brice, A., & Durr, A. (2018). Recent advances in understanding dominant spinocerebellar ataxias from clinical and genetic points of view. *F1000Research*, *7*, 1781. https://doi.org/10.12688/f1000research.15788.1

Courtney, N. A., Bao, H., Briguglio, J. S., & Chapman, E. R. (2019). Synaptotagmin 1 clamps synaptic vesicle fusion in mammalian neurons independent of complexin. *Nature Communications*, *10*(1), 4076. https://doi.org/10.1038/s41467-019-12015-w

D'Angelo, E., & Casali, S. (2013). Seeking a unified framework for cerebellar function and dysfunction: from circuit operations to cognition. *Frontiers in Neural Circuits*, *6*. https://doi.org/10.3389/fncir.2012.00116

Daughters, R. S., Tuttle, D. L., Gao, W., Ikeda, Y., Moseley, M. L., Ebner, T. J., Swanson, M. S., & Ranum, L. P. W. (2009). RNA Gain-of-Function in Spinocerebellar Ataxia Type 8. *PLoS Genetics*, *5*(8), e1000600. https://doi.org/10.1371/journal.pgen.1000600

Davidsson, P., & Blennow, K. (1998). Neurochemical dissection of synaptic pathology in Alzheimer's disease. *International Psychogeriatrics*, *10*(1), 11–23. https://doi.org/10.1017/S1041610298005110

Davis, R. L. (2020). Mechanism of Action and Target Identification: A Matter of Timing in Drug Discovery. *IScience*, *23*(9). https://doi.org/10.1016/J.ISCI.2020.101487

Dell'orco, J. M., Wasserman, A. H., Chopra, R., Ingram, M. A. C., Hu, X.-S., Singh, V., Wulff, H., Opal, P., Orr, H. T., & Shakkottai, V. G. (2015). *Neurobiology of Disease Neuronal Atrophy Early in Degenerative*

Ataxia Is a Compensatory Mechanism to Regulate Membrane Excitability. https://doi.org/10.1523/JNEUROSCI.1357-15.2015

Dickson, Dennis. (2011). *Neurodegeneration : the molecular pathology of dementia and movement disorders*. Wiley-Blackwell.

Donato, F., Rompani, S. B., & Caroni, P. (2013). *Parvalbumin-expressing basket-cell network plasticity induced by experience regulates adult learning*. https://doi.org/10.1038/nature12866

Du, X., Wang, J., Zhu, H., Rinaldo, L., Lamar, K. M., Palmenberg, A. C., Hansel, C., & Gomez, C. M. (2013). XSecond cistron in CACNA1A gene encodes a transcription factor mediating cerebellar development and SCA6. *Cell*, *154*(1), 118. https://doi.org/10.1016/J.CELL.2013.05.059

Durr, A. (2010). Autosomal dominant cerebellar ataxias: polyglutamine expansions and beyond. *The Lancet Neurology*, *9*(9), 885–894. https://doi.org/10.1016/S1474-4422(10)70183-6

Edamakanti, C. R., Do, J., Didonna, A., Martina, M., & Opal, P. (2018). Mutant ataxin1 disrupts cerebellar development in spinocerebellar ataxia type 1. *Journal of Clinical Investigation*, *128*(6), 2252–2265. https://doi.org/10.1172/JCI96765

Emamian, E. S., Kaytor, M. D., Duvick, L. A., Zu, T., Tousey, S. K., Zoghbi, H. Y., Clark, H. B., & Orr, H. T. (2003a). Serine 776 of Ataxin-1 Is Critical for Polyglutamine-Induced Disease in SCA1 Transgenic Mice. *Neuron*, *38*(3), 375–387. https://doi.org/10.1016/S0896-6273(03)00258-7

Emamian, E. S., Kaytor, M. D., Duvick, L. A., Zu, T., Tousey, S. K., Zoghbi, H. Y., Clark, H. B., & Orr, H. T. (2003b). Serine 776 of Ataxin-1 Is Critical for Polyglutamine-Induced Disease in SCA1 Transgenic Mice. *Neuron*, *38*(3), 375–387. https://doi.org/10.1016/S0896-6273(03)00258-7

Emmerich, C. H., Martinez Gamboa, L., J Hofmann, M. C., Bonin-Andresen, M., Arbach, O., Schendel, P., Gerlach, B., Hempel, K., Bespalov, A., Dirnagl, U., & Parnham, M. J. (n.d.). *Improving target assessment in biomedical research: the GOT-IT recommendations*. https://doi.org/10.1038/s41573-020-0087-3

Evers, M. M., Pepers, B. A., van Deutekom, J. C. T., Mulders, S. A. M., den Dunnen, J. T., Aartsma-Rus, A., van Ommen, G.-J. B., & van Roon-Mom, W. M. C. (2011). Targeting Several CAG Expansion Diseases by a Single Antisense Oligonucleotide. *PLoS ONE*, *6*(9), e24308. https://doi.org/10.1371/journal.pone.0024308

Fernandez-Funez, P., Nino-Rosales, M. L., de Gouyon, B., She, W.-C., Luchak, J. M., Martinez, P., Turiegano, E., Benito, J., Capovilla, M., Skinner, P. J., McCall, A., Canal, I., Orr, H. T., Zoghbi, H. Y., & Botas, J. (2000). Identification of genes that modify ataxin-1-induced neurodegeneration. *Nature*, *408*(6808), 101–106. https://doi.org/10.1038/35040584

Ghosh, R., & Tabrizi, S. J. (2013). *Clinical Aspects of Huntington's Disease* (pp. 3–31). https://doi.org/10.1007/7854_2013_238

Glavan, G., Schliebs, R., & Živin, M. (2009). Synaptotagmins in neurodegeneration. *Anatomical Record*, *292*(12), 1849–1862. https://doi.org/10.1002/ar.21026

Greenfied J.G. (1955). The Spino-Cerebellar Degenerations. *Archives of Neurology And Psychiatry*, *73*(1), 121. https://doi.org/10.1001/archneurpsyc.1955.02330070123014

Grekhnev, D. A., Kaznacheyeva, E. v., & Vigont, V. A. (2022). Patient-Specific iPSCs-Based Models of Neurodegenerative Diseases: Focus on Aberrant Calcium Signaling. In *International Journal of Molecular Sciences* (Vol. 23, Issue 2). MDPI. https://doi.org/10.3390/ijms23020624

Gustincich, S., Zucchelli, S., & Mallamaci, A. (2017). The Yin and Yang of nucleic acid-based therapy in the brain. *Progress in Neurobiology*, *155*, 194–211. https://doi.org/10.1016/j.pneurobio.2016.11.001

Heiney, S. A., Kim, J., Augustine, G. J., & Medina, J. F. (2014). Precise control of movement kinematics by optogenetic inhibition of Purkinje cell activity. *Journal of Neuroscience*, *34*(6), 2321–2330. https://doi.org/10.1523/JNEUROSCI.4547-13.2014

Hoebeek, F. E., Stahl, J. S., van Alphen, A. M., Schonewille, M., Luo, C., Rutteman, M., van den Maagdenberg, A. M. J. M., Molenaar, P. C., Goossens, H. H. L. M., Frens, M. A., & de Zeeuw, C. I. (2005). Increased noise level of Purkinje cell activities minimizes impact of their modulation during sensorimotor control. *Neuron*, *45*(6), 953–965. https://doi.org/10.1016/J.NEURON.2005.02.012

Holmes, S. E., O'Hearn, E. E., McInnis, M. G., Gorelick-Feldman, D. A., Kleiderlein, J. J., Callahan, C., Kwak, N. G., Ingersoll-Ashworth, R. G., Sherr, M., Sumner, A. J., Sharp, A. H., Ananth, U., Seltzer, W. K., Boss, M. A., Vieria-Saecker, A.-M., Epplen, J. T., Riess, O., Ross, C. A., & Margolis, R. L. (1999). Expansion of a novel CAG trinucleotide repeat in the 5' region of PPP2R2B is associated with SCA12. *Nature Genetics*, *23*(4), 391–392. https://doi.org/10.1038/70493

Hou, Y., Dan, X., Babbar, M., Wei, Y., Hasselbalch, S. G., Croteau, D. L., & Bohr, V. A. (2019). Ageing as a risk factor for neurodegenerative disease. *Nature Reviews Neurology*, *15*(10), 565–581. https://doi.org/10.1038/s41582-019-0244-7

Ilg, W., Brötz, D., Burkard, S., Giese, M. A., Schöls, L., & Synofzik, M. (2010). Long-term effects of coordinative training in degenerative cerebellar disease. *Movement Disorders*, *25*(13), 2239–2246. https://doi.org/10.1002/mds.23222

Ingram, M. A. C., Orr, H. T., & Clark, H. B. (2012). Genetically engineered mouse models of the trinucleotide-repeat spinocerebellar ataxias. In *Brain Research Bulletin* (Vol. 88, Issue 1, pp. 33–42). https://doi.org/10.1016/j.brainresbull.2011.07.016

Irwin, S., Vandelft, M., Pinchev, D., Howell, J. L., Graczyk, J., Orr, H. T., & Truant, R. (2005). RNA association and nucleocytoplasmic shuttling by ataxin-1. *Journal of Cell Science*, *118*(1), 233–242. https://doi.org/10.1242/jcs.01611

Jacobi, H., Bauer, P., Giunti, P., Labrum, R., Sweeney, M. G., Charles, P., Durr, A., Marelli, C., Globas, C., Linnemann, C., Schols, L., Rakowicz, M., Rola, R., Zdzienicka, E., Schmitz-Hubsch, T., Fancellu, R., Mariotti, C., Tomasello, C., Baliko, L., … Klockgether, T. (2011). The natural history of spinocerebellar ataxia type 1, 2, 3, and 6: A 2-year follow-up study. *Neurology*, *77*(11), 1035–1041. https://doi.org/10.1212/WNL.0b013e31822e7ca0

Kano, M., & Watanabe, M. (2020). Cerebellar circuits. *Neural Circuit and Cognitive Development*, 79–102. https://doi.org/10.1016/B978-0-12-814411-4.00004-4

Kano, M., Watanabe, T., Uesaka, N., & Watanabe, M. (n.d.). *Multiple Phases of Climbing Fiber Synapse Elimination in the Developing Cerebellum*. https://doi.org/10.1007/s12311-018-0964-z

Katsuno, M., Tanaka, F., Adachi, H., Banno, H., Suzuki, K., Watanabe, H., & Sobue, G. (2012). Pathogenesis and therapy of spinal and bulbar muscular atrophy (SBMA). In *Progress in Neurobiology* (Vol. 99, Issue 3, pp. 246–256). https://doi.org/10.1016/j.pneurobio.2012.05.007

Klement, I. A., Skinner, P. J., Kaytor, M. D., Yi, H., Hersch, S. M., Clark, H. B., Zoghbi, H. Y., & Orr, H. T. (1998). Ataxin-1 Nuclear Localization and Aggregation. *Cell*, *95*(1), 41–53. https://doi.org/10.1016/S0092-8674(00)81781-X

Knierim, J. (2020). *Overview: Functions of the Cerebellum.*

Kovacs, G. G. (2016). Molecular pathological classification of neurodegenerative diseases: Turning towards precision medicine. In *International Journal of Molecular Sciences* (Vol. 17, Issue 2). MDPI AG. https://doi.org/10.3390/ijms17020189

Lee, P. J., Kerridge, A., Chatterjee, D., Koeppen, A. H., Faust, P. L., & Louis, E. D. (n.d.). *A Quantitative Study of Empty Baskets in Essential Tremor and Other Motor Neurodegenerative Diseases*. https://doi.org/10.1093/jnen/nly114

Lieberman, A. P., Shakkottai, V. G., & Albin, R. L. (2019). Polyglutamine Repeats in Neurodegenerative Diseases. In *Annual Review of Pathology: Mechanisms of Disease* (Vol. 14, pp. 1–27). Annual Reviews Inc. https://doi.org/10.1146/annurev-pathmechdis-012418-012857

Lim, J., Crespo-Barreto, J., Jafar-Nejad, P., Bowman, A. B., Richman, R., Hill, D. E., Orr, H. T., & Zoghbi, H. Y. (2008). Opposing effects of polyglutamine expansion on native protein complexes contribute to SCA1. *Nature*, *452*(7188), 713–718. https://doi.org/10.1038/nature06731

Liu, C., & Fang, Y. (2019). New insights of poly(ADP-ribosylation) in neurodegenerative diseases: A focus on protein phase separation and pathologic aggregation. In *Biochemical Pharmacology* (Vol. 167, pp. 58–63). Elsevier Inc. https://doi.org/10.1016/j.bcp.2019.04.028

Lopez-Otin, C. , B. M. A. , P. L. , S. M. & K. G. T. hallmarks of aging. C. 153, 1194–1217 (2013). (n.d.). *The hallmarks of aging. Cell 153, 1194–1217 (2013).*

Lorenzetti, D. (2000). Repeat instability and motor incoordination in mice with a targeted expanded CAG repeat in the Sca1 locus. *Human Molecular Genetics*, *9*(5), 779–785. https://doi.org/10.1093/hmg/9.5.779

Ma, J., Wu, C., Lei, J., & Zhang, X. (2014). Cognitive impairments in patients with spinocerebellar ataxia types 1, 2 and 3 are positively correlated to the clinical severity of ataxia symptoms. In *Int J Clin Exp Med* (Vol. 7, Issue 12). www.ijcem.com/

McLoughlin, H. S., Moore, L. R., Chopra, R., Komlo, R., McKenzie, M., Blumenstein, K. G., Zhao, H., Kordasiewicz, H. B., Shakkottai, V. G., & Paulson, H. L. (2018). Oligonucleotide therapy mitigates disease in spinocerebellar ataxia type 3 mice. *Annals of Neurology*, *84*(1), 64–77. https://doi.org/10.1002/ana.25264

Meera, P., Pulst, S. M., & Otis, T. S. (2016). The Journal of Physiology Neuroscience Cellular and circuit mechanisms underlying spinocerebellar ataxias. *J Physiol*, *594*, 4653–4660. https://doi.org/10.1113/JP271897

Menzel P. (1861). *Beitrag zur Kenntnis der hereditären Ataxie und Kleinhirnatrophie Arch Psychiat Nervenkrankh*.

Miyazaki, T., Hashimoto, K., Shin, H.-S., Kano, M., & Watanabe, M. (2004). *Development/Plasticity/Repair P/Q-Type Ca 2 Channel 1A Regulates Synaptic Competition on Developing Cerebellar Purkinje Cells*. https://doi.org/10.1523/JNEUROSCI.4208-03.2004

Mizusawa, H., Clark, H. B., & Koeppen, A. H. (2011). Spinocerebellar Ataxias. In *Neurodegeneration: The Molecular Pathology of Dementia and Movement Disorders* (pp. 273–287). Wiley. https://doi.org/10.1002/9781444341256.ch27

Nóbrega, C. , de A. L. P. , & de A. L. P. (2018). *Polyglutamine Disorders* (Vol. 1049). Springer International Publishing. https://doi.org/10.1007/978-3-319-71779-1

Ogura, Y., Sahashi, K., Hirunagi, T., Iida, M., Miyata, T., & Katsuno, M. (2022). Mid1 is associated with androgen-dependent axonal vulnerability of motor neurons in spinal and bulbar muscular atrophy. *Cell Death & Disease*, *13*(7), 601. https://doi.org/10.1038/s41419-022-05001-6

Paulson, H. L., Shakkottai, V. G., Brent Clark, H., & Orr, H. T. (2017). *Polyglutamine spinocerebellar ataxias — from genes to potential treatments*. https://doi.org/10.1038/nrn.2017.92

Pilotto, F., & Saxena, S. (2018). Epidemiology of inherited cerebellar ataxias and challenges in clinical research. *Clinical and Translational Neuroscience*, *2*(2), 2514183X1878525. https://doi.org/10.1177/2514183x18785258

Purves D, Augustine GJ, & Fitzpatrick D, et al. (2001). *Neuroscience. Organization of the Cerebellum.* (2nd edition). https://www.ncbi.nlm.nih.gov/books/NBK11132/.

Robinson, K. J., Watchon, M., & Laird, A. S. (2020). Aberrant Cerebellar Circuitry in the Spinocerebellar Ataxias. In *Frontiers in Neuroscience* (Vol. 14). Frontiers Media S.A. https://doi.org/10.3389/fnins.2020.00707

Rousseaux, M. W. C., Tschumperlin, T., Lu, H.-C., Lackey, E. P., Bondar, V. v., Wan, Y.-W., Tan, Q., Adamski, C. J., Friedrich, J., Twaroski, K., Chen, W., Tolar, J., Henzler, C., Sharma, A., Bajić, A., Lin, T., Duvick, L., Liu, Z., Sillitoe, R. v., … Orr, H. T. (2018). ATXN1-CIC Complex Is the Primary Driver of Cerebellar Pathology in Spinocerebellar Ataxia Type 1 through a Gain-of-Function Mechanism. *Neuron*, *97*(6), 1235-1243.e5. https://doi.org/10.1016/j.neuron.2018.02.013

Rüb, U., Schöls, L., Paulson, H., Auburger, G., Kermer, P., Jen, J. C., Seidel, K., Korf, H.-W., & Deller, T. (2013). Clinical features, neurogenetics and neuropathology of the polyglutamine spinocerebellar ataxias type 1, 2, 3, 6 and 7. *Progress in Neurobiology*, *104*, 38–66. https://doi.org/10.1016/j.pneurobio.2013.01.001

Ruegsegger, C., Stucki, D. M., Steiner, S., Angliker, N., Radecke, J., Keller, E., Zuber, B., Rüegg, M. A., & Saxena, S. (2016). Impaired mTORC1-Dependent Expression of Homer-3 Influences SCA1 Pathophysiology. *Neuron*, *89*(1), 129–146. https://doi.org/10.1016/j.neuron.2015.11.033

Schöls, L., Bauer, P., Schmidt, T., Schulte, T., & Riess, O. (2004). Autosomal dominant cerebellar ataxias: clinical features, genetics, and pathogenesis. *The Lancet Neurology*, *3*(5), 291–304. https://doi.org/10.1016/S1474-4422(04)00737-9

Sequeiros, J., & Coutinho, P. (1993). Epidemiology and clinical aspects of Machado-Joseph disease. *Advances in Neurology*, *61*, 139–153.

Smeets, C. J. L. M., Ma, K. Y., Fisher, S. E., & Verbeek, D. S. (2021). Cerebellar developmental deficits underlie neurodegenerative disorder spinocerebellar ataxia type 23. *Brain Pathology*, *31*(2), 239–252. https://doi.org/10.1111/bpa.12905

Steffan, J. S., Kazantsev, A., Spasic-Boskovic, O., Greenwald, M., Zhu, Y.-Z., Gohler, H., Wanker, E. E., Bates, G. P., Housman, D. E., & Thompson, L. M. (n.d.). *The Huntington's disease protein interacts with p53 and CREB-binding protein and represses transcription*. www.pnas.orgcgidoi10.1073pnas.100110097

Sullivan, R., Yau, W. Y., O'Connor, E., & Houlden, H. (2019). Spinocerebellar ataxia: an update. *Journal of Neurology*, *266*(2), 533–544. https://doi.org/10.1007/s00415-018-9076-4

Synofzik, M., Puccio, H., Mochel, F., & Schöls, L. (2019). Autosomal Recessive Cerebellar Ataxias: Paving the Way toward Targeted Molecular Therapies. In *Neuron* (Vol. 101, Issue 4, pp. 560–583). Cell Press. https://doi.org/10.1016/j.neuron.2019.01.049

Sze, C. I., Bi, H., Kleinschmidt-Demasters, B. K., Filley, C. M., & Martin, L. J. (2000). Selective regional loss of exocytotic presynaptic vesicle proteins in Alzheimer's disease brains. *Journal of the Neurological Sciences*, *175*(2), 81–90. https://doi.org/10.1016/S0022-510X(00)00285-9

Tanaka-Yamamoto, K., Shakkottai, V., Becker, E. B. E., Laird, A. S., & Robinson, K. J. (2020). *Aberrant Cerebellar Circuitry in the Spinocerebellar Ataxias*. https://doi.org/10.3389/fnins.2020.00707

Tong, X., Gui, H., Jin, F., Heck, B. W., Lin, P., Ma, J., Fondell, J. D., & Tsai, C. (2011). Ataxin-1 and Brother of ataxin-1 are components of the Notch signalling pathway. *EMBO Reports*, *12*(5), 428–435. https://doi.org/10.1038/embor.2011.49

Toonen, L. J. A., Rigo, F., van Attikum, H., & van Roon-Mom, W. M. C. (2017). Antisense Oligonucleotide-Mediated Removal of the Polyglutamine Repeat in Spinocerebellar Ataxia Type 3 Mice. *Molecular Therapy - Nucleic Acids*, *8*, 232–242. https://doi.org/10.1016/j.omtn.2017.06.019

Tsai, C.-C., Kao, H.-Y., Mitzutani, A., Banayo, E., Rajan, H., McKeown, M., & Evans, R. M. (2004). *Ataxin 1, a SCA1 neurodegenerative disorder protein, is functionally linked to the silencing mediator of retinoid and thyroid hormone receptors*. www.pnas.orgcgidoi10.1073pnas.0400615101

Wagner, J. L., O'Connor, D. M., Donsante, A., & Boulis, N. M. (2016). Gene, stem cell, and alternative therapies for SCA 1. In *Frontiers in Molecular Neuroscience* (Vol. 9, Issue AUG). Frontiers Research Foundation. https://doi.org/10.3389/fnmol.2016.00067

Walker, F. (2007). Huntington's Disease. *Seminars in Neurology*, *27*(2), 143–150. https://doi.org/10.1055/s-2007-971176

Walter, J. T., Alviña, K., Womack, M. D., Chevez, C., & Khodakhah, K. (2006). *Decreases in the precision of Purkinje cell pacemaking cause cerebellar dysfunction and ataxia*. https://doi.org/10.1038/nn1648

Watase, K., Weeber, E. J., Xu, B., Antalffy, B., Yuva-Paylor, L., Hashimoto, K., Kano, M., Atkinson, R., Sun, Y., Armstrong, D. L., Sweatt, J. D., Orr, H. T., Paylor, R., & Zoghbi, H. Y. (2002). A Long CAG Repeat in the Mouse Sca1 Locus Replicates SCA1 Features and Reveals the Impact of Protein Solubility on Selective Neurodegeneration. *Neuron*, *34*(6), 905–919. https://doi.org/10.1016/S0896-6273(02)00733-X

Whaley, N. R., Fujioka, S., & Wszolek, Z. K. (2011). Autosomal dominant cerebellar ataxia type I: A review of the phenotypic and genotypic characteristics. *Orphanet Journal of Rare Diseases*, *6*(1), 33. https://doi.org/10.1186/1750-1172-6-33

Yamagata, M., Miyazaki, T., Zhang, B., Sassoè-Pognetto, M., Briatore, F., Pregno, G., di Angelantonio, S., Frola, E., Egle De Stefano, M., Vaillend, C., & Patrizi, A. (2020). *Dystroglycan Mediates Clustering of Essential GABAergic Components in Cerebellar Purkinje Cells*. https://doi.org/10.3389/fnmol.2020.00164

Yang, W.-Y., Gao, R., Southern, M., Sarkar, P. S., & Disney, M. D. (2016). Design of a bioactive small molecule that targets r(AUUCU) repeats in spinocerebellar ataxia 10. *Nature Communications*, *7*(1), 11647. https://doi.org/10.1038/ncomms11647

Yue, S., Serra, H. G., Zoghbi, H. Y., & Orr, H. T. (2001). The spinocerebellar ataxia type 1 protein, ataxin-1, has RNA-binding activity that is inversely affected by the length of its polyglutamine tract. In *Human Molecular Genetics* (Vol. 10, Issue 1).

Zesiewicz, T. A., Wilmot, G., Kuo, S.-H., Perlman, S., Greenstein, P. E., Ying, S. H., Ashizawa, T., Subramony, S., Schmahmann, J. D., Figueroa, K., Mizusawa, H., Schöls, L., Shaw, J. D., Dubinsky, R. M., Armstrong, M. J., Gronseth, G. S., & Sullivan, K. L. (2018). *Comprehensive systematic review summary: Treatment of cerebellar motor dysfunction and ataxia Report of the Guideline Development, Dissemination, and Implementation Subcommittee of the American Academy of Neurology*. https://doi.org/10.1212/WNL.0000000000005055

Zü, G., & Reiser, G. (n.d.). *Calcium Dysregulation and Homeostasis of Neural Calcium in the Molecular Mechanisms of Neurodegenerative Diseases Provide Multiple Targets for Neuroprotection*. Retrieved October 3, 2022, from www.liebertonline.com=ars